STUDIES ON CORE CHARACTERISTICS AND PERTURBATION THEORY BASED TRANSIENT ANALYSIS OF METAL FBRs

By

A. RIYAS

Enrolment Number: PHYS 02 2008 04014

Indira Gandhi Centre for Atomic Research, Kalpakkam, India

A thesis submitted to the
Board of Studies in Physical Sciences
In partial fulfilment of the requirements
For the degree of

DOCTOR OF PHILOSOPHY

of

HOMI BHABHA NATIONAL INSTITUTE

MUMBAI, INDIA

(August, 2014)

Homi Bhabha National Institute

Recommendations of the Viva Voce Committee

As members of the Viva Voce Board, we certify that we have read the dissertation prepared by **Mr. A. Riyas** entitled **"Studies on Core Characteristics and Perturbation Theory Based Transient Analysis of Metal FBRs"** and recommend that it may be accepted as fulfilling the thesis requirement for the Degree of Doctor of Philosophy.

M. Vijayalakshmi Date: 27.7.15

Chairman – Dr. M. Vijayalakshmi

Date: 27/7/15

Convener/Guide – Dr. K. Devan

Date: 27-7-2015

External Examiner- Dr.H.P.Gupta

Date: 27/7/2015

Member – Dr. K. Velusamy

Date: 27/7/15.

Member – Dr. K. Nagarajan

Final approval and acceptance of this thesis is contingent upon the candidate's submission of the final copies of the thesis to HBNI.

I hereby certify that I have read this thesis prepared under my direction and recommend that it may be accepted as fulfilling the thesis requirement.

Date: 27/7/15

Place: Kalpakkam.

(K. Devan)

Guide

STATEMENT BY AUTHOR

This dissertation has been submitted in partial fulfilment of requirements for an advanced degree at Homi Bhabha National Institute (HBNI) and is deposited in the Library to be made available to borrowers under rules of the HBNI.

Brief quotations from this dissertation are allowable without special permission, provided that accurate acknowledgement of source is made. Requests for permission for extended quotation from or reproduction of this manuscript in whole or in part may be granted by the Competent Authority of HBNI when in his or her judgment the proposed use of the material is in the interests of scholarship. In all other instances, however, permission must be obtained from the author.

(A. Riyas)

DECLARATION

I, hereby declare that the investigation presented in the thesis has been carried out by me. The work is original and has not been submitted earlier as a whole or in part for a degree / diploma at this or any other Institution / University

(A. Riyas)

List of Publications Arising From the Thesis

Journal Papers

1. "Perturbation Analysis of Prototype Fast Breeder Reactor Equilibrium Core Using IGCAR and ERANOS Code Systems", A. Riyas, K. Devan and P. Mohanakrishnan, Nuclear Engineering and Design, **2013**, *Vol.*255, 112-122.

2. "ULOF Transient Behaviour of Metal Fuelled Fast Breeder Reactor Cores as a Function of Core Size and Perturbation Methods", A.Riyas and P. Mohanakrishnan, Nuclear Engineering and Design, **2014**, *Vol.*278, 141-149.

Conference Papers

1. A. Riyas and P.Mohanakrishnan, Reactor Physics Studies on Metallic Fuels for Indian Fast Reactor Programme, Paper Submitted to FRA-16, International Conference on Peaceful Uses of Atomic Energy, New Delhi, India (2009).

2. A. Riyas and K. Devan, Physics Optimization of Metal Fuel Pin Design for Enhancement of Breeding Characteristics, IAEA Consultancy Meeting of INPRO Collaborative Project on Fuel Cycles for Innovative Systems based on Integrated Technology, IGCAR, India (2011).

Other Publications

1. "Comparative Study of ULOF analysis of 1000 MWe and 500 MWe FBR-M Cores and their Inherent Safety", T.Sathiyasheela, A. Riyas, P.Mohanakrishnan, S.C.Chetal and Baldev Raj, Annals of Nuclear Energy, **2011**, *Vol.*38, 1065-1073.

2. “Inherent Safety Aspects of Metal fuelled FBR”, T.Sathiyasheela, A.Riyas, R.Sukanya, P.Mohanakrishnan and S.C.Chetal, Nuclear Engineering and Design, **2013**, *Vol.*265, 1149-1158.

3. “A Comparative Study of Severe Loss of Flow Accidents in 500 MWe FBR Metal Cores with PFBR Oxide Core”, R.Harish, G.S.Srinivasan, A.Riyas and P.Mohanakrishnan, Annals of Nuclear Energy, **2009**, *Vol.*36, 1003-1012.

4. “Studies on Physics Parameters of Metal (U–Pu–Zr) Fuelled FBR Cores”, A.Riyas, P.Mohanakrishnan. Annals of Nuclear Energy, **2008**, *Vol.*35, 87-92.

DEDICATED TO MY PARENTS

ACKNOWLEDGEMENTS

First and foremost, praises and thanks to the God, the Almighty, for His showers of blessings throughout my research work to complete the research successfully. I would like to thank my mother, without her continuous support and love I never would have been able to achieve my goals.

I would like to express my deep and sincere gratitude to my research guide, Dr. K. Devan for his support to complete the study. Special appreciation goes to my former guide, Dr. P. Mohanakrishnan for his supervision and constant support. Their invaluable constructive comments and suggestions throughout the thesis works have contributed to the success of this research and thesis.

I would like to thank my doctoral committee members Prof. M. Vijayalakshmi, Prof. K. Velusamy, and Prof. K. Nagarajan for their encouragement and suggestions for the successful completion of the thesis work.

I would like to express my deep thanks to Prof. B. V. R. Tata, Dean Academics-Physics, for his help and advice which helped me to submit the thesis in time.

I am thankful to Dr. P.R. Vasudeva Rao, present Director, IGCAR, Shri. S.C. Chetal and Dr. Baldev Raj former Directors of IGCAR for allowing me to use the facilities for the research work. I am also thankful to Dr. P. Chellapandi, Director, RDG, Shri. P. Puthiyavinayagam Associate Director, CDG for their kind encouragement to my studies.

I am grateful to Smt. T. Sathiyasheela for her efforts that help me to understand and analyse the safety analysis codes that used in the present study. Thanks to my colleague and HBNI classmate Shri. D. Sunil Kumar for his valuable suggestions and helps during course

work and PhD. I would like to acknowledge my colleague, Smt. Debanwita Paul for her helps and suggestions.

There are many colleagues and friends with whom I interacted during my course work and thesis preparation. I thank Shri. Adish Haridas, Shri. V.L. Anuraj Shri. M.L. Jayalal, Shri. M. Ramakrishnan, Smt. V. Bhuvana, Smt. Janaki, Shri. M. Alagan for their valuable helps during this period. Also thanks to our office staff Shri. Ravi.

Most importantly, I am greatly indebted to my wife Sheena, sons Roshan Muhammed and Rizwan Muhammed for their continuous support during the PhD.

SYNOPSIS

Nuclear energy has greater role in India for the faster economic growth and development. Towards this, metal FBRs are planned to be launched during its second-stage of nuclear energy programme. The choice of metal FBRs is due to its advantages of high breeding potential, better capability of radio-toxicity reduction through actinide incineration and amenability for multiple recycling and pyro-reprocessing methods which helps non-proliferation. Though, the benefits are well understood, no commercial power reactors have been built so far based on metal fuels, and the limited data available is based on American experimental reactors, EBR-I, II and FFTF. At the same time, metal FBR designs which enables high breeding poses the safety concern of high positive void coefficient. It necessitates core optimization studies with respect to breeding, safety and economics as a function of fuel pin design, core size, type of metallic fuel used etc. Safety of such systems during unprotected transients also has to be ensured with the uncertainties involved in the calculation. The main scope of the study presented in the thesis is to evaluate the breeding capability, the core performance and the safety characteristics of the metallic fuelled FBR cores as a function of core size, type of metallic fuel used and different reactor core configurations. The effects of approximations and uncertainties to the safety performance are also to be studied.

Ternary metal alloy of U-Pu-Zr is chosen as the fuel for the present study. The first objective of the study is to understand the breeding and safety characteristics of metal fuelled FBR cores of different size and type of fuel. The study is performed using three Zr concentrations of 10%, 6% and 0%. For the first time, the case of U-Pu binary fuel with Zr liner inside the SS clad is studied. It is found that a 500 MWe fast breeder

reactor having 2 rows of blanket can attain a BR of 1.24 with 10% Zr, 1.36 with 6% Zr and 1.47 with a binary fuel of U-Pu alloy with a liner in the fuel pin design. For the case of 1000 MWe FBR core, BR of 1.36, 1.49 and 1.56 are attainable with the Zr content of 10%, 6% and 0% respectively. Internal BR is more than unity is achievable resulting in zero burn-up loss of reactivity. The estimated sodium void worth for the small (120 MWe), medium (500 MWe) and large (1000 MWe) cores fuelled with U-Pu-6%Zr are 0.4 $, 4.5 $ and 5.6 $ respectively. Also, the sodium void worth increases with the reduction of Zr in the fuel pellet. Based on the irradiation data available, it is suggested to use U-Pu-6%Zr as the candidate fuel with maximum BR.

Two methods of reducing the high positive sodium void worth in large metal fuelled FBR cores are applied to a 1000 MWe FBR core. In the first method, the replacement of upper axial blanket with a sodium plenum reduces the sodium void worth to 43% of its original value. The compromise on BR and DT with this modification is found to be small. In the second method, 1% reduction in fuel smear density, sodium void reactivity worth decreases by 0.03% and a corresponding reduction of 0.7% in BR.

The second objective of the study is to find the effectiveness of the first order approximated material removal worths on transient analysis. As a first step of achieving this, an exact perturbation theory code PERTX is developed. By using IGCAR 2D codes, ABBN-93 evaluated multi-group nuclear data and perturbation code PERTX, the errors in the first order estimation of various safety parameters are studied for MOX fuelled 500 MWe PFBR core. The results are validated with the European code system ERANOS 2.1 and JEFF 3.1 data. These comparisons revealed the adequacy of the perturbation

scheme used up to the initiation of sodium voiding. Typical uncertainties are about 10%.

Third objective of the study is to analyse the unprotected loss of flow accident (ULOFA) behaviour of metal fuelled FBR cores as a function of core size and perturbation method. With a flow halving time of 8 sec and with the results of first order perturbation methods, the study shows that small or medium reactors will be in pre-disassembly phase for longer time due to the lower positive reactivity addition from sodium density fall. It is also found that, even with relatively large sodium void reactivity effect, the ULOF in metal FBR cores is benign compared to that of oxide FBR like PFBR and the sodium boiling in metal FBR is delayed up to 900 sec. If a passive safety grade heat removal system (SGDHR) is able to remove the decay heat, the reactor can be brought to safe shutdown state. The study also reveals the adequacy of first order methods for the ULOF transient analysis over exact perturbation calculations. This is due to the fact that the actual perturbation the core suffers during an ULOFA transient is less than 10%.

For accounting uncertainties in first order perturbation based reactivity worths, sensitivity analyses are then performed with 20% uncertainty in Na void reactivity and radial expansion feedback. This resulted in the interesting new finding that the 500 MWe metallic fuelled core continues to be benign even with the pessimistic uncertainty. The reactor power falls below SGDHR capacity before initiation of sodium boiling. But for the 1000 MWe metal core, reactor power reduction below SGDHR capacity is possible only with a 20% reduction in whole core sodium void worth. Thus, it is

important to determine the uncertainties in the perturbation theory based reactivity related parameters.

First important result of the research reported here is the systematic variation of core physics parameters of metallic ternary U-Pu-Zr fuelled FBRs as a function of zirconium content in the fuel and core size. The study shows that both BR and sodium void worth increases with core size and reduction in zirconium. Based on the limitation of irradiation experience, U-Pu-6%Zr is suggested as the fuel for Indian metal fuelled FBRs with maximum BR. The high positive void worth in large FBRs can be reduced by replacing upper axial blanket by a sodium plenum and by reducing fuel smear density. Exact perturbation analysis is made possible by the development of the code PERTX. ULOFA analysis shows that, the 1000 MWe reactor enters the disassembly phase within a shorter interval after the initiation of the event. Also the study proved that, the ULOFA behaviour is found to be similar with the use of exact perturbation results.

Sensitivity analysis is performed with respect to the main feedback components. With an uncertainty of 20% taken for these parameters in the unfavourable direction shows that the 500 MWe reactor shutdown safely and the power reduces below the SGDHR capacity. Another important result of the study is that 20% reduction in the whole core sodium void worth is essential for the safe shutdown of the 1000 MWe reactor during ULOFA.

The study can be extended for core designs with near zero sodium void worths and its transient behaviour. 3D core burn-up and perturbation studies are also of interest. Multichannel representation in a coupled code with neutron diffusion theory and sub-assembly wise thermal hydraulics computation can be also studied.

CONTENTS

LIST OF FIGURES

LIST OF TABLES

LIST OF ABBREVIATIONS

No.	Abbreviation	Meaning
1	ABBN	Starting Letters of Names of Scientists involved in the Russian Nuclear Data Library used in this Study
2	at%	Atom percentage
3	BR	Breeding ratio
4	CDA	Core Disruptive Accident
7	CSDT	Compound System Doubling Time
5	CSR	Control and Safety Rods
6	DSR	Diverse Safety Rods
8	DT	Doubling Time
9	eV	Electron Volt
10	FBR	Fast Breeder Reactor
11	GWd/t	Giga Watt Days/tonne
12	GWe	Giga Watt Electric
13	LAB	Lower Axial Blanket
14	MWe	Mega Watt (Electric)
15	MWt	Mega Watt (Thermal)
16	Na	Sodium
17	pcm	Percent Milli (10^{-5} $\Delta k/k$)
18	PFBR	Prototype Fast Breeder Reactor
19	RB	Radial Blanket
20	RDT	Reactor Doubling Time
21	SA	Sub-assembly
22	SD	Smear Density
23	SDT	System Doubling Time
24	SS	Stainless Steel
25	UAB	Upper Axial Blanket
26	ULOFA	Unprotected Loss of Flow Accident
27	ULOHS	Unprotected Loss of Heat Sink
28	UTOPA	Unprotected Transient Over Power Accident
29	U-Pu-Zr	Uranium-Plutonium-Zirconium
30	wt%	Weight percentage

Chapter 1

INTRODUCTION

1.1 Scope of the Study

Global energy demand is increasing due to growing population, requirement of better economic conditions and higher standard of living. Most of the energy is still being derived from fossil fuels and the continuous use of it has adverse effect on environment. Nuclear energy constitutes one of the main non-renewable sources of clean energy. It contributes 14% of the world's electricity demand [IAEA, 2011] without producing greenhouse gases (GHG). In India, the nuclear power growth scenario is in accordance with the three stage program proposed by H.J.Bhabha and schematically shown in Fig.1.1 [Kakodkar, 2008; Chetal and Chellapandi, 2013] by taking in to account the effective utilization of uranium and thorium resources. The first stage of nuclear program is with water moderated reactors and mainly consists of pressurised heavy water reactors (PHWR). At present, the nuclear contribution to the total electricity demand in India is 5 GWe.

In the second stage, it is planned to achieve electricity generation, fissile fuel production and efficient uranium utilization with fast breeder reactors (FBR). In the third stage, energy security of India can be accomplished from the abundant thorium resources through different reactor concepts, like thermal breeders, fast breeders and molten salt reactors. Starting from present supply of 5 GWe, the nuclear share to the total requirement is expected to be increased to 63 GWe by 2032. In addition, through the efficient utilization of nuclear resources and innovative designs, it can be further enhanced to 600 GWe by 2090. The projected contribution from fast reactors is ~ 20% of total installed capacity by 2052

[Chetal et al., 2011]. To achieve this, a series of metallic fuelled FBR cores are planned with higher breeding potential and lower fuel doubling times. It is also envisaged that, addition of FBR cores help to incinerate actinide waste to background levels within three centuries.

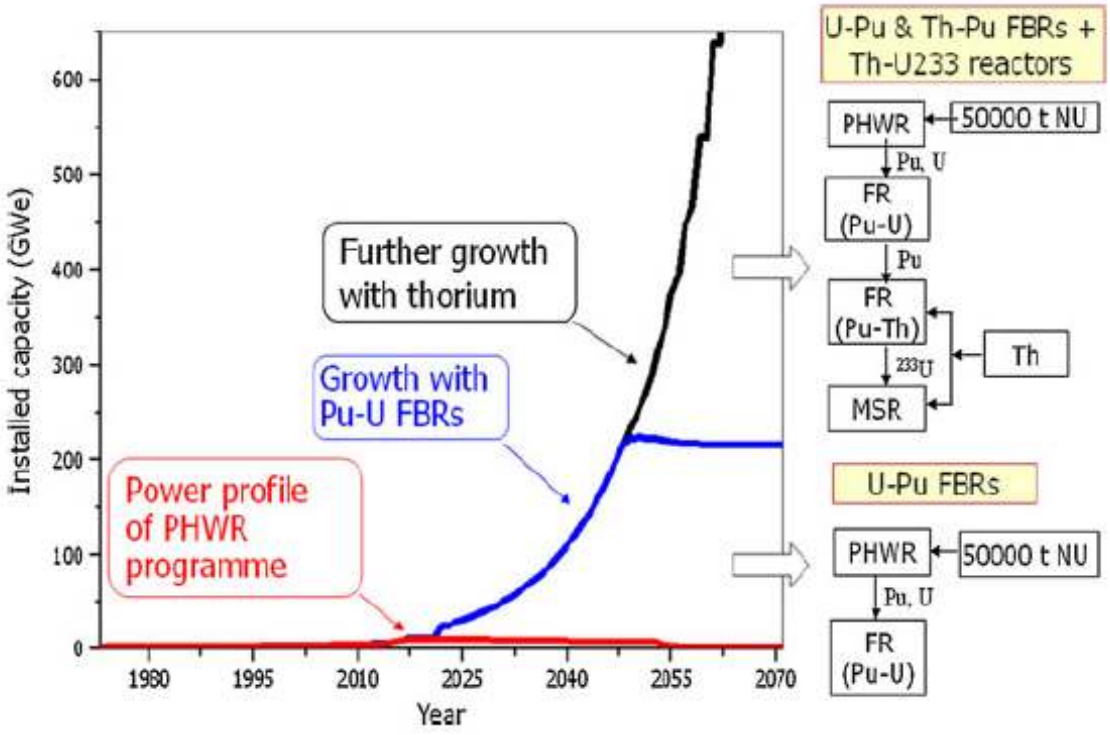

Fig.1.1. The Nuclear Growth Scenario in India

The first fuels used for the early fast reactors were metallic fuels. It includes the reactors of Clementine, EBR-I, EBR-II etc. Metal fuels in EBR-II have shown excellent irradiation behaviour up to higher burn-ups and have improved inherent safety features. Later metal fuel was chosen as the candidate fuel for the integral fast reactor (IFR) concept [Till et al., 1997] for which the EBR-II is considered as the prototype. The IFR concept provided improved safety and waste management, efficient utilization of fuel resources, economic energy production and proliferation resistant nuclear technology.

Since data on metal FBR is limited, Research and development has been started in India in front-end and back end of metal fuel cycle. It includes the development of fuel pins employing different bonding types, manufacturing of various fuel composites and also examining the irradiation behaviour of such fuel pins in Fast Breeder Test Reactor (FBTR). Pyro-processing methods which enable the recovery of actinides using electro refining process also have been commenced. Due to the attractive breeding and safety characteristics compared to ceramic fuels, ternary metallic alloy of U-Pu-Zr has been chosen as the candidate fuel for Indian metallic fuel program. It is important to quantify these parameters for various reactor designs with ternary fuel. The variation of breeding capability and transient safety characteristics are hence studied as a function of core size. Due to the severity of the accident, the transient considered here is the unprotected loss of flow accident (ULOFA). Further, the present study focuses on assessing the calculation methodology of safety analysis and the sensitivity of various reactivity feedbacks on ULOFA. The validity of approximations used in the estimation of reactivity changes using perturbation methods are also studied in detail.

1.2 Basics of Fast Breeder Reactors

1.2.1 Energy from Nucleus

Energy can be liberated from the nucleus of an atom either by the process of nuclear fission or by nuclear fusion. In a nuclear fission, a heavy nucleus splits in to two lighter nuclei, whereas two or more light nuclei are fused together to a heavy nucleus in a nuclear fusion. The importance of these two reactions is that both the process liberates energy. Nuclear fission can be either spontaneous or induced. Isotopes of thorium, uranium and plutonium are some examples of nuclei which can fission spontaneously, but with a small

probability of occurrence. For neutron induced fission, a heavy nucleus fissions after neutron absorption. The probability of such nuclear fission event depends on incident neutron kinetic energy and the target nucleus. For example, a U-235 nucleus absorbs a neutron and splits in to a strontium and xenon nuclei and three neutrons. The fission process can be represented as shown below:

$$^{235}_{92}U + ^{1}_{0}n \rightarrow ^{90}_{38}Sr + ^{143}_{54}Xe + 3^{1}_{0}n \quad (1.1)$$

In this nuclear reaction, the mass of products are less than that of reactants, and the difference in mass is converted in to energy according to Einstein's mass energy relationship ($E=mc^2$) and approximately 200 MeV (million electron volt) of energy is liberated. As shown above each of the nuclear fission process liberates more than two neutrons as an average and can initiate further fissions in the neighbouring U-235 nuclei, and a vast amount of energy can be liberated in a very small interval of time. The process of such continued nuclear fission process is called a chain reaction. But, due to parasitic non-fission captures and leakage of neutrons from the medium, a minimum amount of fissile material is required for a sustained chain reaction and it is called critical mass. The process of uncontrolled chain reaction is employed in fission nuclear explosives. In a nuclear fission reactor, energy is produced by using controlled chain reaction.

Apart from nuclear fission, other neutron induced interactions like scattering (elastic and in-elastic) and radiative capture is also possible and the probability of each of these reactions depends on the incident neutron energy. A measure of the probability of a particular interaction is represented as cross-section [Glasstone and Sesonske, 1994] and it has the unit of 'barn' (1 barn $=10^{-24}$ cm^2). In general**,** most nuclear cross-sections decrease with increase of neutron energy. The nuclei that can be fissioned by neutrons of any energy are called

fissile. Examples are U-233, U-235, Pu-239 and Pu-241. Out of these, U-235 is the only naturally occurring fissile isotope and the others are produced from other nuclei by a process called artificial transmutation in nuclear reactors and accelerated driven systems. The nuclei that can be fissionable by neutrons of high energy are called fertile and examples of such nuclei are Th-232, U-238, Pu-240 and Pu-242. Fertile nuclei can also be converted to fissile nuclei by neutron capture and this process is called breeding.

1.2.2 Nuclear Reactors: Thermal and Fast Reactors

Nuclear reactor is a device used for the liberation of nuclear energy in a controlled manner. In a nuclear reactor, energy is liberated from the nucleus either by nuclear fission or fusion. As controlled nuclear fusion requires extreme physical conditions and the development of such device is still under progress, a nuclear reactor generally refers to a device that liberates nuclear energy by the process of controlled chain reaction. Nuclear reactors can be categorized mainly in to two depending on the kinetic energy of neutrons that causes fission. The first one is called thermal reactors, in which most of the fission reactions are with low energy (thermal) neutrons where as in other type called fast reactors, most of the fissions are taking place with fast neutrons (> 100 keV).

A thermal reactor is possible with less amount of fissile fuel due to the high fission cross-sections at low energies. As the cross-section is small at high energies, fast reactors require higher critical mass. But the conversion of abundant U-238 or Th-232 nuclei is possible with fast reactors using the available Pu-239 from thermal reactors. The higher number of neutrons produced in fast reactors are partly used for sustaining chain reaction and partly used for converting fertile to fissile nuclei. Fast reactors capable of breeding are called fast breeder reactors.

The main difference in thermal and fast reactors is the energy of neutrons causing fission. Accordingly the components and materials comprising the reactor types also differ. In both the reactors, the neutrons produced in fission are having an energy distribution and can be represented by a Maxwell or Watt spectrum with an average energy of 2 MeV [Lamarsh, 1965]. To slowdown neutrons efficiently to low energies and utilize the higher neutron fission cross-sections, fuel in a thermal reactor is embedded in a slowing down medium called moderator. Generally materials like light water, heavy water, beryllium, graphite etc. with light mass numbers are used as moderators. In fast reactors, moderators are absent to keep the neutron energies in fast range to enable breeding. But the spectrum in a fast reactor will be softer than fission spectrum due to the unavoidable moderation mainly by the in-elastic scattering of neutrons with the structural materials. The absence of moderators and high fuel enrichment due to low cross-sections in fast reactors translates to lower core volume and hence higher power density. It necessitates the use of coolants having better heat transfer properties. The main difference between a thermal and fast reactors are summarised in Table 1.1. Harder neutron spectrum in fast reactors has added advantage that enables the incineration of long lived minor actinides by fission and hence reduces the burden of radio-active waste.

1.2.3 Breeding in Fast Reactors

Two most abundant fertile nuclei are U-238 and Th-232. By a process called breeding, these nuclei can be converted in to fissile nuclides Pu-239 and U-233 respectively. The nuclear transmutation reactions with neutrons are shown below.

$$ {}^{1}_{0}\mathrm{n} + {}^{238}_{92}\mathrm{U} \rightarrow ({}^{239}_{92}\mathrm{U})^{*} \xrightarrow[23.5\ \mathrm{m}]{\beta^{-}} {}^{239}_{93}\mathrm{Np} \xrightarrow[2.35\ \mathrm{d}]{\beta^{-}} {}^{239}_{94}\mathrm{Pu} \qquad (1.2) $$

$$ {}^{1}_{0}\mathrm{n} + {}^{232}_{90}\mathrm{Th} \rightarrow ({}^{233}_{90}\mathrm{Th})^{*} \xrightarrow[22\ \mathrm{m}]{\beta^{-}} {}^{233}_{91}\mathrm{Pa} \xrightarrow[27\ \mathrm{d}]{\beta^{-}} {}^{233}_{92}\mathrm{U} \qquad (1.3) $$

Table 1.1: Comparison of Thermal and fast Reactors

Feature	Reactor Type	
	Thermal	Fast
Average neutron energy	Low (0.0253 eV)	High (100-300 keV)
Fissile concentration (%)	Low (0.7-5)	High (15-25)
Fertile conversion	Low	High
Core volume (litre)	Large	Small
Power density (kiloWatt/litre)	10	400
Thermal efficiency (%)	28	40
Fuel burn-up (GWd/t)	7-40	>100
High level wastes	Produced	Partly incinerated
Neutron flux ($n/cm^2/s$)	10^{14}	5-10 x 10^{15}
Maximum neutron fluence (n/cm^2)	10^{22}	2-10 x10^{23}

In nuclear reactors, such transmutation is parameterised as conversion. Conversion ratio (CR) which is defined as the ratio of fissile mass produced to mass destroyed. Thus,

$$\mathrm{CR} = \frac{\text{Fissile mass produced}}{\text{Fissile mass destroyed}}$$

CR greater than 1 is preferable as it leads to a net gain of fissile material from a nuclear reactor. If CR is greater than 1, it is called as breeding ratio (BR) in which the fissile nuclei produced is greater than that of destroyed. A general expression for breeding ratio [Wyckoff and Greebler, 1974] for a nuclear system from the basic nuclear properties of fissile and fertile nuclei is,

$$BR = \frac{\nu - 1 - \alpha + F(\nu' - 1) - A - L}{1 + \alpha} \quad (1.4)$$

where each term have the following meanings,

F - number of fertile atoms fissioned per fission of fissile nuclide

A - number of neutron absorption by the structural and coolant materials per fission of fissile nuclide

L - number of neutrons leaked per fission of fissile nuclide

ν and ν' - number of neutrons emitted per fission of fissile and fertile nuclide

α - the capture to fission ratio of fissile nuclide

The above equation can be approximated as,

$$BR = \eta - 1 \quad ; \quad \text{where} \quad \eta = \frac{\nu}{1 + \alpha} \quad (1.5)$$

η is a quantity called reproduction factor and it is related to the basic nuclear property of a fissile nucleus. This is defined as the number of neutrons produced per neutron absorbed in a fissile nucleus and is a function of incident energy, as both the average number of neutrons produced per fission ν and the capture to fission α are energy dependant. The variation of ν, α and η are shown in Fig.1.2, Fig.1.3 and Fig.1.4 respectively for the main fissile isotopes.

The condition for breeding is,

$$BR > 1 \quad (1.6)$$

From equation 1.5, it gives, $\eta - 1 > 1$

$$\text{or,} \quad \eta > 2 \quad (1.7)$$

Pu-239 offers highest breeding at fast energies due to higher value of ν and lower value of α and hence a higher η. U-233 is significantly better than U-235 by virtue of its lower α and it could give BR higher than unity even in thermal reactors.

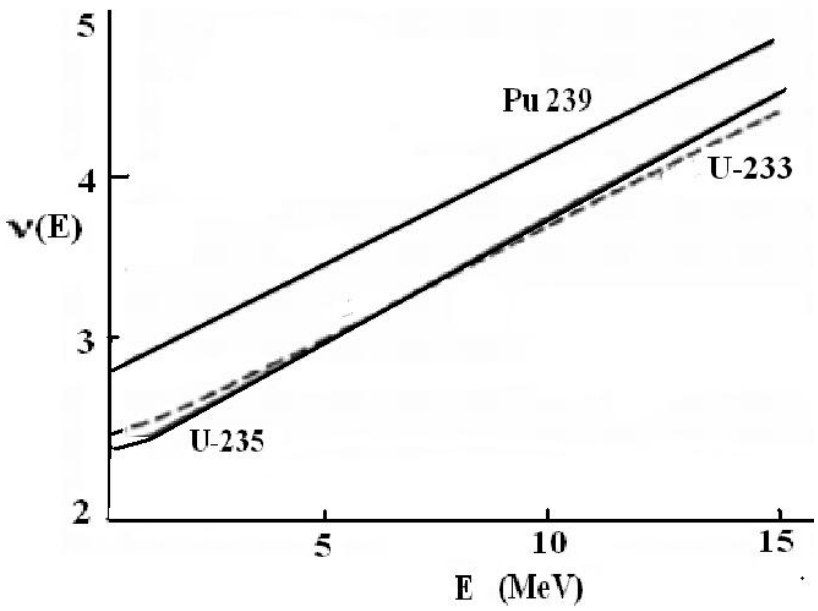

Fig.1.2. Average Number of Neutrons Emitted per fission (ν) for Pu^{239}, U^{235} and U^{233} as a Function of Incident Neutron Energy

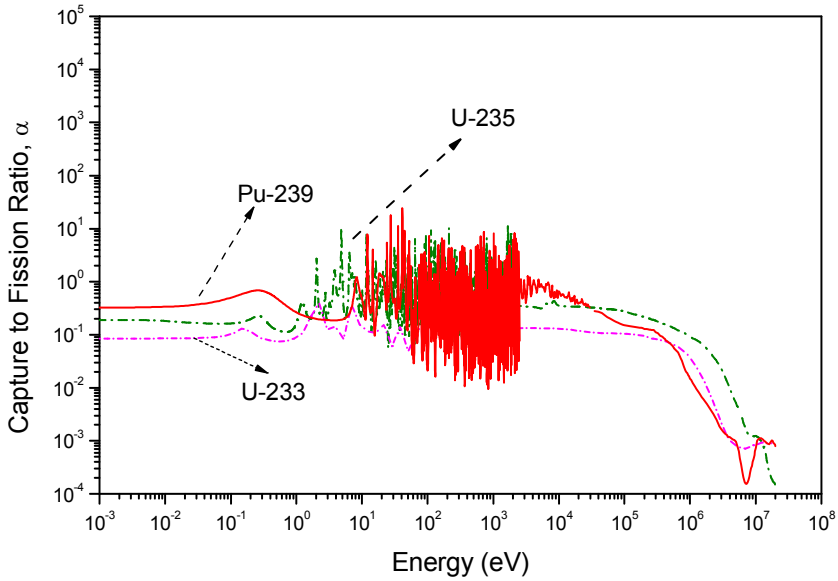

Fig.1.3. Capture to Fission Ratio (α) for Main Fissile Isotopes as a Function of Incident Neutron Energy

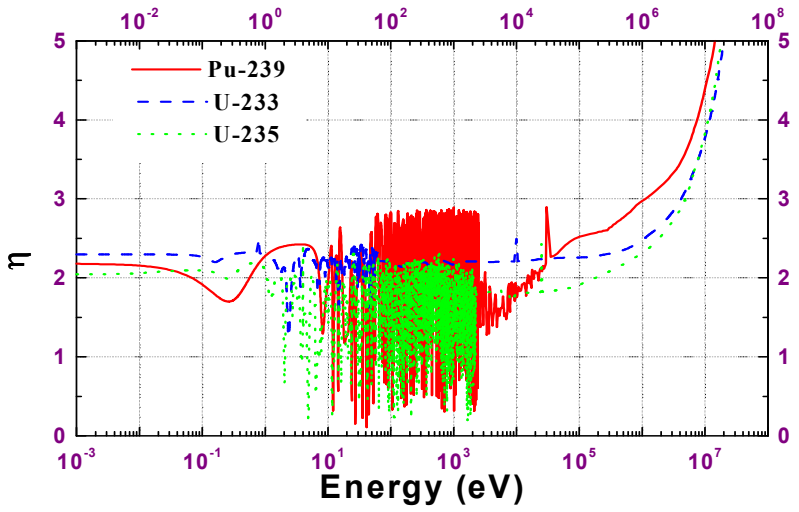

Fig.1.4. Variation of Reproduction Factor (η) with respect to Incident Neutron Energy

The spectrum averaged η for the main fissile isotopes for thermal and fast (medium sized) reactors are given in Table 1.2 [Walter and Reynolds, 1981]. From this table, it is clear that, even η is slightly greater than 2 for Pu-239 or U-235 at thermal energies, thermal breeders are practically difficult to achieve with these fissile fuels due to the neutron losses due to parasitic absorption and leakage. Also the table reveals that it is possible to construct thermal breeders with U-233 as fuel and Pu-239 is a better fuel for fast reactors than U-235.

Table 1.2: Spectrum Averaged η

Flux spectrum	Pu-239	U-235	U-233
LWR	2.04	2.06	2.26
Oxide Fuelled Fast Reactor	2.45	2.1	2.31

1.2.4 The Concept of External and Internal Breeding

Breeding of fissile fuel in fast reactors is possible by using Pu^{239} as the fissile fuel and Th^{232} or U^{238} as fertile material. To achieve breeding, the fissile and fertile material can be

arranged in a fast reactor core in different ways. In external breeding, reactor core is surrounded by pure fertile blanket such that breeding takes place in the blanket due to the neutrons leaking from the core [Walter and Reynolds, 1981]. A schematic of such design is shown in Fig.1.5.

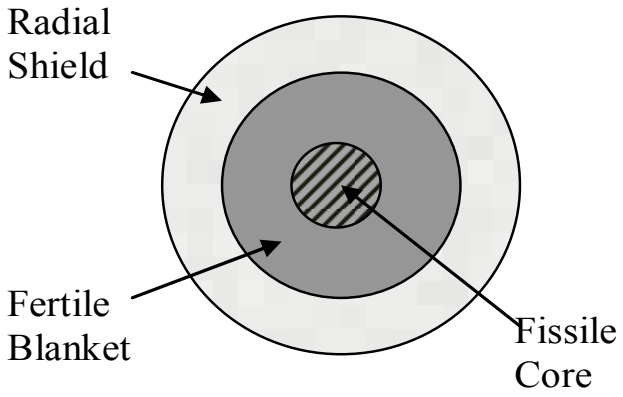

Fig.1.5. Schematic of Fast Reactor Core with External Breeding

In the concept of internal or in-core breeding, the fast reactor core consists of both fissile and fertile materials. Most of the present day fast reactors have adopted this concept. In-core breeding causes less reactivity loss while operation and enable higher fuel burn-up, substantial Doppler effect and enhanced fast fission. The core under this concept can either be homogenous and heterogeneous. In homogeneous cores, fissile and fertile are mixed homogeneously in the fuel sub-assemblies of the core. In heterogeneous designs, sub-assemblies of pure fertile material are interspersed in the core region containing sub-assemblies containing pure fissile or mixture of fissile and fertile material.

Higher breeding ratio and very lower sodium void coefficient are the advantages. Requirement of high fissile fuel inventory and the complexity in the coolant flow channel designs are its main disadvantages. Schematic of homogeneous and heterogeneous designs

are shown in Fig.1.6 [Debanwita Paul et al., 2014]. It has to be noted that, a region of outer fertile blanket can be used in both the homogenous and heterogeneous cores to enhance breeding.

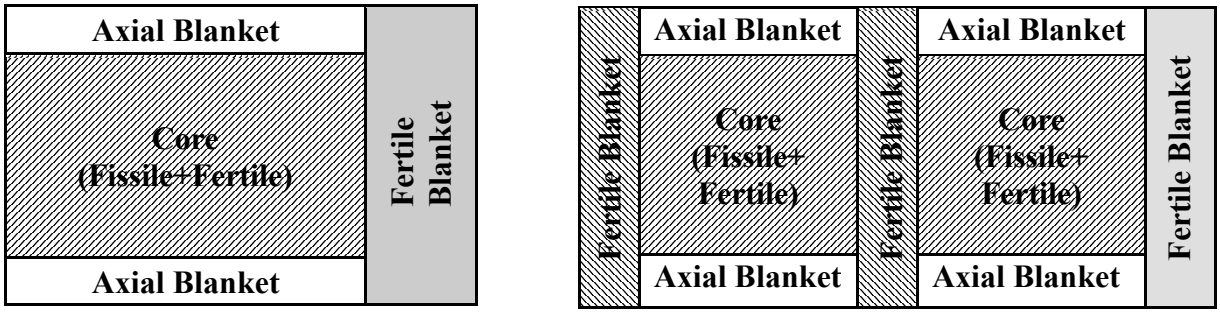

(a) Homogeneous Core **(b) Heterogeneous Core**

Fig.1.6. Typical Sketch of In-Core Breeding using Homogeneous and Heterogeneous Cores

1.2.5 Doubling Time

The rate of production of fissile material compared to the initial inventory is quantified by a term called doubling time (DT). It is the operating time required to produce excess fissile material equal to the initial inventory. For better growth of fissile material, a short DT is desired. It can be defined as,

$$\text{Doubling Time, DT} = \frac{\text{Initial Fissile Mass}}{\text{Net Fissile Mass Production Rate}} \tag{1.8}$$

Based on the scheme of fissile production from fast reactor systems, two types of doubling time are defined. They are simple doubling time and compound doubling time. In simple doubling time, the net bred fissile is removed continuously and stored till it is equal to the initial mass. In compound doubling time, the net bred fissile is returned to the core of the same (or similar) reactor to do further breeding, Now simple doubling time can be further

divided in to reactor doubling time (RDT) and system doubling time (SDT) [Wyckoff and Greebler, 1974].

RDT is the time required for a breeder to produce enough fissile fuel in excess of its own fissile inventory to fuel an identical reactor. It does not account for the fuel cycle external to the reactor. It is defined as,

$$\mathrm{RDT} = \frac{\mathrm{M_0}}{\mathrm{M_g}} \tag{1.9}$$

where M_0 is the initial fissile inventory (kg) and M_g is the fissile inventory gained per year. From the basic core physics properties, RDT can be estimated using the formula [Walter and Reynolds, 1981] given below:

$$\mathrm{RDT} = \frac{2.7\ \mathrm{M_0}}{\mathrm{G}(1+\alpha)\mathrm{Pf}} \tag{1.10}$$

where G is the breeding gain, G=BR-1; P is the reactor thermal power (in MW), α is the capture to fission ratio and ’f’’ is the load factor. For a lower RDT, a small fissile specific inventory (M_0/P) and large breeding gain are desired. This is the minimum time for doubling as it has not considered the fissile fuel losses due to fabrication, reprocessing and nuclear decay.

SDT is defined by considering the fissile fuel mass outside the reactor. Studies show that a breeder reactor will have an out-of-reactor fuel inventory that includes fuel (a) being fabricated (b) being shipped to the plant (c) in storage at the plant awaiting loading or in a cool down period (d) in shipment for reprocessing and (e) being reprocessed. SDT is the time required for a particular reactor to create one additional inventory of fissile for itself and for its requirements of fissile inventory external to reactor. It can be estimated using the formula,

$$\mathrm{SDT} = \frac{\mathrm{EF} \times \mathrm{FBOC}}{(\mathrm{FG} - \mathrm{FL})\mathrm{C}} \tag{1.11}$$

where, FBOC is the fissile material at the beginning of cycle and EF is the ex-reactor factor core. The ex-reactor factor EF is defined such that EF×FBOC gives the total fissile inventory including the inventory outside the reactor. FG and FL are the fissile gained and fissile lost per cycle respectively. The quantity 'C' is the number of cycles per year. (FG-FL) is the net gain per cycle and. SDT will be greater than RDT.

A compound or exponential doubling time assumes that the fissile material produced in a given cycle is continuously re-invested in an identical breeder. It is meaningful only for a power reactor network containing a number of breeder reactors with similar characteristics. In the limiting case of a chain of large number of breeder reactors, compound system doubling time (CSDT) will be less than SDT and it is obtained by the formula [Wyckoff and Greebler, 1974],

$$CSDT = 0.693* SDT \tag{1.12}$$

1.2.6 Advantages of Fast Reactors over Thermal Reactors

In a thermal reactor, the meagre amount of U-235 content is utilized as fissile fuel and the abundant U-238 are largely unused and are disposed as a nuclear waste. With the concept of breeding in fast breeder reactors, using Pu-239 from heavy water reactors as driver fuel, the abundant U-238 can be converted to fissile Pu-239 and hence better fuel utilization is possible in fast reactors. Similarly, the other abundant fertile material Th-232 can also be converted to fissile U-233. Fast reactors using these fuels ensure clean and environmental friendly energy source for the future. As the capture to fission ratio falls at high neutron energies, the actinide elements have more probabilities of fission than capture. The fission of a long lived actinide produces two short lived fission products but the capture converts and retains it as a actinide. It means that fast reactors with low capture to fission ratio can burn

long lived actinides and enables to reduce the problem of long-term storage of radio-active wastes. Hence fast reactors can be chosen to ensure the energy security with reduced radio toxicity.

1.2.7 Fast Reactor Experience

A list of fast reactors operated and/or operating in world are given in Table 1.3. The list consists of Clementine 1&2 which were the first fast reactor, BN-800 of Russia which is just critical in 2014 and PFBR of India which is to be commissioned soon. The power of the reactor and the fuels used are also given in table.

1.2.8 Components of a Fast Reactor

The main components of a fast reactor consists of a suitable nuclear fuel which releases energy by nuclear fission process, a structural material that shields the radioactivity and transfers the heat energy to the coolant, that transfer the heat energy to a heat exchanger. It heats the water to form steam that rotates the turbine of an electric generator to produce electricity. Usually the fuel can be either in ceramic or metallic forms. The ceramic fuels can be classified in to oxide, carbide or nitride and mostly it is oxide due to enough safe operating experience with high burn-up. Most of the fast reactors used liquid metals like sodium as coolant. Pb, NaK, Pb-Bi eutectic etc. are other possible choice. Because of higher fluence and temperature in a fast reactor, stainless steel is used as the structural material.

Table 1.3: A List of Fast Reactors

Reactor	Country	Operation Time	Power (MWt)	Fuel/Fuels Types Used
Clementine	US	1946-1950	0.025	Metallic Pu
Lampre-1/II	US	1961-1963	20/1	Metallic Pu-Fe, Metallic Pu
EBR-I	US	1951-1963	1.0	Metal
EBR-II	US	1964-1994	62.5	Metal
Fermi-1	US	1963-1972	200	Metal U with Zr cladding
FFTF	US	1980-1992	400	MOX
CRBRP	US	Cancelled	975	MOX
SEFOR	US	1969-72	20	MOX
Rapsodie	France	1967-1983	40	MOX
Phenix	France	1973- 2009	563	MOX
Superphenix	France	1985-1997	3000	Oxide
BR-5/BR-10	Russia	1958-2002	8	PuO_2, UC, UN
BOR-60	Russia	1968-	60	Enriched UO_2, UN, (UPu)N
BN-350	Russia	1972-1999	750	Enriched Uranium Oxide
BN-600	Russia	1980- 2010	1470	Enriched Uranium Oxide, MOX
JOYO	Japan	1982-	140	MOX
MONJU	Japan	1980-	714	MOX
DFR	UK	1959-1977	72	Metal
PFR	UK	1974-1994	600	MOX
KNK-II	Germany	1972-1991	58	MOX
FBTR	India	1985-	42.5	Mixed Carbide
CEFR	China	2011-	65	Highly Enriched Uranium
BN-800	Russia	2014-	2100	MOX
*PFBR	India		1250	MOX

**Will be critical soon*

1.2.9 Pool and Loop Type Fast Reactors

Depending upon the arrangement of pumps and heat exchangers in the reactor, fast reactor cores can be either loop type or pool type. In loop type reactors, the primary coolant is circulated through the primary heat exchangers kept outside the reactor vessel. In pool type, the primary heat exchangers and pumps are immersed in the reactor vessel. Each of these has its own advantages and disadvantages. One main advantage of pool type reactors is its large thermal capacity of sodium which can acts as heat sink during transients.

1.2.10 Fast Reactor Fuels

Fast reactor fuels are of different types; ceramic, metallic and dispersion are examples. A ceramic fuel can be further classified in to oxide, carbide and nitride. All are having its merits and demerits. A comparison between these ceramic and metallic fuel types and their important properties are shown in Table 1.4. Among the fast reactor fuels, metal fuels have the maximum fissile and fertile fractions and hence provide the hardest neutron spectrum and gives the maximum BR and hence minimum doubling times. In addition to high breeding, metal fuels have other advantages. Its higher thermal conductivity and coefficient of thermal expansion which enables passive response to the loss of flow and loss of heat sink accidents. Due to the lower absorber rod worth requirement and low reactivity coefficients of metal fuels, the severity of UTOP (unprotected transient over power) accidents will be less. High thermal conductivity causes a reduction in the stored heat in the fuel and helps to reduce the severity of such accidents.

Also, metal fuels have excellent compatibility with liquid metal coolants, helps to have a benign run beyond cladding breach (RBCB) performance compared to oxide fuels. Metal fuels can be fabricated with close dimensional tolerance. Also, they can be recycled

through pyro-reprocessing methods in which low level radioactive fission products are separated and high level actinides are allowed to be with the recycled fuel. It helps the non-proliferation of nuclear materials. Due to the harder neutron spectrum with metal fuels, better actinide incineration is possible. Hence, metal fuel enable the reduction of radio toxicity of the spent fuel to the back ground radiation levels within few hundreds of years compared to tens of thousands of years in once through fuel cycle. It is envisaged that metallic fuelled FBR cores have been chosen in India as it enables safe, non proliferated, economic and faster growing nuclear energy production.

1.2.11 Fast Reactors in India: Present and Future

FBTR is a 40 MWt, loop type and carbide fuelled fast reactor working since 1985 in Kalpakkam [Srinivasan et al., 2006], India. It is a test bed for fast reactor fuels and materials. It has completed 20 irradiation campaigns. The reactor operated up to a maximum power level of 20.3 MWt and sodium outlet temperature of 540 ^{o}C. Its unique carbide fuel has set an international record in burn-up of 165 GWd/t. The performance of sodium systems in FBTR for the past 27 years has been excellent. Also the sodium pumps and steam generators have excellent working experience. PFBR oxide test fuel is irradiated in FBTR to a burn-up of 112 GWd/t and discharged for post-irradiation examination (PIE). Both natural and enriched (14.8%) U-6%Zr fuelled and sodium bonded metallic pins are under irradiation in FBTR [Vasudeva Rao et al., 2013]. Irradiation of three sodium bonded pins of U-19%Pu-6%Zr is initiated and planned to be discharged for PIE after achieving burn-up of 25 GWd/t [IGC Newsletter, 2014]. In addition, a 500 MWe, sodium cooled and MOX fuelled, pool type prototype fast breeder reactor (PFBR) is constructed and planned to be commissioned in 2015 [Chetal et al., 2006].

Table 1.4: Comparison of Fast Reactor Fuels

Properties	Fuel Type			
	Oxide	Carbide	Nitride	Metallic
Fuel Constituents	$(U,Pu)O_2$	(U,Pu) C	(U,Pu)N	U-Pu-10%Zr
Theoretical Density (g/cc)	11.04	13.58	14.32	15.73
Melting Point (^oC)	2810	2477	2799	1127
Thermal Conductivity at 1000 K/2000 K ($W/^oK$)	2.6/2.4	18.8/21.2	15.8/20.1	40
*BR	1.1 – 1.15	1.2 – 1.25	1.2 – 1.25	1.35 -1.4
Swelling	Moderate	High	Moderate	High
Handling	Easy	Pyrophoric	Inert atmosphere	Inert atmosphere
Compatibility- clad	Average	Carburization	Good	Eutectics
Compatibility-Coolant	Average	Good	Good	Good
Dissolution/ Reprocessing	Good	Demonstrated	Risk of C-14	pyro-processing
Fabrication/Irradiation Experience	Large, Good	Limited	Very little	limited

**the value quoted for an FBR core of 500 MWe size*

After getting enough experience in commissioning and commercial operation of fast breeder reactors, it is planned to shift to the use of metallic fuels for a faster growth of nuclear energy [Grover and Chandra, 2006; Chetal et al., 2011]. Towards achieving the goals of closed metal fuel cycle with metal fuel fabrication and reprocessing, research programs have been initiated at IGCAR [Chetal, 2009]. Also heterogeneous cores with better safety and breeding are also envisaged for future.

1.3 Literature Survey on Metallic Fuelled Fast Reactors

The basic thermal and neutronic performance of ternary metal alloys (U-Pu-Zr) as a fast reactor fuel is better than oxide and other ceramic fuels [Chernock and Horton, 1994;

Dubberley et al., 2000]. It includes the harder neutron spectrum which results in higher BR and lower doubling times. Harder spectrum and lower operating temperature leads to lower Doppler feedbacks and hence reduces the positive reactivity to be inserted during reactor start-up. Low burn-up reactivity swing due to high BR and the lower Doppler feedback helps to reduce the control rod reactivity requirement [Fujita and Wade, 1990]. It is possible to achieve a near zero burn-up swing per cycle in metal fuelled reactor core due to high internal conversion ratio [Dubberley et al., 2000]. Metal fuelled core designs with high burn-up of ~150 GWd/t have been reported [Dubberley et al., 2003].

One of the main safety concerns in the selection of metal-fuels in medium and large sized fast reactors is its high positive sodium void worth [Chernock and Horton, 1994; Fujita and Wade, 1990; Yokoyama et al., 2005, Khalil and Hill, 1991] for an unprotected loss of flow (ULOF) accident. It is reported that making the core more tightly coupled and by flattening the core shape results in reduced sodium void worth, though it will lead to a reduced BR and a higher burn-up reactivity swing [Khalil and Hill, 1991]. In another method, by including a sodium plenum as attempted for oxide fuelled BN-800 design [IAEA, 2000] and by using plutonium having less Pu-241 fraction [Yokoyama et al., 2005] its value can be reduced. The compromise of this optimization is less breeding ratio and higher burn-up reactivity swing. In this section, a brief review of irradiation behaviour of metallic fuels and their safety performance during various transients is discussed. Also, the methods of perturbation theory employed for the safety analysis are also reviewed.

1.3.1 Irradiation Experience of Metallic Fuels in Fast Reactors

First prototype fast reactors during the period of 1945-1960 are operated with metallic fuels. It include two reactors of LAMPRE (Los Alamos Molten Plutonium Reactor Experiment) of Argonne National Laboratory (ANL), Experimental Breeder Reactors 1&2 (EBR-I, EBR-II) developed by ANL and Fermi Lab [Hofman, 1980]. All these reactors are situated in United States. Dounreay Fast Reactor (DFR) in United Kingdom is another example with metallic fuels. In general, the metallic fuel can be enriched uranium or plutonium in its pure metallic form or an alloy (binary or ternary) with other metals like Zr, Fe, Mo etc. A survey of different compositions of metallic fuels used in the early reactors have been done and shown in Table 1.5 [Kittel et al., 1993]. Fissium (Fs) mentioned in the table is a group of noble fission products Mo, Ru, Rh, Pd, Zr and Nb retained with the metallic fuel used in EBR-II.

Achievable burn-up of metallic fuels in initial reactor designs were limited due to the poor fuel pin performance. The main concern was the fission gas retention due to higher smear density and the resulting enhanced radial swelling. The other major concern was its poor chemical compatibility with the steel cladding and the resulting eutectic formation [Hofman et al., 1997]. To prevent fuel-clad chemical interaction (FCCI), fuel composition is modified such that elements like Zr, Mo etc. is added in the fuel that prevents the inter-diffusion of fuel and clad constituents by forming a diffusion barrier at the fuel-clad interface. Out of these elements, Zr is the best option due to its better compatibility. Addition of Zr helps to increase the solidus temperature of the fuel; it increases by $\approx 13\ ^{o}C$ for each percent of zirconium present for a 20% plutonium alloy. Also the addition of Zr improves its dimensional stability during irradiation.

Reduction of thermal conductivity and decrease in BR achievable are the disadvantages of Zr addition.

The studies revealed that the selection of the ternary fuel U-Pu-Zr could give higher burn-up. Tests to study the impact of design parameters like fuel smear density, zirconium content in the fuel, fission gas plenum volume and cladding types, which can affect the overall fuel performance, was carried out in EBR-II. This irradiation experiments was called DP-1 (design parameters). In this test, these key design parameters were systematically varied from the reference fuel of U-Pu-Zr alloy with 19 wt% Pu. The following parameters are changed and the impact on the fuel performance was studied.

- Effect of fuel smear density on fuel-clad mechanical interaction (FCMI) and fission gas release.
- Effect of Zr in fuel restructuring and fuel/cladding compatibility.
- Impact of plenum to fuel length ratio (P/F) on fission gas pressure on cladding.

  The values of P/F used were 1.1, 1.5 and 2.1.
- Effects of different cladding materials (Martensitic steel HT9 or austenitic stainless steel D9).

The effect of smear density on the gas release is studied and the results are shown in Fig.1.7. The smear densities considered are 70, 75, and 85% of theoretical density (TD). As shown in figure, the maximum gas release occurs at smear density of around 75% with minimum clad-strain. It is also observed that a constituent redistribution occurs in high plutonium fuels. The effect of Zr on the fuel restructuring is studied by varying Zr in the fuel. Zr concentrations chosen were 6, 10, and 14 wt%.

Table 1.5: Metallic Fuel Compositions Used in Early Reactors

Reactor Name	Core	Fuel Composition	Initial Operation	Country
Clementine		Pu	1949	USA
EBR-I	MARK-I	U	1951	USA
	MARK-II	U-Zr	1954	
	MARK-III	U-Zr	1957	
	MARK-IV	Pu-Al	1962	
LAMPRE-I		Molten Pu-Fe	1959	USA
LAMPRE-II		Molten Pu-Fe	1962	
DFR	MARK-II	U-Cr	1963	UK
	MARK-IIA,B,C	U-Mo	1963	
	MARK-IIIA,B,C	U-Mo	1964	
EBR-II	MARK-I. IA	U-Fs	1964	USA
	MARK-II	U-Fs	1973	
	MARK-III.IIIA, IVA	U-Zr	1990	
	MARK-V	U-Pu-Zr	1995	
Fermi		U-Mo	1966	USA

Fig.1.8 shows the results of such post irradiation studies of U-Pu-Zr fuel (Pu-19 wt% and Zr-10 wt%) pins corresponding to 1.9% atom burn-up. Significant migration of fuel constituents is clearly seen in the figure. There is an accumulation of Zr at the centre and at the boundary with depletion of U at these positions. U concentration is increased in the middle [Pahl et al., 1990]. The redistribution of Zr in the central increase the fuel solidus temperature and at the outer regions helped to increase the fuel-clad eutectic temperature and compatibility. Significant changes in the Pu concentration are also observed. These types of restructuring are found to be seen for fuel compositions containing 15 wt% Pu or greater; fuel containing 8 wt% Pu or less did not show significant restructuring except for a rather

homogeneous development of fission gas bubbles and grain boundary cavities. It is reported that Zr starts to migrate to the centre region, only when the temperature in the centre region exceeds 1020 K. It is also found that there is no effect of Zr on fission gas release and fuel axial elongation. Even the fuel restructuring increases the radial swelling, it causes a reduction of axial expansion.

Different clad materials like 20% cold worked D9, SS-316 steel etc. are chosen for the test. The results of such tests are given in Fig.1.9. It is found that clad of 20% cold worked HT9 shows the minimum strain with burn-up. The clad-strain as a function of Zr content in the fuel and plenum to fuel ratio is estimated and the variation is as shown in Fig.1.10. From the figure, it is clear that the amount of zirconium in the fuel pellet don't have an influence on the clad-strain. Also clad-strain is measured as a function plenum to fuel ratio. It is found that the clad-strain is almost constant with respect to the ratio of plenum to fuel lengths.

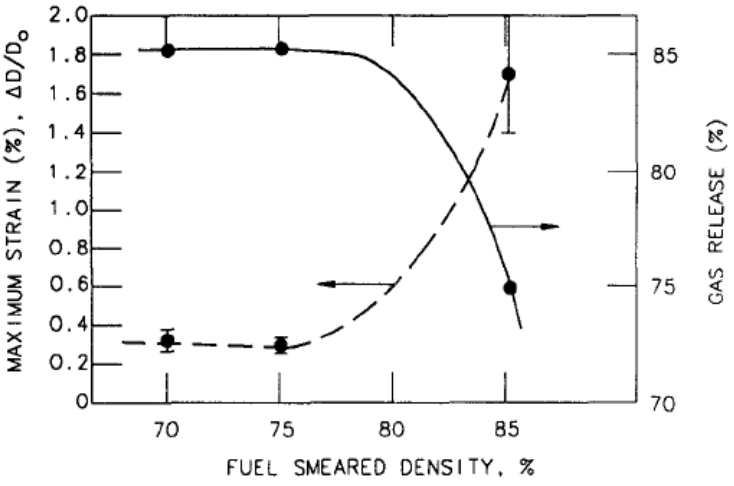

Fig.1.7. Effect of Smeared Density on Gas Release and Clad-Strain for HT-9 clad with U-19%Pu-10%Zr Fuel

It was concluded from the results of the tests that an optimum design parameters for better reliability and high burn-up could be taken like:

- Ternary fuel of U-20Pu-10Zr
- Smear density ≈75% TD
- Low swelling HT-9 cladding
- Sodium bonded pins
- Plenum/fuel ratio ≈1.5.

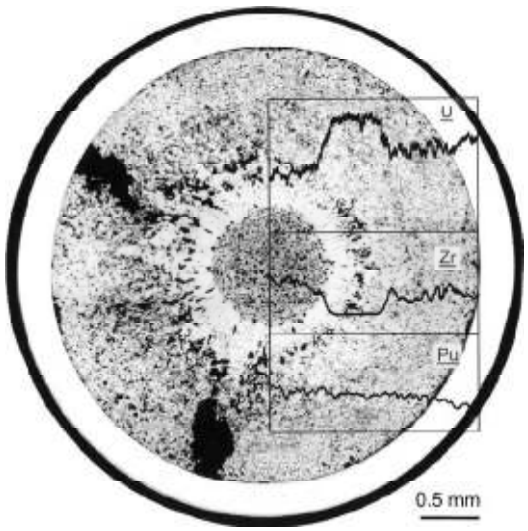

Fig.1.8. Distribution of Pu, U and Zr in the U-19Pu-10Zr Fuel Pin at 1.9 at% Burn-up

With this choice of fuel composition and pin design as above, more than 19 at% burn-up have been successfully attained in EBR-II [Walters, 1999] with fuel pin size of 4.4 mm diameter and 34.3 cm long [Chang, 2007]. The tests are repeated in Fast Flux Test Facility (FFTF) with 90 cm long [Wright, 1990] fuel pins of commercial reactors and similar results are obtained [Carmack et al., 2009].

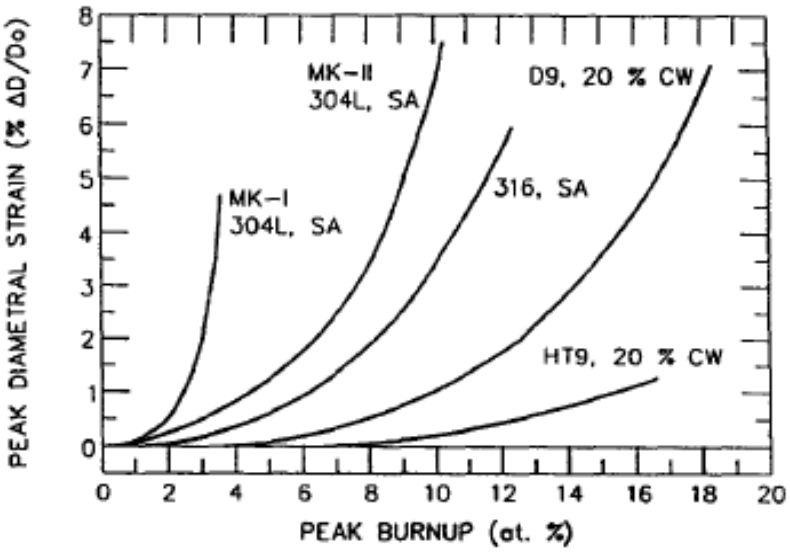

Fig.1.9. Cladding Strain as a Function of Peak Burn-up of Metal Fuels for Different Clad Materials

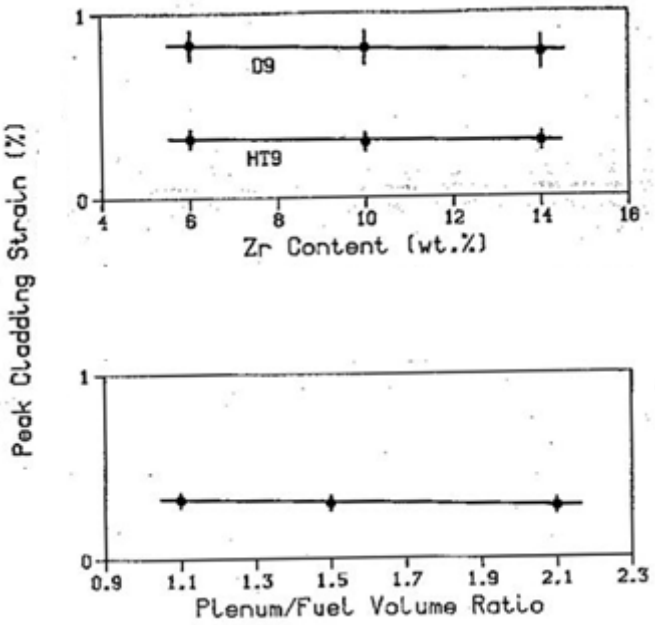

Fig.1.10. The Variation of Clad-Strain as a Function of Zr Content in the Fuel and the Ratio of Plenum to Fuel Volume Ratio

As already stated, breeding potential possible with metallic fuels decreases with the addition of Zr in the fuel. It means that binary metal fuels without zirconium can provide the

maximum BR, but the use of such fuels are constrained by the lack of irradiation experience. Irradiation experience of metallic fuels having Zr up to a minimum of 6 wt% is available in the literature [Pahl et al., 1992].

1.3.2 Inherent Safety of Metal Fuels during Transients

Because of better thermo-dynamic and neutronic properties, metal fuel behaviour during transients is superior to ceramic fuels. The main transients considered are the unprotected accidents of loss of flow (ULOFA), transient over power (UTOPA) and loss of heat sink (ULOHS). This has been proved in EBR-II. ULOFA in EBR-2 demonstrated the benign behaviour [Ott, 1988; Planchon et al., 1987]. Due to higher thermal conductivity, the stored heat in the metal fuels during the transient is less. Higher thermal conductivity of metal fuels and higher gap conductance of sodium helps to have lesser temperature gradient across the fuel pin. Also operating temperature of metal fuels is lesser compared to oxide fuel, and provides lesser temperature gradient across the fuel pin. The Doppler feedback during a transient is less for metallic fuel and causes lesser feedback in reactivity. The higher gap conductance of sodium bonded metal fuel implies a reduced thermal time constant (Hummel and Okrent, 1970) and small temperature swing between zero and nominal powers which reduces the amount of reactivity required to bring the reactor to zero power during ULOFA.

Due to the accident, primary flow reduces and causes rise in outlet coolant temperature. This rise in temperature causes thermal expansion of core components (mainly fuel SA) and enhances neutron leakage and slows down chain reaction. It introduces a negative feedback, rise in power and temperature stops and eventually brings to a asymptotic value. The variation of outlet temperature during such an incident is shown in Fig.1.11

[Chang, 2007]. Also it can be seen that the experimental results are matching with the predictions.

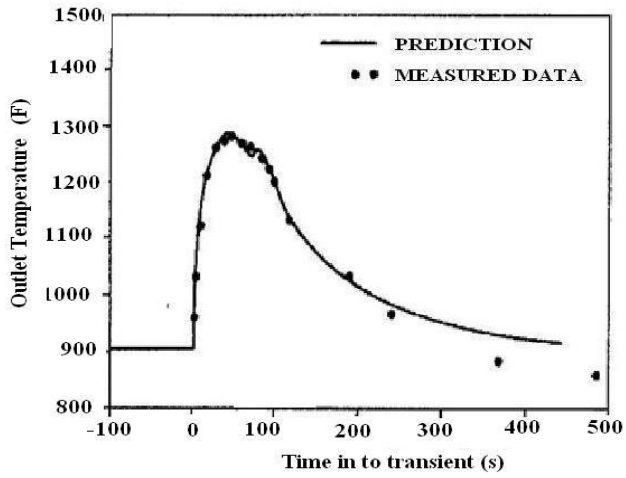

Fig.1.11. Experimental and Predicted Temperature Profiles in EBR-II during ULOFA as a Function of Time

Uncontrolled withdrawal of control rods without SCRAM (UTOPA) causes increase in reactivity, power and rise in temperature of fuel and coolant. The low operating temperatures of metallic fuels provides reduced Doppler feedback and the high breeding helps to reduce the burn-up reactivity swing. Both reduces the control rod requirement and lesser positive addition during a UTOP and hence reduces the severity of UTOP in metal fuelled FR. Low burn-up reactivity swing also helps to extend core life. A transient overpower (TOPA) test performed in Transient Reactor over Power Facility (TREAT) shows that metallic fuels having larger margins to cladding failure threshold compared to oxide fuels [Chang, 2007].

Unprotected loss of heat sink occurs due to the shutdown of intermediate pumps. The primary is isolated and the inlet temperature increases. Due to the thermal expansion and

enhanced neutron leakage power reduces and the outlet temperature reduces. This has been proved in EBR-II experiment and shown in Fig.1.12. All the above discussion shows the superior inherent passive safety features of metallic fuels.

1.3.3 Perturbation Theory in the Safety Analysis of FBR Cores

Perturbation theory has been used for reactor analysis and design calculations [Gandini, 1967]. In the standard perturbation theory, first-order and exact perturbation analysis is performed to find the changes on neutron multiplication factor with a perturbation to the core. For small perturbations applied to a reference core, first order perturbation theory is a useful approximation [Ronen, 1986]. This can be often used in FBR analysis, to find the reactivity change due to sodium density changes and to find the feedback reactivities during a transient [Kobayashi and Hirakava, 1987]. This has been used for various sensitivity analysis in core physics [Saito and Katsuragi, 1969] and shielding applications [Daniel Fieno, 1972].

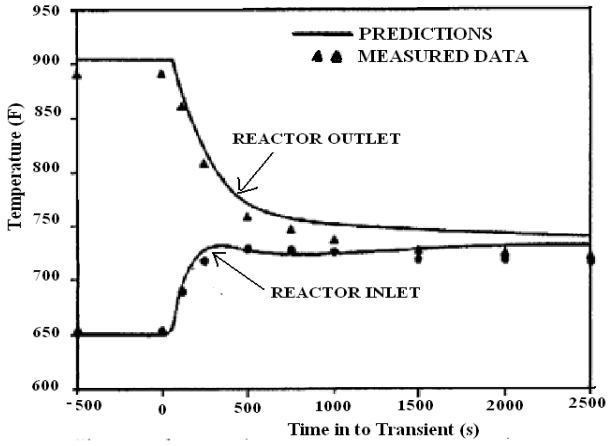

Fig.1.12. Temperature Vs Time for ULOHS Prediction and Experiment from EBR-2

The advantage of using perturbation calculations in reactor analysis over the direct methods are as follows. First, for very small perturbations, an exact perturbation analysis can provide accurate results as it is free from convergence errors. Second is that it can give the total reactivity change with perturbation as the sum of the individual components like

leakage, capture, fission etc. Also, the spatial distribution of the total reactivity change in the reactor zones, is possible with perturbation calculations, and this will be a useful input in the transient analysis to find the feedback reacitivites. In addition to the sodium void worth estimations, Doppler reactivity effect, material removal worths and core expansion feedbacks also can be estimated using perturbation theory. For example, the reactivity feedback with a possible core deformation is reported [Shikhov, 1960].

Sodium voiding is an important safety concern for medium and large fast reactors as it is a positive reactivity feedback effect. It is shown that for small sodium void perturbations, exact perturbation estimation with transport theory corrections predicts the experimental results within 10% accuracy [Kappler, 1984]. As there is a difference between the predictions of first order and exact results of even small sodium void reactivity, the adequacy of the use of the former for the sodium void worth prediction of medium and large sized power reactors has to be investigated. The effectiveness of the first order approximation to the estimation of reactivity change due to any arbitrary perturbations can be tested by an exact perturbation theory codes [Azekura and Hayase, 1989].

The results of such a first order analysis have been widely used in IGCAR for the safety analysis of PFBR [Harish et al., 2009] as the perturbations involved are assumed to be small. Transients analyzed are restricted up to the time of initiation of sodium boiling. Also a first order perturbation analysis has been performed for the safety analysis of FBR cores using different fuel types [Singh et al., 1994]. In all these analysis, first order perturbation code NEWPERT [John, 1984] has been used to find the approximate reactivity change with perturbation and its spatial distribution.

1.3.4 Behaviour of FBR Cores during ULOFA

As the fuel in a fast reactor is not in the most reactive configuration, safety analysis of FBR cores during transients is important. The safety systems can be classified in to active, passive and inherent. SCRAM provided to active systems requires an activation signal to function. Passive systems do not depend on activation signal, but function automatically based on some physical criteria like temperature, magnetic property etc. Even though, it is not rely on any activation signals, safe shutdown may further prevented by additional failures of the system. In depth safety of a fast reactor can be ensured by inherent safety phenomenon, as they are the result of inherent physical phenomenon like thermal expansion and gravity that don't have a probability of failure [Wigeland, 2011]. It is important to analyze the capability of a FBR core to shutdown inherently during severe accidental conditions. Among the three FBR accidents, the severity of UTOPA can be minimized by control rod design optimization such that the reactivity insertion due to uncontrolled withdrawal can be restricted within allowed safety limits [Yokoo and Ohta, 2001]. This is especially true for metallic fuelled FBR cores which have low excess reactivity, low control rod worth and favourable thermo-physical properties. The severity of ULOHS accident can be minimized by pool type designs which provide longer time constants.

The ULOFA is assumed to be initiated by a total loss of offsite power and the resulting failure of pumps. It is also assumed that the SCRAM systems are not available in the event and the reactor power varies in accordance with the feedback reactivity only. Now the reactivity feedback is a function of flow coast down of pumps, which depends on their inertial characteristics only [Cahalan et al., 1990]. During a ULOFA, the core will undergo through 3 phases of pre-disassembly, transition and disassembly [Chellapandi, 2103]. In the

pre-disassembly phase, reactor power decreases due to the dominating negative feedback from core radial expansion. In the transition phase, reactor power starts to increases due to the initiation of positive feedback from sodium voiding. Once the voiding spreads to core centre, power excursion and rapid temperature rise happens, and ultimately leads to core meltdown. It constitutes the dis-assembly phase.

Various studies are reported on the inherent safety properties of FBR cores. Inherent safety performance of oxide and metal fuels during transients are studied on a large sized FBR core [Royl et al., 1990; Cahalan et al., 1990; Ott, 1988]. In these studies, the net reactivity of the core is calculated as the sum of feedback reactivities. Flow coast down due to pump failure is represented by a flow halving time – the time required for flow reduction by 50%. The net reactivity and temperatures are obtained as a function of time after the initiation of the event. These studies ensure the better inherent safety performance of metal fuels over oxide and other ceramic fuel types. Most of the above studies are performed using different versions of the SAS code.

The shutdown capability of a medium sized (500 MWe) liquid-metal FBR during ULOFA as a function fuel type has been reported using static and dynamic analysis methods from IGCAR scientists [Singh et al., 1994]. Oxide, carbide and metal fuels are chosen for this analysis and the analysis has shown the superior safety of metal fuels. In this study, the feedback reactivity are estimated using the code PREDIS [Harish et al., 1999], which predicts the transient behaviour in the pre-disassembly phase. The various feedback reactivities due to a temperature change in the core due to flow reduction were estimated from the distribution of material removal worths, Doppler effects and boundary movement

worths, which were predicted with the first order perturbation code NEWPERT. The main inherent reactivity feedbacks during ULOFA event is given in the following paragraph.

The first and abrupt feedback is from the Doppler effect of neutron absorption cross-section in reactor materials. Among the different reactor materials, the main contribution to this feedback is from fuel and its magnitude depends on fuel choice. The net reactivity feedback due to Doppler effect is governed by the value of Doppler coefficient and the temperature gradient during a transient and hence depends indirectly on other properties like fuel thermal conductivity and sodium flow rate. The feedback contribution from coolant is due to the density changes that alter its moderating, leakage and capture properties. As the coolant temperature is immediately affected by the transient, this feedback is also quick. The magnitude of this reactivity feedback is highly space dependant for a particular core and the net value is decided by the size and compactness of core. The reactivity feedback due to dimensional changes along the axial direction during a transient will be decided by the thermal expansion coefficient of fuel and cladding along with the temperature changes. As fuel SA worth shows a clear radial dependence in FBR cores, core dimensional changes during a transient also lead to reactivity feedbacks. The net feedback due to this effect can be further divided in to the effects of SA bowing and grid plate expansion, the latter shows a slower response. The expansion or contraction of control rod driveline changes the insertion length of control rods inside the core and provides a feedback on the net core reactivity. As coolant temperature increases during a transient, sodium expansion provides positive feedback and other feedbacks give negative contribution to the net reactivity. With temperature reduction, feedbacks show the reverse trend to the net reactivity.

1.3.5 Sensitivity Studies in FBR Safety Analysis

As mentioned, the response during a transient is decided from the feedback reactivities of Doppler, fuel axial expansion, coolant expansion, core radial expansion and control rod drive line expansion. In addition, the flow coast-down time has an important effect on the coolant peak temperature during ULOFA. Now the uncertainties in the neutronic calculations strongly affect the core radial expansion due to the strong radial dependence of fuel SA worth in an FBR core. Axial expansion of fuel is governed by the fuel–clad interaction. Doppler feedbacks are sensitive to the accuracy of nuclear cross-sections. In short, all the feedback parameters which govern the core response during ULOFA are sensitive to the models, methods, codes, time constants and nuclear cross-sections used for their estimation. To ensure a safe and reliable reactor operation, a sensitivity analysis of transient behaviour with respect to the accuracy of feedback parameters is necessary. A sensitivity study on unprotected transient behaviour with respect to flow halving time and core radial axial expansion are reported [Endo et al., 1990]. This study reveals the high dependence of flow halving time on the peak coolant temperature and proves that the core radial expansion is the main negative feedback component during transient. A similar analysis is performed on a medium sized FBR core with respect to the flow coast down time [Singh et al., 1994].

1.4 Works Performed for the Thesis

In India, fast breeder reactors having shorter DT are essential for faster growth of energy production and enabling energy security. In this context, metal FBRs are chosen for future reactors as they have higher BR compared to oxide and carbide based FBRs. The experience based on EBR-II and FFTF experiments revealed that metal FBRs have the

capacity of high breeding and improved safety characteristics. But, the core characteristics in a commercial power reactor could be different from these experimental reactors due to the changes in power, fuel composition, core geometry, neutron spectrum etc. In addition, the main design rationale of the above experimental reactors was not breeding, it is important to re-assess the neutronic behaviour of commercial metal FBR cores including breeding and safety before their actual launching.

A safe and reliable commercial FBR design is possible to be conceived if the above characteristics (neutronics and safety) are properly assessed for different cores having varied power. With this background, a study is made on the FBR core optimization with respect to breeding and safety parameters.

1.4.1 Breeding Potential and Safety Parameters of Metal Fuelled FBR Cores as Function of Core Size and Zr Content

First topic of the research is to find the dependence of BR on the Zr content in ternary metallic alloy U-Pu-Zr for various reactors having different size. Variation of BR with Zr is studied in the range of 0% - 10%. This study is important to choose a metallic fuel type to achieve maximum possible BR, but, at the same time they should have enough irradiation experience. The analysis is performed in three FBR cores of different sizes. It consists of a small core (120 MWe) of experimental size, a medium sized (500 MWe) commercial reactor and a large core of 1000 MWe size. In addition to BR, the dependence of reactor doubling time with fuel type and core size is also analysed as it governs the production rate of fissile fuel and the associated fuel doubling. Important safety parameter of sodium void worth as a function of Zr content and core size is also computed. Other core physics parameters of Doppler constant, core enrichments, delayed neutron fraction and neutron life times are also investigated.

One important problem with metallic fuel is its swelling characteristics and the associated pellet-clad interaction and the resulting burn-up limitations. This pellet-clad interaction is more in fuels with lesser Zr which can provide more breeding. The pellet clad interaction can be reduced by the introduction of a barrier material to prevent the clad interaction. The influence of these barrier materials on breeding characteristics and other important core physics parameters is also studied. To improve the safety during transients, two methods available for reducing sodium void worth are applied to a 1000 MWe metallic core and their influence on the main core physics parameters are investigated. The above study is performed with 2D diffusion analysis.

Based on the available irradiation experience of metallic fuels, Zr in the ternary metallic fuel is chosen as 6% and the present study helped to find the breeding and safety parameters corresponding to this fuel as a function of core size. In addition, the study is important to understand the variation of breeding and safety characteristics of metallic fuelled FBRs with respect to core size, fuel pin designs and the methods adopted to reduce sodium void worth. Hence, the study helps to design safe and economic metallic FBR core designs with high breeding.

1.4.2 1st Order and Exact Perturbation Analysis of FBR Cores

In IGCAR, the data based on first order perturbation theory has been used for FBR safety analysis. The basic assumption is that the perturbation applied to the core is small during a transient and before initiation of disassembly phase. But during the transient, sodium voiding may occur in a large scale and the 1st order approximations to flux change may fail. The effectiveness of the first order approximation to the estimation of reactivity change due to any arbitrary perturbations has been tested by developing an exact perturbation

theory code PERTX. Both the first order and exact option of perturbation analysis is possible with PERTX. The direct (2-k) methods are performed to validate the worths estimated using exact methods. In direct method, the multiplication factors of the reference and perturbed core are estimated by diffusion calculations and are used to find the exact reactivity change due to perturbation. The newly developed perturbation code system consists of a 2D diffusion code ALCIALMI, ABBN-93 evaluated multi-group nuclear data and the code PERTX. This can be further used for the estimation of the errors involved in the 1st order prediction of safety parameters and material removal worths. This system has the capability to compute the first order and exact estimated material worths, boundary movement worths and Doppler constant. The errors involved in safety parameters due to 1st order perturbation approximation are studied in a 500 MWe oxide core. This code system has been validated against the results based on well known ERANOS 2.1 system. Details of these studies are discussed in this thesis.

1.4.3 Transient Behaviour of Metallic fuelled FBRs as a Function of Core Size and the Approximations in Perturbation Methods

The third topic of the research is to investigate the ULOFA transient behaviour of metallic fuelled cores as a function of core size. Three different sizes of cores, ie, small, medium and large are taken in the analysis. The code PREDIS is used for the analysis up to the initiation of dis-assembly phase. Here the analysis is carried out using the material removal and Doppler worths estimated using the 1st order perturbation theory assuming the perturbations during transients are small. The feedback reactivity effects are from sodium (expansion and voiding), core radial expansion, fuel axial expansion and Doppler effects in fuel. All these feedbacks are a function of temperature change and perturbation worths. With respect to safety, the duration of pre dis-assembly phase during a transient is also important.

In reality, a large perturbation occurs in the core during a transient, especially in the case of sodium voiding from core centre. Thus, the first order perturbation assumption fails. Transient analysis using exact perturbation theory is also carried out for all these cores by using the data generated using PERTX code. This study is performed to check the applicability of first order approximation of reactivity changes in the transient analysis. The temperature coefficient, power coefficient and its components are estimated as a function of core size and approximations in perturbation method.

A sensitivity analysis on the ULOFA transient behaviour of metallic fuelled FBR cores with respect to the main feedback contributions are also carried out. Main feedbacks considered for sensitivity analysis are sodium density changes and core radial expansion. These feedbacks cause positive and negative contributions to the net reactivity respectively. An uncertainty of 20% is considered for the main feedbacks in the unfavorable direction. The analysis is carried out for both the medium and large reactor cores for which the sodium void worth is highly positive. This study is important for the optimization of metallic FBR cores with respect to ULOFA transient behaviour.

1.5 Organization of the Thesis

Chapter 1 of the thesis gives the scope of study, literature survey of both static and transient performances of metallic fuelled FBR cores. It also gives various topics addressed in the present research. Then the problems addressed in the present study are explained briefly. Chapter 2 describes the basic calculation scheme of static diffusion, perturbation and ULOFA transients. Chapter 3 describes the results of research performed on metallic fuels of different Zr contents and as a function of core size. Effects of design modifications for reduction of sodium void worth are also explained. Chapter 4 describes the study performed

on the first order and exact perturbation analysis of material void worths and safety parameters. Chapter 5 gives the variation of ULOF transient behaviour of metallic fuelled FBR cores as a function of FBR core size and the approximations in perturbation method for the reactivity feedback parameters. Chapter 6 gives the conclusions and the possible future studies.

Chapter 2

CALCULATION SCHEME

2.1 Introduction

The neuron distribution inside the reactor core is described by the time dependant Boltzmann transport equation which is a linear integro-differential equation with seven variables and given below [Lewis and Miller, 1993].

$$\frac{1}{\upsilon(\mathrm{E})}\frac{\partial\Phi(\mathbf{r},\mathrm{E},\Omega,\mathrm{t})}{\partial\mathrm{t}}$$
$$= -\Omega.\nabla\,\Phi(\mathbf{r},\mathrm{E},\Omega,\mathrm{t}) - \Sigma_{\mathrm{t}}(\mathrm{r},\Omega,\mathrm{E})\Phi(\mathbf{r},\mathrm{E},\Omega,\mathrm{t})$$
$$+ \frac{\chi(\mathrm{E})}{4\pi}\int_0^{\infty}\mathrm{dE}'\,\nu(\mathrm{E}')\Sigma_{\mathrm{f}}(\mathbf{r},\mathrm{E}')\int_{4\pi}\Phi(\mathbf{r},\mathrm{E}',\Omega',\mathrm{t})\mathrm{d}\Omega$$
$$+\int_0^{\infty}\mathrm{dE}'\int_{4\pi}\mathrm{d}\Omega'\,\Sigma_{\mathrm{s}}\big(\mathbf{r},\Omega'.\Omega,\mathrm{E}'\to\mathrm{E}\big)\Phi(\mathbf{r},\mathrm{E}',\Omega',\mathrm{t})$$
$$+\,\mathrm{Q}(\mathrm{r},\Omega,\mathrm{E},\mathrm{t}) \qquad (2.1)$$

where, Φ is the neutron angular flux, Σ_t, Σ_f and Σ_s are the macroscopic total, fission and scattering cross sections of the medium respectively. The nuclear quantities are assumed to be time independent. The neutron transport equation is a balance equation for angular neutron density n($\mathbf{r}$,E,Ω,t), which is the expected number of neutrons per unit volume, per unit energy interval per unit solid angle per unit time around the phase space point $(\mathbf{r},\mathrm{E},\Omega)$ at time t. The angular neutron density is related to the angular neutron flux $\Phi(\mathbf{r},\mathrm{E},\Omega,\mathrm{t})$ and the neutron speed (υ) by the equation:

$$\Phi(r, E, \Omega, t) = n(r, E, \Omega, t) \times v \quad (2.2)$$

Equation 2.1 is a balance equation for the net rate of change of neutron angular density in terms of the neutrons getting accumulating and leaving the unit phase space volume per unit time. The terms in the RHS of equation 2.1 represent the rate of gain/loss of neutrons to/from the phase space volume due to different interactions and neutron streaming in the medium:

1^{st} term - streaming term which gives loss of neurons due to leakage.

2^{nd} term - removal of neutrons from phase space due to interactions.

3rd term - the gain of neutrons in the phase space due to total fissions in the medium

4^{th} term - gain of neutrons in the phase space due to interactions from other energies and solid angles.

5^{th} term - external source

χ (E) is the fraction of total fission neutrons that belongs to an unit energy interval around E and can be obtained from fission spectrum and ν(E) is the average number of neutrons released at energy E per fission. Σ_s (r, $\Omega'.\Omega$, E′→E) is the differential macroscopic scattering cross section and it gives the cross-section corresponding to the differential scattering of neutrons from initial energy and solid angle (E′, Ω') to final energy and direction (E,Ω).

Due to the property of the concerned medium and/or neutron energies, the neutron distribution may show a week angular dependence. The resulting weak angular dependence of neutron flux and density can be approximated by first order Legendre polynomial expansion with cosine of the angular variable. In that case, equation 2.1 simplifies to a five variable neutron diffusion equation. Such equation is generally used for fast reactors because of large neutron free-paths. It simplifies the geometrical complexity of fuel sub-assemblies

and the angular dependence. The complex and continuous dependence of cross-sections with neutron energy can be approximated by multi-group approach. The resulting equation is called multi-group neutron diffusion equation and can be written for the time independent case as:

$$-\nabla.\,D_g(r)\nabla\Phi_g(r)+\Sigma_{rg}(r)\Phi_g(r)=\sum_{\substack{g'=1\\ g'\neq g}}^{G}\Sigma_{sg'g}\,\Phi_{g'}(r)+\frac{\chi_g}{k}\sum_{g'=1}^{G}(\nu\Sigma_f)_{g'}\,(r)\Phi_g,(r) \qquad (2.3)$$

'g' is the index for energy grouping and can vary from 1 to G. 'k' represents the effective neutron multiplication factor. Different terms have the following meaning:

D_g - Diffusion coefficient for group 'g'

Φ_g - Group flux

Σ_{rg} - Removal cross-section for group 'g'

$\Sigma_{sg'g}$ - Differential scattering cross-section from group g' to g

χ_g - Fission spectrum–fraction of fission neutrons in the g^{th} group

ν - Number of neutrons emitted per fission

Σ_{fg} - Fission cross-section for the g^{th} group

The group flux, fission spectrum and cross-sections can be estimated using appropriate flux shapes as,

$$\Phi_g(r)=\int_g dE\,\Phi(r,E)$$

$$\chi_g=\int_g dE\,\chi(E)$$

$$and,\ \ \Sigma_{\alpha g}(r)=\frac{\int_g dE\Sigma_\alpha\,(r,E)\Phi(r,E)}{\int_g dE\Phi\,(r,E)} \qquad \alpha=\ r\ (\text{removal}),\qquad f\ (\text{fission}) \qquad (2.4)$$

$$\text{and,} \quad \Sigma_{sg'g}(r) = \frac{\int_g dE \int_{g'} dE' \Sigma_s(r, E' \rightarrow E)\Phi(r, E')}{\int_g dE \Phi(r, E)}$$

In equation 2.3, the removal cross-section $\Sigma_{rg}(r)$ is defined as,

$$\Sigma_{rg}(r) = \Sigma_{tg}(r) - \Sigma_{sg\rightarrow g}(r)$$

With the assumption of no up-scattering, the equation 2.3 appears the form,

$$-\nabla . D_g(r)\nabla\Phi_g(r) + \Sigma_{rg}(r)\Phi_g(r) = \sum_{g'=1}^{g-1} \Sigma_{sg} \Phi_{g'}(r) + \frac{\chi_g}{k} \sum_{g'=1}^{G} \nu \Sigma_{fg'}(r)\Phi_{g'}(r) \quad (2.5)$$

$$-\nabla . D_g(r)\nabla\Phi_g(r) + \Sigma_{rg}(r)\Phi_g(r) = \sum_{g'=1}^{g-1} \Sigma_{sg'g} \Phi_{g'}(r) + \frac{1}{k} S_g(r) \quad (2.6)$$

$$\text{where,} \quad S_g(r) = \chi_g \sum_{g'=1}^{G} \nu \Sigma_{fg'}(r)\Phi_{g'}(r) \quad (2.7)$$

The above equation can be written as an Eigen value equation;

$$M\Phi = \frac{1}{k} F\Phi \quad (2.8)$$

Above equation can be solved by different methods for the unknown parameters of flux and multiplication factor.

Now, macroscopic cross-sections are essential for solving the neutron diffusion equation. The macroscopic cross-sections are computed by the product of number densities of the concerned nuclei in the medium and the basic multi-grouped microscopic nuclear cross-sections. The effects of energy self shielding has also to be computed by proper methods [Walter and Reynolds, 1981]. The same neutron diffusion equation can be used with proper rearrangements to find the adjoint flux also [Ronen, 1986]. Using a perturbation theory code, the direct and adjoint fluxes are computed which help to obtain material removal worths, Doppler worths and kinetic parameters. These results of perturbation

analysis along with basic thermo-physical data of the reactor materials can be used to estimate the reactivity feedbacks and the consequent reactor behaviour during a transient.

The static, perturbation and transient analyses quoted in the present research are performed with neutron diffusion equation. Ideally neutron transport theory has to be used for computing void reactivity effects in FBRs. But it has been found that due to larger mean path of neutrons and the homogenized approximation generally used in diffusion theory calculations (smearing of fuel and steel over the volume of subassembly), the void reactivity effect within the core and axial blankets is well computed by the diffusion theory also [IAEA, 2001]. It is not true for all the core configurations. While estimating the reactivity change due to voiding of sodium plenum region (which is just above the core and replacing axial blankets), use of diffusion theory can lead to larger errors. The replacement of axial blankets with plenum is to reduce the positive void effect of core, the amount of this reduction is over-predicted by diffusion theory by 20 to 30% [IAEA, 1994]. Thus the reduction in void reactivity due to the replacement of axial blanket by a sodium plenum is only approximate as computed by diffusion theory, for more reliable estimates, transport computations are essential. At the same time, the use of diffusion codes are adequate for the present study as it is mainly concerned to the comparative performance of different metallic fuelled cores with respect to their static and transient behaviours.

2.2 Estimation of Static Core Physics Parameters

In the present study, metal fuelled FBR cores are analysed with respect to its breeding potential and safety characteristics. For this, the number densities of various nuclei in different regions of the reactor are essential. The number densities of various nuclei present in the homogenous regions of the metal fuelled FBR core are calculated using the modified

version of the code ATOMIX [Devan et al., 2003]. The metallic fuel considered here is U-Pu-Zr, a ternary alloy of uranium, plutonium and zirconium. The fissile (plutonium) enrichment E_{Pu} is defined as the percentage of plutonium in the total heavy metal (U+Pu) mass.

ie., $$E_{Pu} = \frac{\text{Mass(Pu)}}{\text{Mass(U)} + \text{Mass(Pu)}} * 100\% = W_{Pu} \times 100\ \% \quad (2.9)$$

where, W_{Pu} is the weight fraction of plutonium in the heavy metal. The weight fraction of W_{Zr} in the fuel is a key parameter that decides its neutronic and thermo-physical properties; it is the fraction of zirconium weight to the total metal weight.

ie, $$W_{Zr} = \frac{\text{Mass(Zr)}}{\text{Mass (U + Pu + Zr)}} \quad (2.10)$$

The number density (number of atoms per unit volume) n_i of an element 'i' with atomic mass A_i and weight fraction W_i in an alloy of density ρ is calculated by the formula as,

$$n_i = \frac{W_i \times N_A \times \rho}{A_i} \quad (2.11)$$

The above formula can be used for the number density estimation of steel, sodium and fuel isotopes. For example, the number density of Pu-239 in a ternary alloy of uranium, plutonium and zirconium can be calculated by the formula given above.

$$n_{Pu239} = (1 - W_{Zr}) \times Fr_{Pu239} \times \frac{W_{Pu} \times N_A \times \rho}{A_{239}} \quad (2.12)$$

where W_{Zr} is the weight fraction of zirconium in the fuel, Fr_{Pu239} is the weight fraction of Pu-239 in the plutonium metal, W_{Pu} is the weight fraction of plutonium, N_A is the Avogadro number and A_{239} is the atomic mass of Pu-239. The number density of zirconium is calculated by the formula,

$$n_{Zr} = W_{Zr} \times \frac{N_A \times \rho}{A_{Zr}} \quad (2.13)$$

A_{Zr} is the atomic mass of zirconium. The actual number density of a particular isotope or element in a homogeneous mixture containing fuel, steel and sodium is then computed using the corresponding volume fraction and the temperature dependent density values. The temperature dependence can be accounted by redefining the density with the help of proper expansion coefficients.

After knowing the number densities of the various constituent nuclei types in the homogenised media of the reactor, self shielded cross-sections can be estimated. This is important from the fact that the effective cross-section of a particular nuclei is determined by the number of its own atoms and the presence of other atoms by a process called energy self shielding, The self-shielded cross-sections from 26 group ABBN-93 cross-section data are calculated using the CONSYST/EFCONSY [Devan, 2003] code system [Manturov, 1997]. The k–effective is calculated using the two-dimensional diffusion theory code ALCIALMI using R-Z geometry. A flowchart of the calculation scheme is given in Fig.2.1.

From the knowledge of neutron fluxes, mesh and region specifications and macroscopic cross-sections the code ALEX calculates the reaction rates in all meshes and regions using the relationship,

$$\text{Reaction Rate} = \Sigma\Phi \text{ per unit volume per unit time} \tag{2.14}$$

In addition, region averaged group fluxes, breeding ratio, peak linear pin powers and capture to fission ratio are also calculated by ALEX. Using reaction rates and the value of energy released per fission, power densities can be computed. Knowing the power densities as a function of mesh, number of pins/sub-assembly and area of sub-assembly, the linear heat rating (LHR) can be computed using the formula,

$$\text{LHR (W/cm)} = \frac{\text{P} \times \text{A}}{\text{N}} \tag{2.15}$$

where, P : power density (W/cm^3)

A : area of SA (cm^2) and,

N : number of pins/SA

In addition to power density, area of SA and number of pins/SA can be different for different core designs.

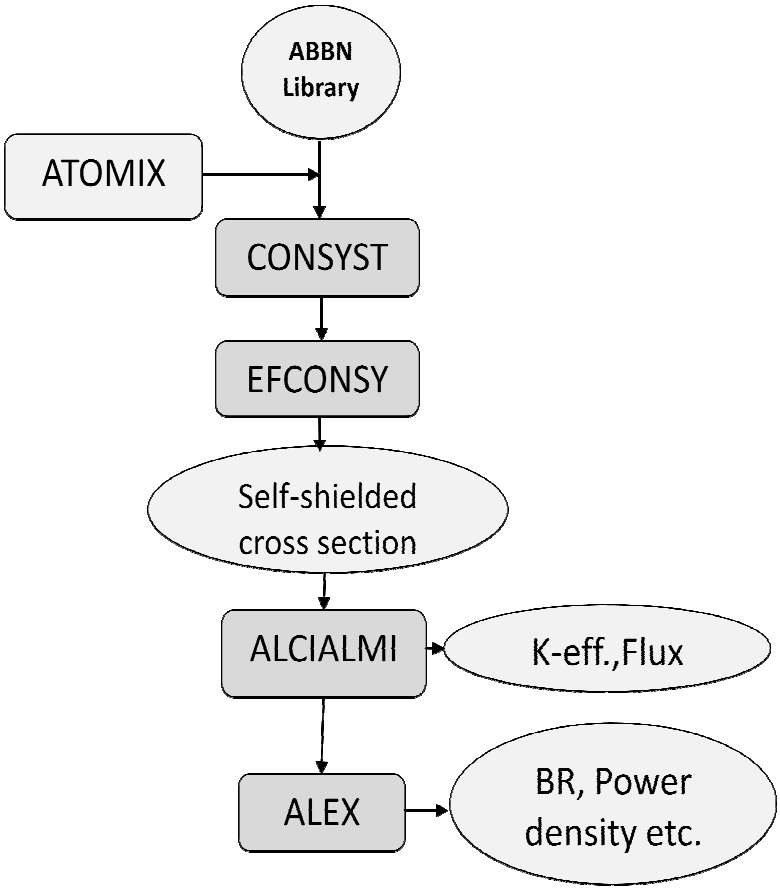

Fig.2.1. Calculation Scheme-Static Core Physics Parameters

The radiation damage in structural materials is estimated by computing its displacement per atom (dpa), which depends on neutron flux, neutron energy, irradiation time and temperature. For different reactors, the dpa in the structural materials have been calculated using the appropriate flux, steel-concentrations and displacement cross-sections.

2.3 Calculation Scheme for Perturbation Calculations

The fundamental eigen-value problem of an unperturbed reference neutron multiplying system can be written in operator form as [Ronen, 1986],

$$L\Phi = \lambda P\Phi \tag{2.16}$$

where L represents the loss operator representing the leakage and scattering out terms of neutron diffusion equation and P is the production operator representing the fission and in-scattering terms and λ is the eigen-value related to the neutron multiplication factor k by the relation:

$$\lambda = \frac{1}{k} \tag{2.17}$$

For the perturbed system, the eigen-value equation becomes,

$$(L + \Delta\Phi)(\Phi + \Delta\Phi) = (\lambda + \Delta\lambda)(P + \Delta P)(\Phi + \Delta\Phi) \tag{2.18}$$

If we define the reactivity ρ as given below,

$$\rho = 1 - \frac{1}{k} \tag{2.19}$$

The exact change in reactivity '$\Delta\rho$' due to the perturbation are given by,

$$\Delta\rho = \frac{\lambda < \Phi^{+}(\Delta P)(\Phi + \Delta\Phi) > - < \Phi^{+}(\Delta L)(\Phi + \Delta\Phi) >}{< \Phi^{+}(P + \Delta P)(\Phi + \Delta\Phi) >} \tag{2.20}$$

The quantity Φ^{+} is called the adjoint function or neutron importance function. The denominator is called the importance integral and is given by the expression in multi-grouping scheme as,

$$I = \sum_{g} \int_{v} \Phi_{g}^{+} \chi_{g} \left(\sum_{g'} (\nu\Sigma_{g'}^{f}) \Phi_{g'}^{'} \right) dV \tag{2.21}$$

For the first order perturbation, the perturbation is assumed to be small so that it can be assumed that the perturbed flux not differs from the un-perturbed flux;

$$\Phi' = \Phi + \Delta\Phi \approx \Phi \ ;$$

and from equation 2.20, we can obtain,

$$\Delta\rho = \frac{\lambda < \Phi^{+} (\Delta P)\Phi > \ - < \Phi^{+} (\Delta L)\Phi >}{< \Phi^{+} (P + \Delta P)\Phi) >} \tag{2.22}$$

as the 1st order approximate expression for reactivity change.

Fig.2.2 shows the scheme used in the code PERTX to evaluate the reactivity change and its components. The direct and adjoint fluxes, multiplication factor (k_1) of the unperturbed reference core is obtained first. For a given perturbation, using equation 2.22, the first order approximated reactivity change can be obtained. The perturbation may be either a change in isotopic concentration, dimensional changes or change in temperature of nuclides. Now the core is subjected to the assigned perturbation, perturbed fluxes (both direct and adjoint) and multiplication factor (k_2) are obtained for the modified core. The reference and perturbed macroscopic cross-sections are used for estimating the change in leakage due to perturbation. Equation 2.20 then can be used to estimate the exact reactivity change due to perturbation. The multiplication factors of the reference and perturbed core k_1 and k_2 will give the exact reactivity change through direct methods. The detailed scheme of calculation is given in chapter 4.

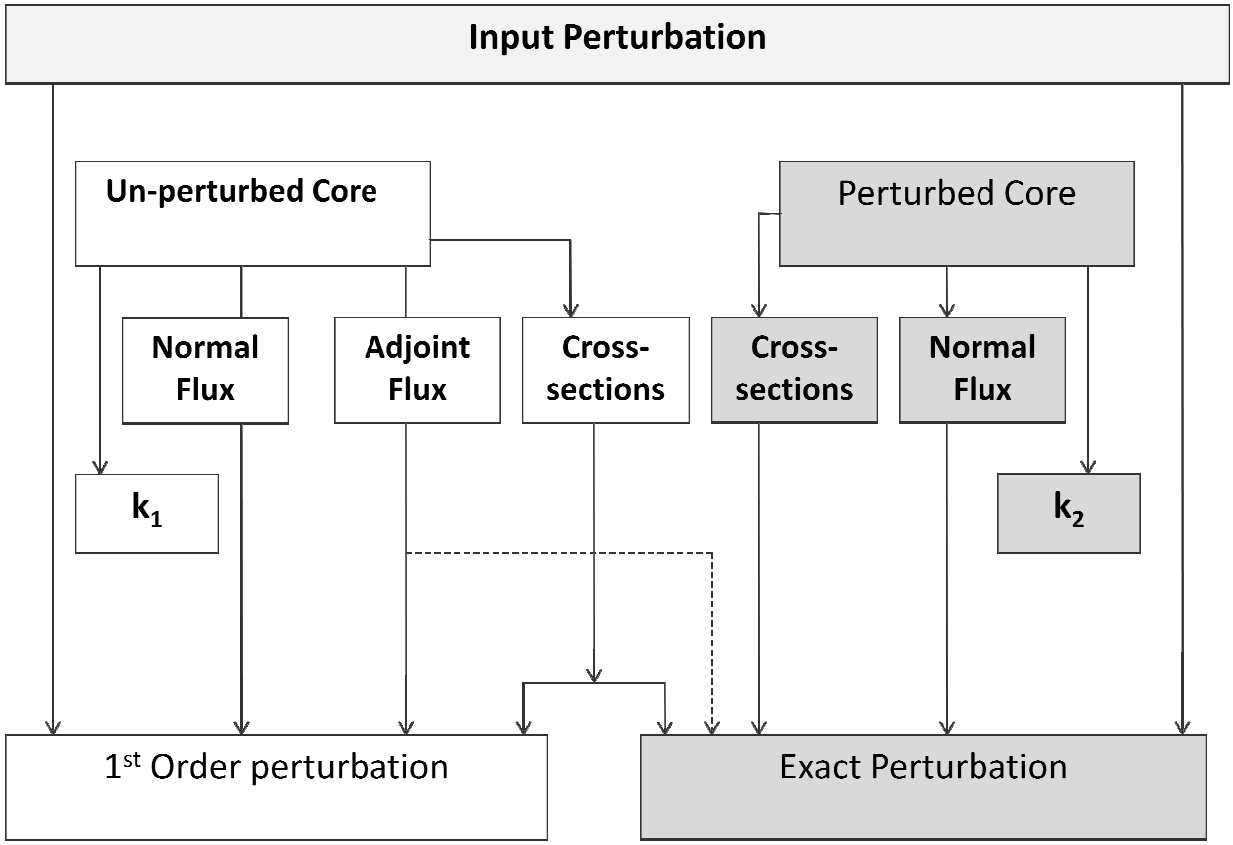

Fig.2.2.Calculation Scheme used for IGCAR Perturbation Analysis

The parameters estimated by perturbation methods are given below,

a. Void reactivity worths of fuel, steel and sodium

b. Boundary movement worths

c. Doppler worths

d. Delayed neutron fraction

e. kinetic parameters

The removal worths are estimated by removing the particular isotopes of interest in the concerned mediums. It is also called void reactivity worth. Boundary movement worth is the reactivity change due to the expansion of one region to the neighbouring region. For the estimation of this reactivity worth, the material in the first region is assumed to be displaced

from its original position and added to the second region. This value along with the reactivity change due to variation of material density is used to estimate the reactivity feedback caused by core radial expansion and SA bowing during a transient. For estimating the Doppler constant, it is assumed that the rate of change of multiplication factor with temperature is inversely proportional to temperature as in the case of oxide fuels.

ie; $$\frac{dk}{dT} \propto \frac{1}{T} \qquad \text{or;} \qquad \frac{dk}{dT} = \frac{C}{T} \tag{2.23}$$

For a temperature rise from T_1 to T_2, the Doppler constant (C) is obtained by integrating Eqn.2.23,

$$C = \frac{\Delta k}{\ln\left(\frac{T_2}{T_1}\right)} \text{ with } \Delta k = k_2 - k_1 \tag{2.24}$$

The delayed neutron fraction and kinetic parameters are estimated after proper weighting with the adjoint flux [Walter and Reynolds, 1981]. Its distributions in the core regions and along the assigned mesh volumes are also computed which are essential for transient analysis.

2.4 Perturbation Calculations using ERANOS System

For comparing and validating the results of perturbation results obtained with IGCAR codes, the diffusion and perturbation modules [Tommasi, 2007] available in ERANOS 2.1 [Rimpault et al., 2002] along with JEFF 3.1 nuclear data have been used. ERANOS is a code system that has been developed and validated to provide a suitable basis for reliable neutronic calculations of current and advanced fast reactor cores. It consists of data libraries, deterministic codes and calculation procedures and also has the options of perturbation calculations of 2D and 3D diffusion and 2-D transport. The schematic of the calculation is

shown in Fig.2.3. The combination of JEFF3.1 nuclear data, diffusion and perturbation modules available in ERANOS 2.1 is referred to ERANOS scheme of calculation.

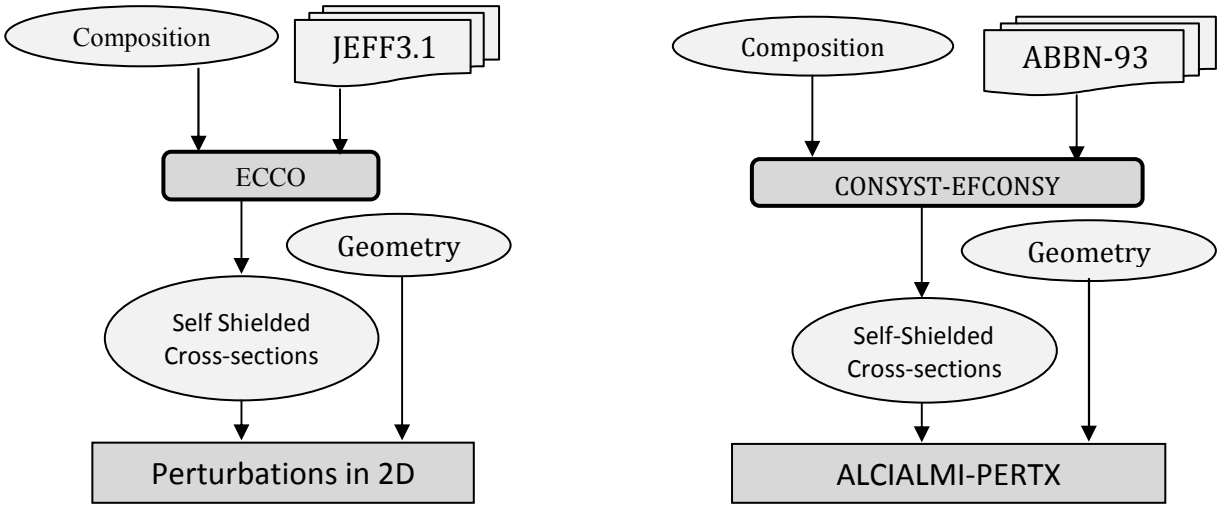

ERANOS ALCIALMI-PERTX

Fig.2.3. Flow charts of ERANOS and ALCIALMI-PERTX Perturbation Analysis

For comparison, a simplified schematic of ALCIALMI-PERTX system used in the IGCAR is also given. In ERANOS, the calculation is performed using various input modules. The modules can be used for the estimation of different parameters like effective multiplication factor and perturbation worths. The ECCO finds the self shielded cross-sections by combining a slowing down treatment in many groups (1968 groups) with the subgroup method within each fine group and collision probabilities calculation for many types of geometries [Ruggieri et al., 2006]. For the estimation of effective multiplication factor and perturbation worths, 33-group cross-section data has been used. The ERANOS have the options of standard perturbation theory (SPT) [Gandini, 1978; Gandini 1981],

generalized perturbation theory (GPT) [Gandini, 1967] and equivalent generalized perturbation theory (EGPT) [Gandini, 1986]. Out of these, the standard perturbation theory tools available in the code are used for the present analysis. First order and exact perturbation theory results are derived from SPT option. These self-shielded cross-sections are then used along with the SA details and material distribution is then used to find the reactivity worth caused by a given perturbation applied to the core. Unlike PERTX, in ERANOS, the distribution of the reactivity change along the core sub-zones is not available, but group and region wise break-ups are available.

2.5 Estimation of Pu Equivalence

The isotopic composition of a nuclear fuel changes due to burn-up that causes a non-uniform depletion/accumulation of fissile and fertile isotopes in the fuel. Therefore, the net reactivity effect or worth of reprocessed fuel can be different in different batches as compared to the initial assigned value. Also, the fuel isotopes suffer losses and decay during reprocessing and manufacturing. In addition, during manufacturing, plutonium containing high fissile content from other sources like blanket is used for fuel fabrication to compensate the higher fertile fraction. To quantify this reactivity change and the relative worth of a fuel, a ^{239}Pu equivalence concept for fuel isotopes can be used [Mohanakrishnan, 2005]. This can be defined as the relative worth of a fuel isotope compared to ^{239}Pu. This gives the effectiveness of any fuel isotope with respect to plutonium ^{239}Pu [Riyas and Mohanakrishnan, 2006a]. This in turn can be used to re-estimate the enrichment requirement of the reprocessed fuel so that the worth of the reprocessed fuel can be retained same as that of reference fuel [Pandikumar et al., 2009]. Generally first order perturbation methods are

used to find the ^{239}Pu equivalence of the main fissile and fertile isotopes. It is estimated using the formula;

$$^{239}\text{Pu Equivalence of Fuel Isotope} = \frac{\text{Worth of Fuel Isotope}}{\text{Worth of } ^{239}\text{Pu}} \tag{2.25}$$

Now the worth of ^{239}Pu is the reactivity change occurs by adding or removing a small quantity of ^{239}Pu to the core. The quantity added is small such that first order approximation is valid so that Equation 2.22 can be applied for finding the worth. Similarly, same amount of fuel isotope is added or removed to/from the core and the worth is estimated. Use of Equation 2.25 then will give the value of ^{239}Pu equivalence of that particular fuel isotope.

2.6 Nuclear Data Used in IGCAR Scheme

ABBN cross-section set is used for the IGCAR static and perturbation calculations of metallic fuelled FBR cores. The data set was generated from Russian nuclear data library FOND-2. This library contains data carefully selected from JENDL-3 (Japanese), BROND-2(Russian), ENDF/B-VI (American) and JEF-2 (European) evaluated nuclear data libraries. This selection had been based on a detailed study of the relative performance of the above libraries in predicting several integral parameters measured on the Russian and other international fast critical facilities [Manturov, 1997]. The selection criteria include completeness of the data, year of evaluation, comparison of group cross-sections, comparison of thermal cross-sections, and resonance integrals with measured values etc. The validation of ABBN-93 has been performed by analyzing experiments conducted on compact spherical assemblies with different reflectors, critical assemblies with different neutron spectra, uranium and plutonium solution critical systems, heterogeneous uranium-water, plutonium-water and MOX-water critical assemblies. Many experiments are carried out at on the BFS

and KBR facilities at IPPE and irradiation experiments done at BN-350 reactor have been used in the validation. The self shielded cross-sections are prepared in 26, 28 or 299 group structure by the code CONSYST. The code EFCONSY is used to suit the processed cross-sections from CONSYST [Devan, 2003] to the IGCAR diffusion theory codes ALCIALMI and FARCOB [Mohanakrishnan, 2008]. Integral validation of ABBN-93 is also carried out in IGCAR [Devan et al., 1999]. The ABBN-93 cross-section set has been used for the benchmark analysis of BN-600 reactor using IGCAR codes [IAEA, 2010]. The 26-group calculations based on ABBN-93 nuclear data has been performed for the physics design and perturbation studies of oxide fuelled Indian PFBR [Harish et al., 2009]. The 26 group energy structure used in IGCAR calculations using ABBN nuclear data is given in Table 2.1.

2.7 Nuclear Data Used in ERANOS Scheme

European Reactor Analysis Optimized calculation System ERANOS 2.1 [Ruggieri et al., 2006] along with JEFF 3.1 nuclear data is also used for the perturbation analysis of PFBR core. JEFF 3.1 is the joint European Fission and Fusion nuclear data library version 3.1 released on 2005 [Koning et al., 2006]. It is an updated version of JEF 2.2. From this library, multi-group data are prepared in 1968 groups for the main nuclides and 33 groups for the fast spectrum applications, and used for the present analysis. Criticality calculations of MOX fuelled fast critical facilities using JEFF 3.1 nuclear data has been reported [Rowlands, 2010]. Also better predictions of safety parameters like sodium void worth of small critical facilities have been estimated with JEFF 3.1 and ERANOS 2.1 [Tommasi et al., 2010].

Recently in IGCAR, physics design and safety parameters of a small experimental metal fuelled fast reactor are performed with ERANOS 2.1 using this data library [Devan et al., 2011]. More recently, using FARCOB and ERANOS code systems, comparative studies

have been performed to predict the Phenix control rod withdrawal end-of-life experimental results [Devan et al., 2012]. For fast reactor applications, 33-group library is provided for all the important nuclides. A fine group library in 1968 group structure is also available for 37 nuclides of interest to fast reactors. These nuclear data libraries were processed from JEF-2.2, JEFF-3.1 and ENDF/B-VI.8 libraries using NJOY and CALENDF codes. The 33 group energy structure used in ERANOS data is given in Table 2.2.

Table 2.1: 26 Group Neutron Energy Structure in ABBN Library

Group No.	Upper Energy (eV)	Group No.	Upper Energy (eV)
1	10.5E+06	14	2.154E+03
2	6.5E+06	15	1.0E+03
3	4.0E+06	16	464.16
4	2.5E+06	17	215.44
5	1.4E+06	18	100.0
6	0.8E+06	19	46.416
7	0.4E+06	20	21.544
8	0.2E+06	21	100
9	100E+03	22	4.642
10	46.416E+03	23	2.154
11	21.544E+03	24	1.0
12	10.0E+03	25	0.464
13	4.642E+03	*26	0.215
		*Lower limit of 26th group is 0.025 eV	

2.8 Transient Analysis Using the Code PREDIS

The ULOF transient in the pre-disassembly phase is carried out using the code PREDIS which is a part of the general code KALDIS [Harish et al., 1999]. This code is validated against European LOFA benchmark problem [Singh et al., 1994] and the BN800

benchmark exercise [IAEA, 2000] up to onset of sodium boiling. PREDIS uses the point kinetics model for the calculation of reactor power during a transient. Point kinetics approximation is well valid for smaller tightly coupled cores. The eigen-value separation between the fundamental mode and the first mode is found to be greater than 5000 pcm for a 500 MWe reactor (Mohanakrishnan and Singh, 2000). By comparing the fast neutron diffusion length with core size, it is possible to assume the wide separation of first two modes in 1000 MWe FBR core too. It further justifies the use of point kinetics approach in PREDIS code for the transient analysis of this reactor. PREDIS is a multi-channel code, where each flow channel is represented by a fuel pin with its associated coolant flow and surrounding structure. The net reactivity is a sum of the input reactivity and the feedback reactivity and the heat transfer is calculated using Fourier heat conduction law.

For the purpose of calculations, the core is divided into different radial and axial zones and zone allocation will be different for three cores. 140 zones created for the perturbation analysis of 500 MWe FBR core is shown in Fig.2.4. Size of zones, number of SA per zone, number of meshes and mesh widths are also shown in figure. The distribution of void worths, Doppler worths, boundary movement worths and boundary movement worths are estimated by perturbation methods. Using these data, feedback reactivities due to axial fuel expansion, radial expansion of the core, clad and coolant expansion, Doppler effect and coolant voiding during a transient can be obtained. The radial expansion reactivity includes contributions due to boundary movement from the one radial zone to another and also flowering of the core due to spacer pad expansion. Using the temperatures and expansion coefficients of the spacer pad locations, the reactivity feedback due to spacer pad expansion can be estimated using a cantilever type bending for fuel SA.

Table 2.2: 33-Group Energy Structure in ERANOS

Group No.	Upper Energy (eV)	Group No.	Upper Energy (eV)
1	1.96403E+07	18	3.35463E+03
2	1.00000E+07	19	2.03468E+03
3	6.06531E+06	20	1.23410E+03
4	3.67879E+06	21	7.48518E+02
5	2.23130E+06	22	4.53999E+02
6	1.35335E+06	23	3.04325E+02
7	8.20850E+05	24	1.48625E+02
8	4.97871E+05	25	9.16609E+01
9	3.01974E+05	26	6.79040E+01
10	1.83156E+05	27	4.01690E+01
11	1.11090E+05	28	2.26033E+01
12	6.73795E+04	29	1.37096E+01
13	4.08677E+04	30	8.31529E+00
14	2.47875E+04	31	4.00000E+00
15	1.50344E+04	32	5.40000E-01
16	9.11882E+03	*33	1.00000E-01
17	5.53084E+03	*lower limit of 33rd group is 0.0001 eV	

The static power coefficients and isothermal temperature coefficients are calculated in the steady state mode of PREDIS code. During a loss of flow accident, it is assumed that the coolant flow coasts down in the form,

$$V(t) = \frac{V(0)}{1 + \frac{t}{\tau}} \tag{2.25}$$

where, V(0) is the initial flow velocity, τ is the flow halving time and t is the time. Flow halving time of 8s is considered for the three reactor cores considered in the present analysis.

Flow halving of 8 s had been chosen for the pump used in PFBR. High flow halving time is preferred with respect to safety of reactors during unprotected transients. In general, the cost of pump increases as the flow halving time is increased as it depends on the higher mass of flywheel used. It was found for PFBR that, the flow halving time of 8 s is adequate to control the consequences of short power failures within the design safety limits. Thus 8s flow halving time has been chosen as a median value for the three reactors. A schematic of a PREDIS is shown in Fig 2.5. Finally a summary of codes used for calculations are given in Table 2.3.

2.1	7	15.0	UAB	14								.	140
1.1	14	15.0		13								.	139
1.0	10	10.1	Core	12								.	138
2.0	5	10.1		11								.	137
2.0	5	10.1		10									136
2.0	5	10.1		9									135
2.0	5	10.1		8									134
2.0	5	10.1		7									133
2.0	5	10.1		6									132
2.0	5	10.1		5									131
2.0	5	10.1		4	.								130
1.0	10	10.1		3	.								129
1.1	14	15.0	LAB	2	.								128
2.1	7	15.0		1	.								127
			Region	*Core-1				*Core-2			Radial blanket		
		Width (cm)		7.2	32.7	12.4	12.4	10.2	12.4	6.4	6.0	12.4	8.8
	Number of meshes			4	16	7	12	10	6	6	6	6	4
Mesh size				1.8	2.0	1.8	1.0	1.0	2.0	1.1	1.0	2.1	2.2
No.of SA in the zone				1	30	24	30	30	42	24	24	54	42

**Core-1 and Core-2 are the inner and outer regions of the core respectively*

Fig.2.4. Zone Distribution used for the Perturbation Analysis of 500 MWe FBR Core

It is assumed that clad expansion is independent of fuel expansion. Also it is to be noted that control rod drive line expansion feedback is not modeled in PREDIS. The code works well in the pre-disassembly phase and fails when fuel melting and boiling starts or when the reactor becomes prompt-critical.

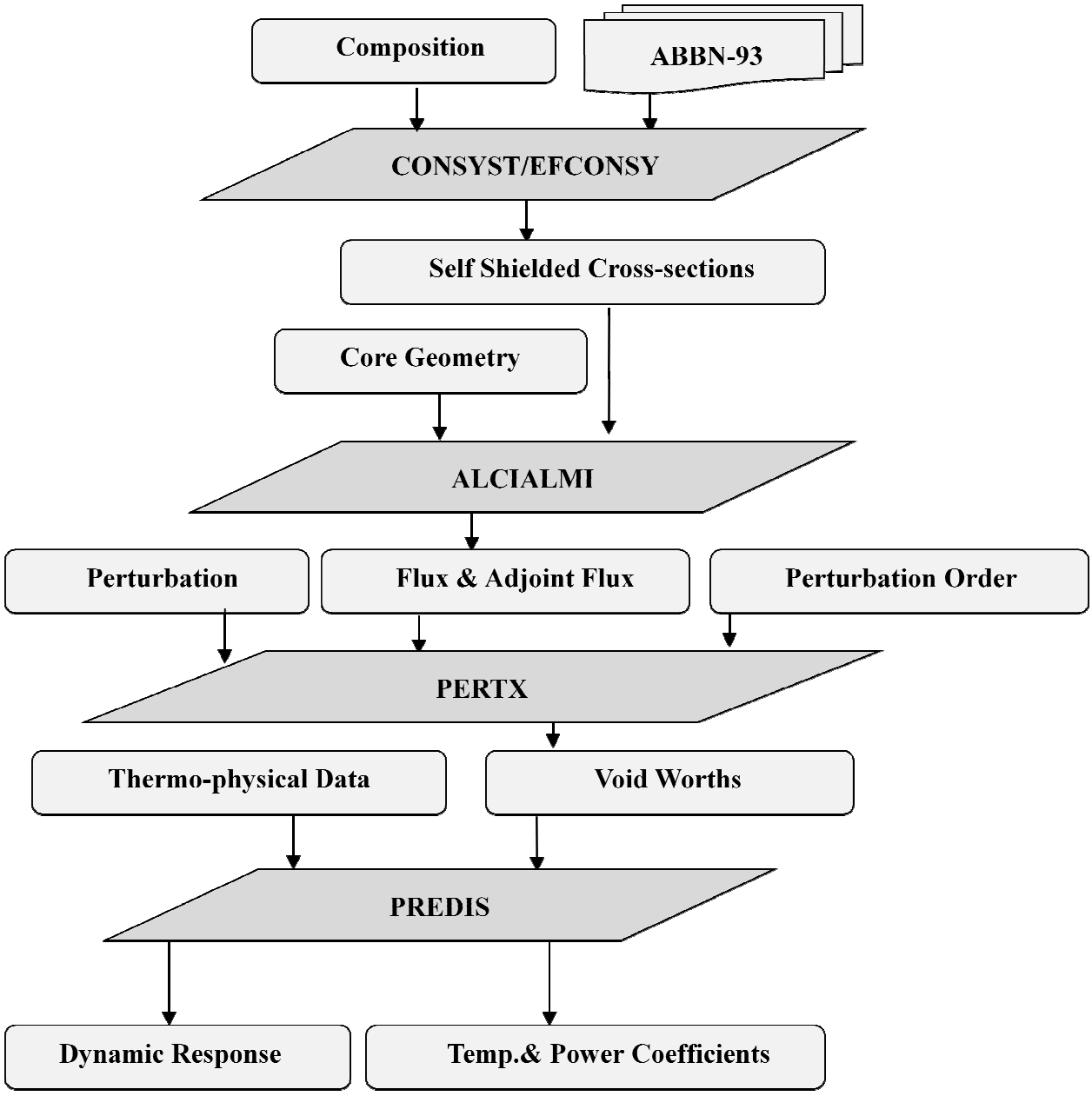

Fig.2.5. Calculation Scheme- PREDIS

Table 2.3: Summary of Codes used and Their Description

No.	Code	Use
1	ATOMIX	Number density calculation for mixtures
2	CONSYST&EFCONSY	Self shielded cross-section computation from ABBN-93
3	ALCIALMI	Direct, adjoint fluxes and k by R-Z model computation
4	NALEX	Computes reaction rates, power density, BR etc. using output data from ALCIALMI
4	PERTX	1^{st} order and exact perturbation calculations to estimate the material removal and Doppler worths
5	PREDIS	Point kinetics code for pre-disassembly phase accident analysis

2.9 Summary

A brief outline of calculation methods employed for the present studies on metallic fuels are given in this chapter.

Chapter 3

BREEDING POTENTIAL AND SAFETY PARAMETERS OF METALLIC U-PU-Zr FUELLED REACTORS

3.1 Introduction

In this study, three metal-fuelled cores having different sizes are analysed to understand their breeding and safety characteristics. It consists of a 120 MWe experimental reactor core and two commercial reactor cores of 500 MWe and 1000 MWe respectively. The fuels chosen in these cores are the ternary metallic alloy of U-Pu-Zr with three different Zr compositions varying from 0% to 10%. It has to be noted that, most of the available irradiation experience of the ternary alloy was with 10% Zr [Chernock and Horton, 1994; Khalil and Hill, 1991] as it has the optimum thermo-dynamic properties. As it is the aim in Indian context to maximise the BR without compromise on safety, breeding characteristics of U-Pu-Zr fuels with lesser Zr concentrations are also investigated in this study. Impact of zirconium concentration on the main reactor physics parameters are only examined here. In addition to BR and sodium void worth, fuel doubling time, fast and total fluxes, Doppler coefficient, plutonium inventory and delayed neutron fraction etc. are some of the other physics parameters investigated. It has to be noted that the doubling time mentioned in the present study is the RDT, which indicates a theoretical minimum time for fissile doubling. In addition to the core size and fuel type used, the dependence of BR with increase of radial blanket thickness and with smear density in fuel are also investigated.

In the first part of analysis, two commercial sized metal fuelled FBR cores of power 500 MWe and 1000 MWe are analyzed with metallic fuels of two Zr concentrations 0% and 10%. These will give the extreme limits of BR and sodium void worth with ternary alloys

containing uranium, plutonium and zirconium in these reactors. Zr concentrations beyond 10% are omitted due to degradation of breeding and thermo-physical properties. Due to the available irradiation experience of ternary fuels with a minimum Zr concentration of 6%, and the aim in Indian context is to maximize BR, fuels with 6% is proposed as the candidate fuel for Indian FBR program. All the FBR cores are then analysed with this chosen fuel. Modified fuel pin designs with reduced fuel-clad interactions and extended fuel burn-up are proposed and its influence on the breeding characteristics is also investigated. Detailed burn-up studies and safety analysis have not been performed. Since metal FBRs have high positive sodium void coefficient, emphasis is given to find out various options of reducing its value. The influence of two possible methods to reduce the value of sodium void effect is also studied.

3.2 Basic Core Design Parameters

The thermo-physical properties of metallic U-Pu-Zr fuels are given in Table 3.1. Even metal fuels with three different Zr concentrations are discussed in this study, the properties corresponding to 6% zirconium is only given in the table for simplicity. As the thermo-dynamic and physical properties are heavily dependent on the Pu concentration, the data corresponds to average Pu concentration of ~15% is chosen here. Also the temperature dependence on the fuel density, expansion coefficient, conductivity, expansion coefficient and specific heat has been neglected due to paucity of data.

The core configuration of the small 120 MWe experimental breeder reactor is similar to one reported in the recent IGCAR metal fuelled FBR studies [Devan et al., 2011] and is shown in Fig.3.1. The core design of 500 MWe metallic FBR core with two rows of radial blanket is same as that of the PFBR except fuel pin bonding material and smear density, the latter uses helium bonded pins with higher fuel smear density. The core configuration is

shown in Fig.3.2. The core configuration of the 1000 MWe reactor with two rows of radial blanket is given in Fig.3.3 [Riyas and Mohanakrishnan, 2005b]. FBR cores with three rows of radial blankets are also considered but their core configurations are not given here.

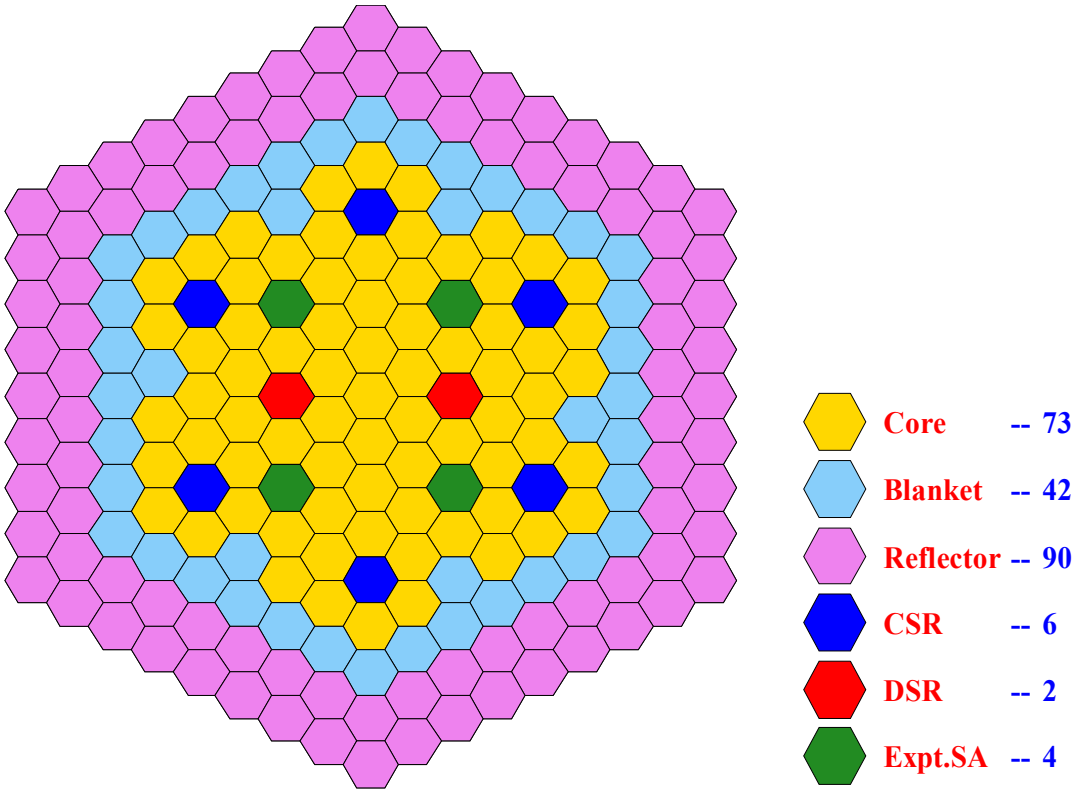

Fig.3.1. Core Configuration of 120 MWe FBR

The fuel pin diameter of a fast breeder reactor is one of the key parameters that determine the BR, doubling time and fuel inventory. Small diameter is favorable to reduce the fuel inventory, even though it will lead to a reduction in breeding ratio. The pin diameter is chosen as 6.6 mm for the 120 MWe and 500 MWe FBR cores in order to minimize the fuel inventory. In these reactors, the pin diameter, maximum allowed heat rating and fuel sub-assembly pitch are kept same as that of PFBR. For the 1000 MWe FBR core, pin diameter of

8 mm is chosen. This is backed by the recent study done to find the optimum pin diameter in such cores [Riyas and Devan, 2013]. In general, for all the reactor cores discussed here, sodium bonded fuel pins with 75% smear density is used. The important design parameters of the FBR cores are given in Table 3.2.

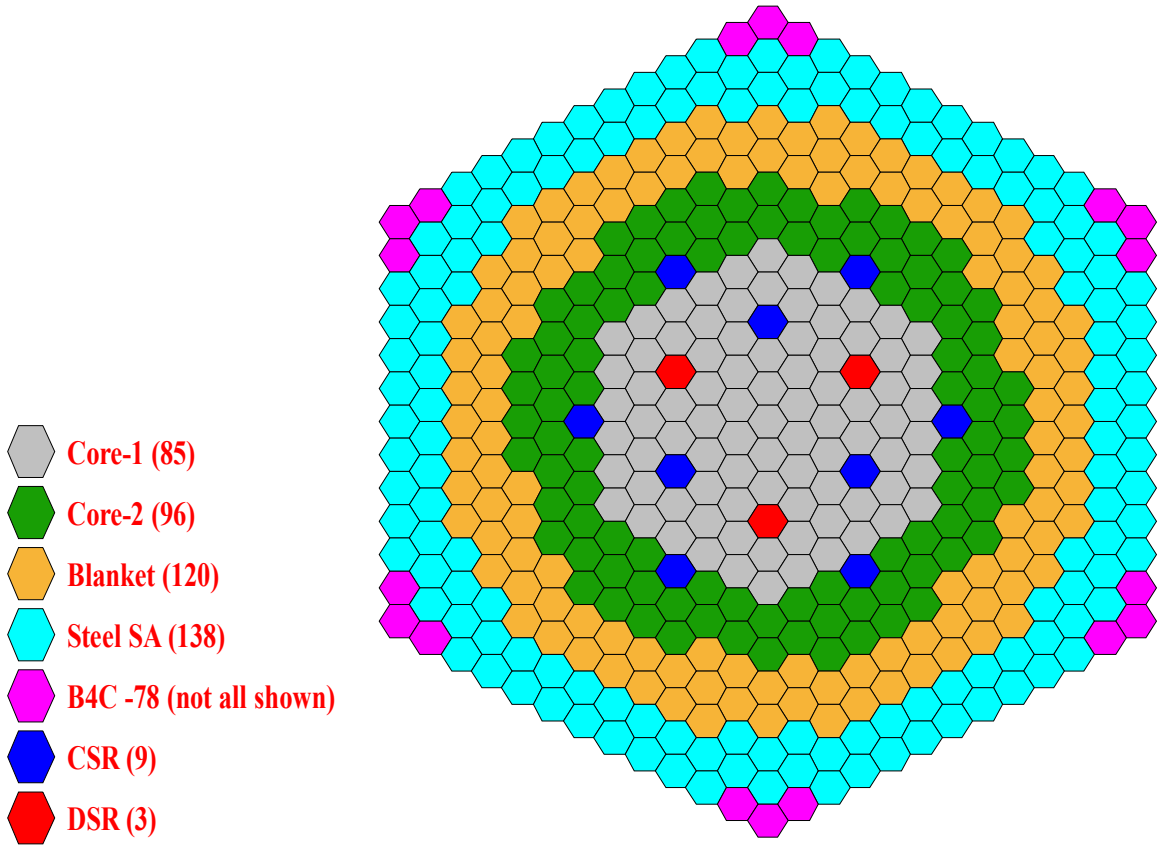

Fig.3.2. Core Configuration of 500 MWe FBR

It is assumed that both uranium and plutonium have the isotopic composition similar to that of typical PHWR reprocessed fuel. The plutonium vector is given in Table 3.1 and the uranium is depleted to 0.25%. The effects of radial blanket SA to breeding is studied on 500 MWe core in which the analysis is performed with two and three rows of RB.

Table 3.1: Thermo-Physical Properties of Metallic Fuels

Number	Parameter	Value
1	Fuel Type	U-Pu-6%Zr
2	Fuel Density (g/cm^3)	17.1
3	Smeared Density (g/cm^3)	12.8
4	Plutonium Isotopic Composition: Pu239/Pu240/Pu241/Pu242 (%)	68.8/24.6/5.3/1.3
5	Melting Point (^oC)	1067
6	Boiling Point (^oC)	3932
7	Thermal Conductivity ($W/cm/^oC$)	0.25
8	Linear Expansion Coefficient ($^oC^{-1}$)	19.7×10^{-6}
9	Gap Conductance ($W/cm^2/^oC$)	27
10	Specific Heat ($J/g/^oC$)	0.2
11	Latent Heat of Fusion (J/Kg)	38
12	Latent Heat of Vaporization (J/g)	1641

The allowed heat rating of 1000 MWe reactor is taken as 500 W/cm, which is more than that in the small and medium reactors, to minimise the specific fuel inventory. Also it is to be noted that the control rods mentioned in the core designs are only tentative with respect to its number, absolute and relative positions in the core, the enrichment of control material used and the related safety implications during an uncontrolled withdrawal accident, as detailed analysis is required for such an optimization. Two dimensional diffusion analysis has been performed with ABBN-93 cross-sections to find the static core physics and safety parameters of three different FBR cores and the results are presented in the next sections separately.

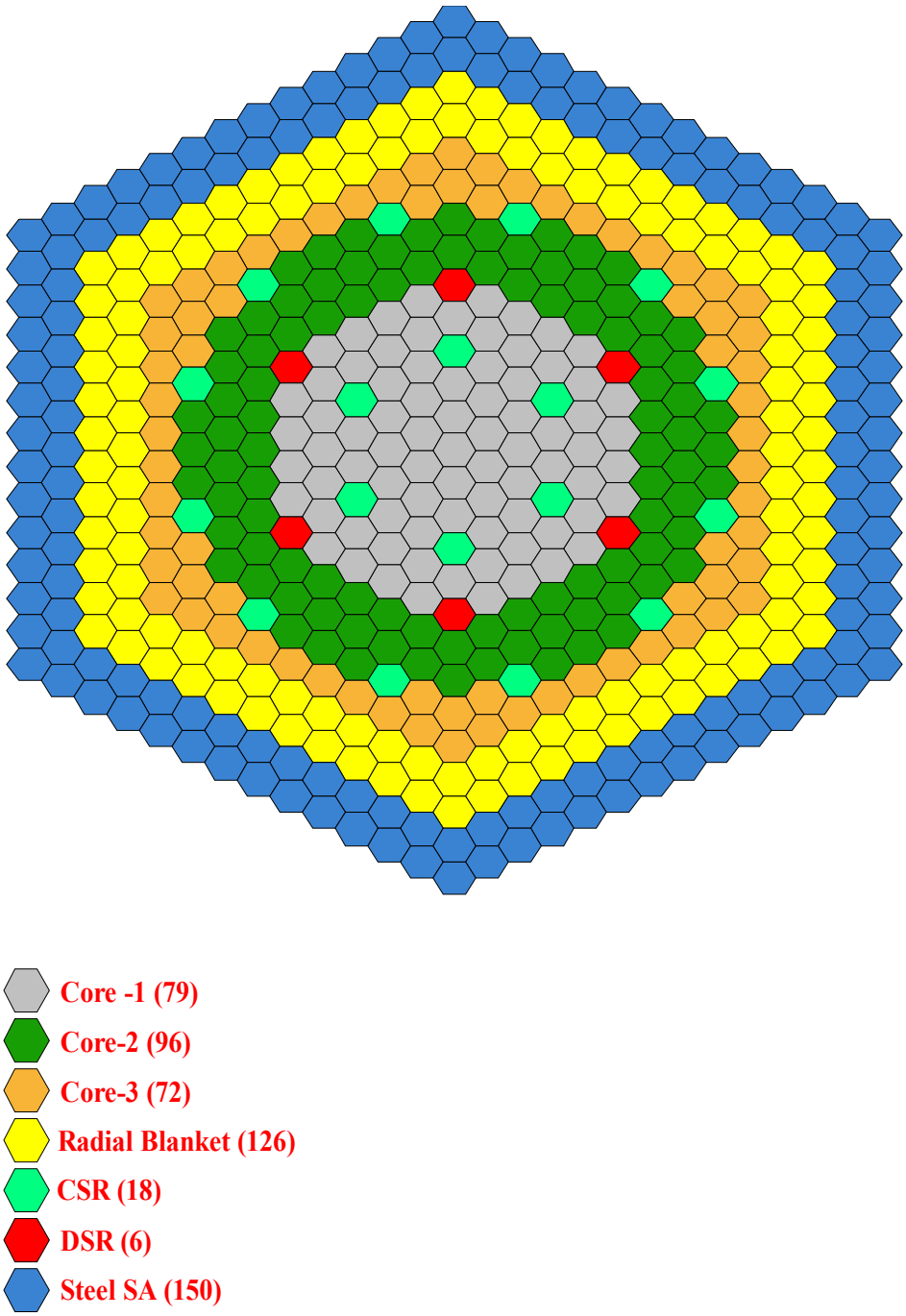

Fig.3.3. Core Configuration of 1000 MWe FBR

Table 3.2: Basic Core Design Parameters

Core Parameter		Core Size		
		Small	Medium	Large
Thermal Power (MWt)		320	1250	2630
Electrical Power (MWe)		120	500	1000
Maximum Allowed Linear heat Rating (W/cm)		450	450	500
Fuel Pin Diameter (mm)		6.6	6.6	8.0
Clad Thickness – Fuel (mm)		0.45	0.45	0.53
Assembly Pitch (mm)		135	135	168
Number of Pins per Sub-assembly –Fuel		217	217	271
Number of Rows of Radial Blanket		1	2/3	2
Pin Diameter - Blanket (mm)		14.3	14.3	12.8
Clad Thickness-Blanket (mm)		0.55	0.55	0.6
Number Pins per Sub-assembly- blanket		61	61	127
Volume Fractions of Fuel/ Steel/ Sodium	Core	26/24/50	26/24/50	32/23/45
	Radial Blanket	42/19/39	42/19/39	44/20/36
Number of Fuel Enrichments		1	2	3
Number of Fuel SA in Core Regions (Total SA)		73 (73)	85/96 (181)	79/96/72 (257)
Number of Sub-assemblies in Radial Blanket		42	120/180	126/198
Number of CSR		6	9	18
Number of DSR		2	3	6
Total Height Core		100	100	100
Total Heights-Lower/Upper Axial Blankets		30/30	30/30	30/30

3.3 Breeding and Safety Performance of 500 MWe Metal Fuelled FBR Cores

The important core physics parameters obtained for the 500 MWe fast reactors are given in Table 3.3. For comparison, the results of 500 MWe oxide fuelled PFBR core with two rows of radial blanket is also given. It is found that breeding ratio changes with Zr concentration and the number of rows of radial blanket. While the breeding ratio of the PFBR

core is 1.05 with a fuel doubling time of 65 years [Riyas and Mohanakrishnan, 2005a], FBR cores of same size, with two rows of RB can provide BR of 1.25 and 1.49 with U-Pu-10%Zr and U-Pu fuels respectively. A smear density of 0.75 is taken for the metal fuelled cores. The corresponding doubling times are 14.2 y and 8.1 y.

It is observed that the sodium void worth of 500 MWe FBR core increases from +1.7 $ to +4.4 $ as the fuel changes from oxide to metallic U-Pu-10%Zr. It has to be noted that its value further increases to +5.0 $ as the fuel changes to U-Pu. It corresponds to an increase of 200% compared to oxide fuels. This increase in U-Pu fuels is due to the higher ratio of fast flux to total flux in the U-Pu fuel compared to U-Pu-Zr fuel, though both the fast flux and the ratio of fast flux to total flux is less for the former. The schematic variation of sodium void worth and BR of metal fuels with variation of Zr in the range 10% to 0% for a 500 MWe FBR core is shown in Fig.3.4 [Riyas and Mohanakrishnan, 2006b]. It can be seen from the figure that the breeding ratio increases linearly as zirconium fraction decreases from 10% to 0%. Sodium void worth increases with the decrease in zirconium in fuel, but the rate of increase is small in the range of 0% - 5% of zirconium. It should be noted that estimated sodium void worths mentioned above using 2-D calculations are expected to be about 20% lesser compared to 3-D calculations [Mohanakrishnan et al., 1999].

Due to harder neutron spectrum, the Doppler constant in both U-Pu-Zr and U-Pu fuels are less compared with that of the oxide fuel. In metal fuels, the value of Doppler constant becomes slightly more negative with reduction in Zr content. Delayed neutron fraction increases in metal fuels due to lower enrichments and resulting increased uranium inventory. Due to the same reasons, its value shows further increase in fuels with reduced Zr content.

Also it can be seen that sodium void worth, Doppler constant and delayed neutron fraction are not varying by increasing the radial blanket thickness.

Table 3.3: Core Physics Parameters of 500 MWe FBR Core

No	Parameter		Number of Rows of Radial Blanket				
			2			3	
			Fuel Type			Fuel Type	
			Oxide	Metal U-Pu-10%Zr	Metal U-Pu	Metal U-Pu-10%Zr	Metal U-Pu
1	Plutonium Inventory (t)		1.99	1.93	2.05	1.93	2.05
2	Core Enrichments (%)		20.7/27.7	15.4/20.6	12.1/16.2	15.4/20.6	12.1/16.2
3	Breeding Ratio	Internal	0.60	0.73	0.91	0.73	0.91
		External	0.45	0.52	0.58	0.57	0.62
		Total	1.05	1.25	1.49	1.30	1.53
4	Fast Flux (10^{15} $cm^{-2}s^{-1}$)		3.23	3.78	3.48	3.78	3.48
5	Total Flux (10^{15} $cm^{-2}s^{-1}$)		5.54	5.70	5.14	5.70	5.14
6	Ratio of Fast to Total Flux		0.58	0.66	0.68	0.66	0.68
7	Reactivity Swing (pcm)		3500	2000	1000	2000	1000
8	RDT (years)		65	14.2	8.1	12.4	7.6
9	Doppler Constant (pcm)		-735	-408	-412	-411	-411
10	Delayed Neutron Fraction -pcm		340	389	418	389	418
11	Sodium Void Worth ($)		1.7	4.4	5.0	4.4	5.0
12	dpa ($year^{-1}$)		51	54	50	54	50

The residence time of the fuel and the fuel burn-up in any reactor is mainly decided by the fissile fuel availability, pellet-clad interaction and the maximum material damage that the structural material can withstand during irradiation. Even enough high internal breeding in FBR cores can provide enough excess reactivity for higher burn-up; higher neutron

fluence and temperatures existing in these cores limits the burn-up by the irradiation damage in structural materials. The dpa per year for core-1 region of the mentioned FBR cores have been estimated as a function of fuel used are also shown in Table 3.4. It has been found that, the dpa/year in the case of oxide fuel is 51, its value increases to 54 as the fuel changes to metal U-Pu-10%Zr. As the zirconium content in the metal fuel becomes zero, the dpa/year decreases to 50, due to the reduced fast and total fluxes in the latter. The only marginal changes in dpa in different fuel types are due to the nearly same ratio of fast flux to total flux in these reactor cores.

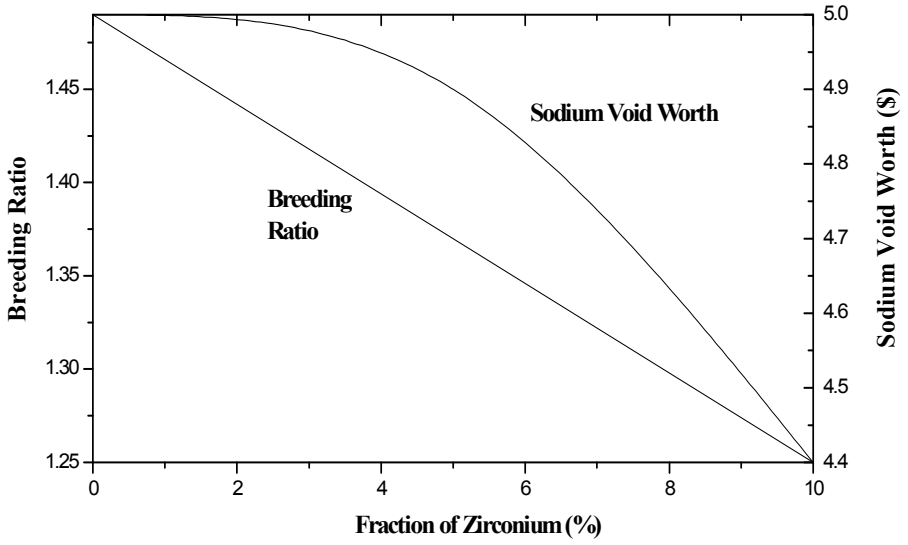

Fig.3.4. Schematic Variation of Breeding Ratio and Sodium Void Worth of a 500 MWe FBR Core as a Function of Zr Content in the Fuel

3.4 Breeding and Safety Parameters of 1000 MWe Metal Fuelled FBR Cores

The results for 1000 MWe reactors using the two types of metal fuels U-Pu-10%Zr and U-Pu are given in Table 3.4. The breeding performance with three rows of radial blanket is not attempted in this core due to the negligible influence of radial blanket on BR in large

reactors. The plutonium inventory requirement for this core is 4 tonnes and 4.3 tonnes for U-Pu-Zr and U-Pu systems respectively, which is almost twice that required for 500 MWe reactors with similar fuels. The breeding ratio obtained with the U-Pu-Zr fuel and U-Pu fuel is 1.38 and 1.61 respectively. The corresponding reactor doubling time is 9.7 years and 6.6 years. It has to be noted that, internal BR of 1.1 is possible in the 1000 MWe core with U-Pu metal fuel. An internal BR equal or greater than 1.0 translates to a zero reactivity swing and associated high fuel burn-up, provided with the availability of a suitable high irradiation resistant structural material. This could be possible even with fission products, as the loss of neutrons from fission product absorption is only about 4%. In addition, a possible small reactivity loss due to fission product formation will be compensated by the reactivity gain in the blankets.

The sodium void reactivity worth of the 1000 MWe core with both U-Pu-Zr and U-Pu fuels are high (~ 6.0 $) compared to 500 MWe oxide (~2 $) and metal-fuelled cores (~4 $). This high positive reactivity worth is an important concern for the safety of such FBR cores with high breeding. It has to be noted that, the Zr content don't have an influence on the sodium void worth. But, the Doppler constant in the operating range is higher for 1000 MWe reactors compared with that of 500 MWe reactors due to higher U-238 content.

From Table 3.4, it can be seen that, the structural material in the core-1 region have a dpa/year of 52 with metal U-Pu-10%Zr fuel. In the case of U-Pu fuel its value has been reduced to 47, due to the reduction in fast and total fluxes. The delayed neutron fraction also increases compared with 500 MWe FBR cores and fuelled with similar fuels due to the higher uranium contents.

Table 3.4: Core Physics Parameters of 1000 MWe FBR Core

No.	Parameter		Zr Content in the Ternary Fuel U-Pu-Zr	
			10%	0%
1	Plutonium Inventory (t)		4.0	4.3
2	Core Enrichments (%)		12.6/13.9/18.9	10.2/11.0/15.2
3	Breeding Ratio	Internal	0.92	1.12
		External	0.46	0.49
		Total	1.38	1.61
4	Fast Flux (10^{15} $cm^{-2}s^{-1}$)		3.67	3.36
5	Total Flux (10^{15} $cm^{-2}s^{-1}$)		5.68	5.08
6	Fast Flux to Total Flux Ratio		0.65	0.66
7	Reactivity Swing (pcm)		1000	0
8	RDT (years)		9.7	6.6
9	Doppler Constant		-501	-479
10	Delayed neutron fraction (pcm)		404	432
11	Sodium void worth ($)		6.3	6.2
12	dpa ($year^{-1}$)		52	47

3.5 Effect of Modified Fuel Pin Designs on Breeding Characteristics

From previous discussions on the breeding characteristics of FBR cores fuelled with U-Pu-Zr ternary alloys, it is clear that BR can be increased by reducing Zr in the fuel pellet. Zr has been added to the fuel to improve its physical and chemical properties. In addition, it has a role in deciding the pellet-clad interactions. At the same time, it has to be noted that, the efforts to enhance the BR by reducing Zr may limit the burn-up of metallic fuels due to the increased pellet-clad interaction. One way of reducing the pellet-clad interaction and to retain the benefits of both higher breeding and burn-ups is to provide a physical barrier between fuel-pellet and clad. The barrier called liner can be made of different materials like

Chromium, Zirconium, Molybdenum, Titanium and Tungsten [Kim et al., 2009]. The effects of these liner materials on the breeding performance are studied and found that both Cr and Zr are having the same breeding effects [Riyas and Mohanakrishnan, 2007a]. But, due to the better compatibility with fuel, Zr is chosen as the liner material in the present study. Schematic of such modified fuel pin designs with liner is shown in Fig.3.5. A comparison of reference and modified pins are given in Table 3.5.

The outer diameter of reference pin is 8 mm with a clad thickness of 0.53 mm. Fuel smear density of 75% has been taken with pellet radius to 3.0 mm. In the modified pin design, 0.150 mm thick zirconium liner is attached inside the clad. Since the same SD of 75% is retained, pellet diameter reduces to 5.75 mm in the modified design. Due to the introduction of liner, the fuel and sodium volume fractions of the modified pin become slightly less than that of the reference pin as shown in the Table 3.5 [Riyas and Mohanakrishnan, 2007b; Riyas and Mohanakrishnan, 2009a].

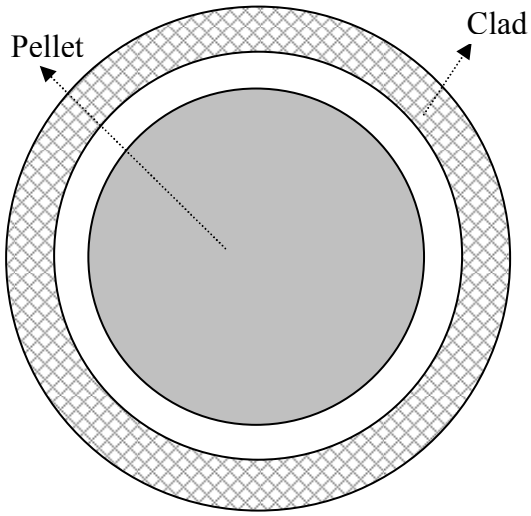

Fig.3.5a. Cross-sectional View of the Reference Pin (Not to the Scale).

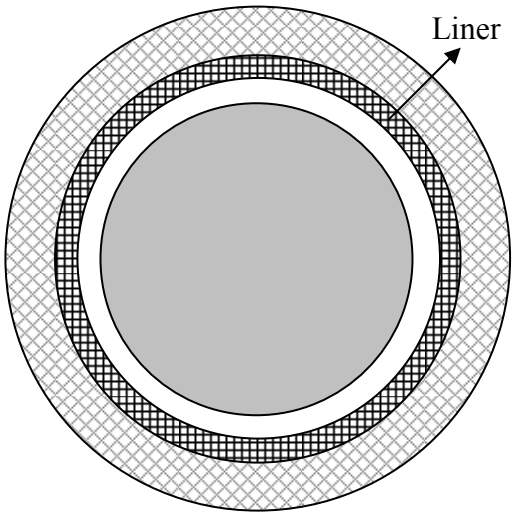

Fig.3.5b. Cross-sectional View of the Modified Pin (Not to the Scale).

Table 3.5: Reference and Modified Fuel Pin Designs

Parameter		Pin Type	
		Reference Pin	Modified Pin
Pin Outer Diameter (mm)		8	8
Clad Thickness (mm)		0.53	0.53
Liner Thickness (mm)		Not applicable	0.150
Pin Inner Diameter (mm)		6.94	6.64
Pellet Diameter (mm)		6.01	5.75
Volume Fractions (%)	Steel	23.16	23.16
	Fuel	41.94	38.39
	Sodium	45.37	44.48
	Sodium Bonding	10.5	9.6
	Liner Material	No liner	3.547

Table 3.6: Physics Parameters of the 1000 MWe Metal FBR with Zirconium Liner

Parameter	Pin Type	
	Reference Pin	Pin with Zr-Liner
Core Enrichments in Core1/Core2/Core3	10.2/11.0/15.2	10.8/11.7/16.2
Breeding Ratio	1.61	1.55
RDT (years)	6.6	7.7
Delayed Neutron Fraction (pcm)	432	422
Sodium Void Worth ($)	6.2	6.3

The effects of modified fuel pin design on the breeding and main safety characteristics are investigated on a 1000 MWe FBR core fuelled with binary U-Pu alloy, which constitutes the reference core. In the modified core, a zirconium liner of 150 μm is introduced in the fuel pin inside the clad. The study is performed on the modified core and the main results are given in Table 3.6. To compare the effect of zirconium liner, the results

of reference core analysis are also given in table. The breeding ratio and doubling time obtained with the core of modified fuel pins are 1.55 and 7.7 years respectively. For the reference case these were 1.61 and 6.6 years respectively. From Table 3.6, it can be seen that the sodium void worth remains almost same in the two cases (~6.2 $).

3.6 Methods to Reduce the Sodium Void Worth

High positive sodium void worth is a safety concern for medium and large sodium cooled FBR cores. Also, its value is more positive in metal fuelled FBR cores as compared to ceramic fuelled cores. Core designs with near zero or negative sodium void coefficients are of great importance in emerging sodium cooled fast reactor designs with enhanced safety. Here two methods of reducing sodium void worth are examined without much compromise on breeding ratio and doubling time. In the first method, a sodium plenum is included in place of upper axial blanket. This is in accordance with the methods adopted in the BN-800 reactor to reduce sodium void worth [IAEA, 2000]. In the present study, the method is adopted in a 1000 MWe FBR core fuelled with U-Pu-10%Zr ternary alloy [Riyas and Mohanakrishnan, 2008]. As described in the previous section, the reference core is having an active fuel region length of 100 cm with axial blankets of 30 cm above and below the core. In an effort to reduce sodium void worth, the core is modified such that the upper axial blanket is replaced with a sodium plenum. The R-Z model of the reference core and the modified core are given in Fig.3.6 and Fig.3.7, respectively.

From Table 3.7, it can be seen that sodium void worth of the reference core is equal to 6.3 $. It has to be noted that the bonded sodium is not voided while calculating the sodium void worth. By adopting modified core design with a sodium plenum reduces the sodium void worth to 3.6 $, a reduction by 43% and is very favorable from safety point of view. The

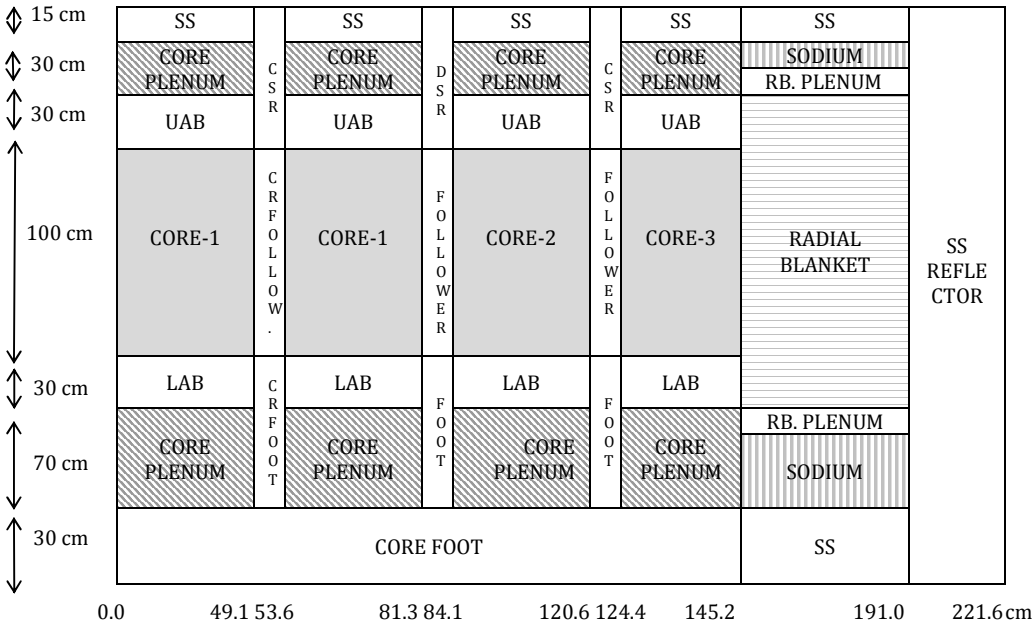

Fig.3.6. R-Z Model of the Reference Core

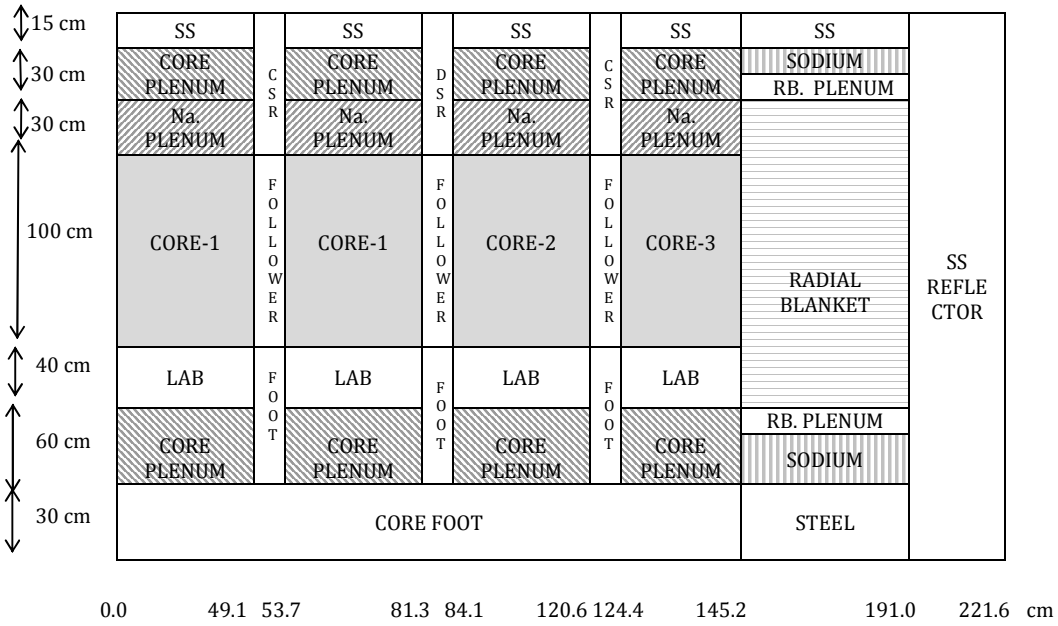

Fig.3.7. R-Z Model of the Modified Core with Sodium Plenum

compromise on breeding ratio and doubling time with the modification are found to be small. With the sodium plenum, the breeding ratio decreases from 1.38 to 1.31, with a

corresponding increase of doubling time from 9.7 years to 11.8 years [Riyas and Mohanakrishnan, 2005b]. As metal fuel pins have gas plenum in the top region, it is easy to have the sodium plenum above the fuel region. Also Doppler constant increases with this modification in the core design. All this increases reactor safety without much compromise on breeding.

Table 3.7: The Reduction of Sodium Void Worth by Sodium Plenum

Parameters	Core Type	
	1000 MWe, U-Pu-10%Zr	
	Reference Core	Modified Core with Sodium Plenum
Core Enrichments	12.6/13.9/18.9	12.7/14.0/19.1
Breeding Ratio	1.38	1.31
RDT (years)	9.7	11.8
Doppler Constant (pcm)	-527	-608
Sodium Void Worth ($)	6.3	3.6

In another method, the sodium void worth is reduced by decreasing the fuel smear density and the study is performed in a 1000 MWe, U-Pu fuelled core. Table 3.8 shows how the smear density affects the physics parameters. As the fuel smear density changes from 75% to 62%, sodium void worth decreases from 6.2 $ to 5.8 $, it leads to a small reduction in BR too. BR reduces from 1.61 to 1.50 for this core with a corresponding increase in doubling time from 6.6 years to 7.3 years.

Table 3.8: The Effect of Fuel Smear Density to Reduce the Sodium Void Worth

Parameters	Core Type	
	1000 MWe, U-Pu	
	Reference Core SD = 0.75	Modified Core SD = 0.62
Core Enrichments (%)	10.2/11.0/15.2	11.4/12.4/17.3
Breeding Ratio	1.60	1.50
RDT (years)	6.6	7.3
Doppler Constant (pcm)	-479	-500
Sodium Void Worth ($)	6.2	5.8

As the fuel smear density decreases, the ratio of fast flux to total flux decreases and causes a reduction in sodium void worth. At the same time it gives an increase in Doppler constant and a slight decrease in plutonium inventory. As compared to the first method, the reduction in sodium void worth is less in the present method. It has been seen that both the modifications in the core design leads to reduction in sodium void worth, even though the latter gives only a marginal reduction. The reduction in sodium void worth in large FBR cores is important with respect to its ULOFA transient behaviour.

3.7 Core Physics Analysis of Experimental Fast Breeder Reactor

The core design of the small experimental breeder reactor reported here is similar to one reported by the research team of IGCAR recently [Devan et al., 2011]. The radial core configuration is as shown in Fig.3.1 with 73 fuel SA and plutonium enrichment of 20%. The possible plutonium enrichment in the core is limited up to a maximum of 20%. This reactor design is planned and designed to achieve experience in metallic fuel irradiation.

It has been seen from the discussions in chapter-1, irradiation experience of various U-Pu-Zr metallic fuels are available from EBR-II with Zr concentrations of 6%, 10% and

14%. Out of these, due to the optimum thermodynamic properties, achieved higher burn-ups and possible nonproliferation features, U-Pu-10%Zr fuel was chosen as the candidate for IFR [Wade and Chang, 1988]. In addition, choice of metallic fuels with Zr concentrations more than 10% will cause reduction of thermal conductivity; problems in fuel fabrication due to increased of melting point and a reduction of achievable BR. But, the higher BR and shorter doubling times possible with metallic fuels of U-Pu-6%Zr makes it attractive for the Indian fast reactor program. So, from the reported international experience and national requirement it is better to choose metallic ternary alloys with 6% zirconium as a promising and challenging fuel type for better BR as compared to the well experienced 10% Zr fuels. It is assumed that, the possible enhanced fuel-clad interactions and associated limited burn-up in such fuel types could be minimized with advanced fuel pin designs and materials.

Due to the reasons mentioned above, a Zr content of 6% is chosen for the metallic fuel for the experimental breeder. Two dimensional analyses are performed to find the breeding capacity of such reactors and found that a small breeder reactor core is possible with 73 fuel SA of single enrichment and with one row of RB. Te results of such analysis are shown in Table 3.9. To compare the breeding potential and safety characteristics of FBR cores with respect to core size, the 500 MWe and 1000 MWe cores also analysed with the chosen fuel type of U-Pu-6%Zr and the results are given in the table.

It is found that the BR possible with small, medium and large reactors is 1.1, 1.36 and 1.49 respectively [Riyas and Mohanakrishnan, 2009b]. The corresponding RDT are 67 years, 10.5 years and 7.5 years respectively. The sodium void worth is less than 1 $ in the case of experimental reactor and 4.5 $ and 6.3 $ for the medium and large reactors. But the Doppler constant shows the reverse trend and becomes more negative with core size.

Table 3.9: Breeding and Safety Parameters of Metal FBR Cores Fuelled with U-Pu-6%Zr Alloy

No.	Parameter		Reactor Size (Power- MWe)		
			Small (120)	Medium (500)	Large (1000)
1.	Core Excess Reactivity (pcm)		7000	4500	3000
2	Number of Core Enrichments		1	2	3
3	Plutonium Enrichment (wt%)		19.6	13.6/18.2	11.15/12.4/16.7
4	Number of Fuel SA		73	181	247
5	Number of Radial Blanket SA		42	120	126
6	Breeding Ratio	Internal	0.63	0.83	1.03
		External	0.47	0.53	0.46
		Total	1.10	1.36	1.49
7	Reactor Doubling Time (years)		60	10.5	7.5
8	Delayed Neutron Fraction (pcm)		385	403	419
9	Sodium Void Worth (pcm)		+164	+1830	+2340
10	Doppler Constant (pcm)		-336	-470	-524
11	Prompt Neutron Life Time (μs)		0.248	0.278	0.264
12	Effective Delayed Neutron decay constant (s^{-1})		0.0921	0.0941	0.0965
13	Effective delayed neutron life time (s)		7.52	7.36	7.18
14	Effective neutron life time (s)		0.041	0.043	0.044

Other properties like prompt and delayed neutron parameters are also shown in the table and found that they don't have significant dependence on core size. It is clear that, the breeding and sodium void worth of FBR cores have strong core size dependence. It means that, a proper decision has to be taken for the Indian metal fuelled FBR cores with respect to core size, sodium void worth and breeding potential for a safe, faster and sustainable nuclear

growth. Also the renewed safety concern on nuclear reactors, especially on the sodium cooled fast reactors with positive void coefficient necessitates alternate core design concepts with better safety coefficients. Heterogeneous cores with better safety and breeding performance can be one of such options.

3.8 Summary and Conclusions

In this study, breeding and safety parameters of U-Pu-Zr metal-fuelled cores have been analyzed with respect to core size, Zr content and RB thickness. While the BR achievable with oxide fuelled, 500 MWe PFBR core is 1.05, it is found to be 1.25 for 500 MWe U-Pu-10%Zr metal FBR of same size. At the same time, metallic FBR has higher sodium void worth of 4,5 $ compared to 1.7 $ in oxide core. It is also found that, both BR and sodium void worth shows an increasing trend with reduction of Zr content in the fuel and core size. BR of 1.49 and doubling time of 7.5 years are possible with U-Pu-6%Zr fuelled 1000 MWe FBR core. However, it has sodium void worth of +6.3 $. In-core breeding of 1.0 is possible with 1000 MWe metal fuelled FBR cores and thus very high burn-up cores could be designed. Core designs with higher BR are advisable for faster nuclear growth, but higher sodium void worth in these cores is a safety concern. The study also reveals that, thickness of RB doesn't have a significant influence on the breeding performance of medium and large FBR cores. Two methods to reduce sodium void worth are applied in large FBR cores. In one of the method, by replacing the upper axial blanket with sodium plenum can cause a reduction of sodium void worth by 43%. The Doppler constant becomes more negative with core size and reduction of Zr. The effects of advanced fuel pin designs on the breeding characteristic are also studied.

Chapter 4

PERTURBATION THEORY IN NUCLEAR REACTOR ANALYSIS AND SAFETY OF FAST BREEDER REACTOR CORES

4.1 Introduction

Static and transient analysis of FBR cores in IGCAR uses reactivity worth data based on the results of 1st order perturbation theory. The important data are sodium void, Doppler, material removal and boundary movement reactivity worths. Even the net reactivity change due to the above effects can be estimated using 2-k methods also; its spatial decomposition is possible with perturbation method. The spatial distribution of this worth change from the core zones can be used to find the feedback reactivity during a transient in the dis-assembly phase. It has to be noted that the temperature changes and the transient response is space and time dependant. The code NEWPERT is used for the 1st order perturbation studies.

Even though the first order approximation is valid only for small perturbation in core, the same method is usually employed for larger perturbations like 100% voiding of coolant, steel and fuel from PFBR core. The estimated material removal worth corresponding to 100% voiding is used for the arbitrary small and space dependant perturbations during a transient after linear scaling. The Doppler distribution in the given temperature limits are used appropriately for finding the feedback for the spatial and time dependant temperature changes during a transient.

The validity of the above approximation is verified with the help of an exact perturbation code. An exact perturbation code PERTX [Riyas, 2011; Riyas and Mohanakrishnan, 2011] is developed for this purpose by modifying the code NEWPERT. In

this study, the errors in the first order estimated worths are obtained with respect to the exact perturbation theory.

IGCAR perturbation studies performed with PERTX code is verified by the ERANOS code system [Rimpault et al., 2002]. 2D perturbation options available in ERANOS 2.1 along with JEFF 3.1 nuclear data have been performed for the comparison and validation studies [Riyas et al., 2013].

The required theory used for the development of exact perturbation code PERTX is presented in Section-4.2. Core design parameters and calculation scheme is given in section 4.3. The results obtained with IGCAR and ERANOS code systems are explained in Section-4.4. The results include the prediction of sodium void worth, fuel void worth and steel void worth. The estimation of Doppler constant and plutonium equivalence (a parameter used to find the relative worth of a fuel isotope in continuing the neutron chain reaction compared to plutonium-239) are also discussed. It is estimated by first order methods. The main conclusions of the study are presented in Section-4.5.

This study helped to verify the results of IGCAR 1st order perturbation scheme with exact results and enabled validation with ERANOS system. The validation studies are performed in an equilibrium core of oxide fuelled PFBR [Riyas et al., 2013]. The first order and exact perturbation scheme is then used for the ULOF transient analysis of metallic fuelled FBR cores. The results of such studies will be explained in the next chapter.

4.2 Reactivity Change Using Standard Perturbation Theory

The fundamental eigen-value problem of a neutron multiplying system can be written as [Ronen, 1986];

$$L\Phi(x) - \lambda P\Phi(x) = 0 \qquad (4.1)$$

Where, Φ : neutron flux which is a function of energy and space,

x : symbolic representation of all independent variables like energy, space and direction coordinates.

L : neutron loss operator, defines the rate at which neutrons disappear from the system,

P : neutron production operator, defines the rate at which neutrons are produced in the system, and

λ : eigen-value.

The eigen-value λ is related to the neutron multiplication factor k by, $k=1/\lambda$

By taking the inner product of both sides of Equation 4.1 with an arbitrary, non-zero weight function W(x), the following expression for λ can be determined as,

$$\lambda = \frac{< W\ L\ \Phi >}{< W\ P\ \Phi >} \tag{4.2}$$

When the system is perturbed, operators L and P change to L+ΔL and P+ΔP respectively. The flux and eigen-value correspondingly change to Φ+ΔΦ and λ+Δ λ. Similar equation can be written for the perturbed system as,

$$(\mathrm{L} + \Delta\mathrm{L})\ (\Phi + \Delta\Phi) = (\lambda + \Delta\lambda)(\mathrm{P} + \Delta\mathrm{P})(\Phi + \Delta\Phi) \tag{4.3}$$

ΔL and ΔP are the operators that represent the change in loss and production rates due to perturbation. ΔΦ and Δ λ are the change in flux and eigen-value due to the perturbation. Applying the weight function W(x) on both sides of the equation 4.3 and on rearrangement gives,

$$\Delta\lambda = \frac{< W\ (\Delta\mathrm{L} - \lambda\Delta\mathrm{P})(\Phi + \Delta\Phi) > + < W(L - \lambda P)(\Delta\Phi) >}{< W\ (\mathrm{P} + \Delta\mathrm{P})(\Phi + \Delta\Phi) >} \tag{4.4}$$

If W is chosen as the λ-mode adjoint flux function of the unperturbed core, that obeys the equation,

$$L^{+}\Phi^{+}(x) - \lambda P^{+}\Phi^{+}(x) = 0 \tag{4.5}$$

where,

Φ^{+} : adjoint neutron flux which is a function of energy and space,

L^{+} : adjoint neutron loss operator, and

P^{+} : adjoint neutron production operator,

With this substitution, it can be shown that,

$$< W(L - \lambda P)\Delta\Phi > = < \Phi^{+}(L - \lambda P)\Delta\Phi > = < \Phi^{+}(L^{+} - \lambda P^{+})\Delta\Phi > = 0$$

Then, the expression of exact change in eigen-value given by equation 4.4 reduces to,

$$\Delta\lambda = \frac{< \Phi^{+}(\Delta L - \lambda\Delta P)\Phi^{'})}{< \Phi^{+} P\Phi^{'})} \tag{4.6}$$

Φ'= Φ+ΔΦ and P'=P+ΔP represent the flux function and production operator of the perturbed state respectively.

Now,

$$\Delta\lambda = \lambda_2 - \lambda_1 = \frac{1}{k_2} - \frac{1}{k_1} = \frac{k_1 - k_2}{k_1 k_2} = -\Delta\rho \tag{4.7}$$

where, Δρ is the reactivity change occurs due to the perturbation. λ_1 and λ_2 are the eigen-values associated with unperturbed and perturbed cores respectively. From equations 4.6 and 4.7, the exact expression for reactivity change can be written as,

$$\Delta\rho = \frac{< \Phi^{+} (\lambda\Delta P - \Delta L) \Phi^{'} >}{< \Phi^{+} P \Phi^{'} >}$$

or,
$$\Delta\rho = \frac{\lambda < \Phi^{+} (\Delta P) \Phi^{'} > - < \Phi^{+} (\Delta L) \Phi^{'} >}{< \Phi^{+} P \Phi^{'} >} \tag{4.8}$$

and, $< \Phi^{+} \, P\Phi^{'} > is\ called$ imporatnce function

Now, total change in loss ΔL can be represented as the sum of changes in leakage, capture, fission, scattering and (n,xn) reactions. The change in production can be written as the sum of changes in fission rate and fission spectrum in the core. That is,

$$\Delta L = \Delta L_{leakage} + \Delta L_{capture} + \Delta L_{fission} + \Delta L_{scattering} + \Delta L_{(n,xn)} \quad (4.9)$$

and, $\Delta P = \Delta P_{fission} + \Delta P_{fission\ spectrum}$ (4.10)

It is seen that, the total change in reactivity due to a perturbation can be given as the sum of the change in individual components of leakage, capture, scattering, fission, fission spectrum, and leakage [McMurry, 1956; Ronen, 1986]. Thus the total reactivity change, Δρ can be expressed as,

$$\Delta\rho = \Delta\rho_{fission} + \Delta\rho_{fission\ spectrum} + \Delta\rho_{leakage} + \Delta\rho_{scattering} + \Delta\rho_{(n,xn)} \quad (4.11)$$

The individual terms can be computed as,

$$\Delta\rho_{fission} = \lambda < \Delta P_{fission} > -\lambda < \Delta L_{fission} > \quad (4.12a)$$

$$\Delta\rho_{fission\ spectrum} = \lambda < \Delta P_{fission\ spectrum} > \quad (4.12b)$$

$$\Delta\rho_{capture} = -< \Delta L_{capture} > \quad (4.12c)$$

$$\Delta\rho_{leakage} = -< \Delta L_{leakage} = -\left(< \Delta L^{axial}_{leakage} > + < \Delta L^{radial}_{leakage} >\right) \quad (4.12d)$$

$$\Delta\rho_{scattering} = -< \Delta L_{scattering} >= -(< \Delta L^{elastic}_{scattering} + \Delta L^{inelastic}_{scattering} >) \quad (4.12e)$$

and, $\Delta\rho_{n,xn} = -< \Delta L_{n,xn} >$ (4.12f)

The total leakage component of reactivity due to perturbation can be written as the sum of axial and radial contributions. Similarly the scattering contribution can be written as the sum of elastic and in-elastic components.

Thus,

$$\Delta\rho_{\text{leakage}} = -\left(\Delta\rho_{\text{leakage}}^{\text{axial}} + \Delta\rho_{\text{leakage}}^{\text{radial}}\right) \tag{4.13a}$$

$$\Delta\rho_{\text{scattering}} = \Delta\rho_{\text{elastic}} + \Delta\rho_{\text{inelastic}} \tag{4.13b}$$

The individual production and loss components in the perturbation equation can be calculated from the following expressions. The integration has to be replaced by a summation over the mesh volumes of interest for an actual calculation using computer program. Similarly, the summation through all the neutron groups is also essential.

$$< \Delta L_{\text{leakage}}^{\text{axial}} > = \frac{\sum_{\mathbf{g}} \int_{\mathbf{v}} \delta \mathrm{D}_{\mathrm{g}}^{\text{axial}} \left(\nabla \Phi_g^{+} \nabla \Phi_g^{'}\right) dV}{\mathrm{I}} \tag{4.14a}$$

$$< \Delta L_{\text{leakage}}^{\text{radial}} > = \frac{\sum_{\mathrm{g}} \int_{\mathrm{v}} \delta \mathrm{D}_{\mathrm{g}}^{\text{radial}} \left(\nabla \Phi_g^{+} \nabla \Phi_g^{'}\right) dV}{\mathrm{I}} \tag{4.14b}$$

$$< \Delta \mathrm{L}_{\text{capture}} > = \frac{\sum_{\mathrm{g}} \int_{\mathrm{v}} \delta \Sigma_{\mathrm{g}}^{\mathrm{c}} \left(\Phi_g^{+} \Phi_g^{'}\right) dV}{\mathrm{I}} \tag{4.14c}$$

$$< \Delta \mathrm{L}_{\text{fission}} > = \frac{\sum_{\mathrm{g}} \int_{\mathrm{v}} \delta \Sigma_{\mathrm{g}}^{\mathrm{c}} \left(\Phi_g^{+} \Phi_g^{\prime}\right) dV}{\mathrm{I}} \tag{4.14d}$$

$$< \Delta \mathrm{P}_{\text{fission}} > = \frac{\sum_{\mathrm{g}} \int_{\mathrm{v}} \Phi_g^{+} \chi_g \sum_{g'} \delta \left(\nu \Sigma_{\mathrm{g}'}^{\mathrm{f}}\right) \Phi_{g'}^{'} dV}{\mathrm{I}} \tag{4.14e}$$

$$< \Delta \mathrm{P}_{\text{fission spectrum}} > = \frac{\sum_{\mathrm{g}} \int_{\mathrm{v}} \Phi_g^{+} \sum_{g'} \left(\delta \chi_{g'} \nu \Sigma_{\mathrm{g}'}^{\mathrm{f}} \Phi_{g'}^{'}\right) dV}{\mathrm{I}} \tag{4.14f}$$

$$< \Delta L_{elastic} >= \frac{\sum_g \int_v \Phi_g^+ (\sum_{g'>g} (\Phi_{g'}^{'} - \Phi_g^{'}) \Sigma_{g' \to g}^{elastic}) dV}{I} \quad (4.14g)$$

$$< \Delta L_{inelastic} >= \frac{\sum_g \int_v \Phi_g^+ (\sum_{g'>g} (\Phi_{g'}^{'} - \Phi_g^{'}) \Sigma_{g' \to g}^{inelastic}) dV}{I} \quad (4.14h)$$

$$< \Delta L_{n,xn} >= \frac{\sum_g \int_v \Phi_g^+ ((\sum_{g'=1} \Phi_{g'}^{'} \delta\Sigma_{g' \to g}^{n,xn}) - \delta\Sigma_g^{n,xn} \Phi_g^{'}) dV}{I} \quad (4.14i)$$

The summation is over the energy groups and the integral is over the region of interest. Practically, the integral is replaced with a summation over the mesh volumes. The suffix 'g' denotes the energy group 'g'. The expressions for the reactivity change due to the change in fission spectrum and (n, xn) reactions are taken from the ERANOS manual [Tommasi, 2007] as they are not used in the code PERTX. The importance integral, *I* is given by the expression,

$$I = \sum_{\mathbf{g}} \int_v \Phi_g^+ \chi_g \left(\sum_{g'} \nu\Sigma_{g'}^f \Phi_{g'}^{'} \right) dV \quad (4.15)$$

The notations used in the above expressions are as follows:

Φ ,Φ^+ - direct and adjoint flux of the unperturbed core

Φ' - direct flux of the perturbed core

D^{axial} - axial component of the diffusion coefficient

D^{radial} - radial component of the diffusion coefficient

D - total component of the diffusion coefficient

Σ^c - macroscopic capture cross-sections

Σ^f - macroscopic fission cross-sections

$\Sigma^{elastic}$ - macroscopic elastic scattering cross-sections

$\Sigma^{in\text{-}elastic}$ - macroscopic in-elastic scattering cross-sections

χ - fission spectrum

δD - change in diffusion coefficient

$\delta\Sigma^c$ - change in capture cross-section

$\delta\Sigma^f$ - change in fission cross-section

$\delta\Sigma^s$ - change in scattering cross-sections with $\Sigma^s = \Sigma^{elastic} + \Sigma^{inelastic}$

$\delta\chi$ - the change in fission spectrum due to perturbation

$\delta(\nu\Sigma^f)$ - change in the product $\nu\Sigma^f$

All theses quantities are functions of energy group and mesh.

If Σ_{tr} and Σ'_{tr} are the macroscopic transport cross-sections of the un-perturbed and perturbed core respectively, the diffusion coefficients are given by [Pitterle and Paik, 1972],

$$D = \frac{1}{3\Sigma_{tr}} \quad \text{and } D' = \frac{1}{3\Sigma'_{tr}} \tag{4.16a}$$

Therefore, $$\delta D = D' - D = \frac{\delta\Sigma_{tr}}{\Sigma_{tr}\Sigma'_{tr}} \tag{4.16b}$$

4.2.1 First Order Approximation

In the first order approximation, the perturbation is assumed to be small so that the flux is not appreciably changed with perturbation [Ronen, 1986]. Thus,

$$\Phi'_g = \Phi_g + \delta\Phi_g \approx \Phi_g \quad \text{for first order perturbation.} \tag{4.17a}$$

Therefore, in the first order approximate estimation of the reactivity change, the direct flux of the perturbed core used in the above integrals can be replaced with the unperturbed direct flux. Also, the changes in transport cross-section $\delta\Sigma_{tr}$ are assumed to be small for small perturbations, so that for the for first order,

$$\Sigma'_{tr} = (\Sigma_{tr} + \delta\Sigma_{tr}) \approx \Sigma^2_{tr} \tag{4.17b}$$

For first-order approximation, the change in diffusion coefficient (see equation 4.16b) is given by,

$$\delta D = \frac{\delta \Sigma_{tr}}{\Sigma_{tr}^2} \qquad (4.17c)$$

4.2.2 Reactivity Change by Direct Method

The reactivity change associated with a perturbation can be estimated with direct method. If k_1 and k_2 are the multiplication factors of the reference and perturbed core, the reactivity change can be estimated as,

$$\Delta\rho = \rho_2 - \rho_1 = \frac{1}{k_1} - \frac{1}{k_2} = \frac{\Delta k}{k_1 k_2} \;\; ; \;\; with, \qquad \Delta k = k_2 - k_1 \qquad (4.18)$$

The value of total reactivity change predicted from exact perturbation method can be well verified with the above expressions.

4.3 Core Design Parameters and Calculation Scheme

The PFBR core at beginning of equilibrium (BOEC) is used for the analysis [Devan et al., 2011a]. The basic design parameters are shown in Table 4.1. The radial distribution of is same as that of the 500 MWe FBR core mentioned before in chapter 3 and the R-Z model is shown in Fig.4.1 [Riyas and Mohanakrishnan, 2011]. The height of PFBR core and sub-assembly area at hot temperature state is taken as 101.7 cm and 162.04 cm^2 respectively. Average concentration of various fuel isotopes and fission products corresponding to PFBR equilibrium core has been used for calculation. IGCAR scheme consists of ATOMIX-CONSYST-EFCONSY-ALCIALMI-ALEX-PERTX codes for the perturbation calculations along with the ABBN-93 cross-sections. The ERANOS scheme consists of the diffusion and perturbation codes along with the JEFF 3.1 data.

The isotopic concentrations of different mixtures of the reactor core are directly feed to the IGCAR and ERANOS calculation procedures, to avoid the effects of core expansion which are taken differently in two systems. To match with the ABBN-93 representation of fission products, number densities of fission products are doubled for ERANOS.

4.4 Results and Discussion

The main results of the first order and exact perturbation calculations are discussed in this section. The predicted multiplication factor of the reference unperturbed core using the IGCAR two dimension diffusion calculations is 1.0436 while it is 1.0467 with ERANOS assuming homogeneous fuel and absorber rods. Thus ERANOS 2.1 with JEFF3.1 over-predicts the estimated IGCAR k_{eff} by 308 pcm. This may be due to the difference between the nuclear data and calculation methods employed in the two schemes.

Comparison between the two schemes of perturbations IGCAR code system and ERANOS is done for voiding worth of sodium, fuel, steel and for the estimation of Doppler constant. The individual contributions from leakage, capture, fission, fission spectrum, elastic and inelastic scatterings and (n, xn) reactions can be possible with ERANOS perturbation methods. Even though, self-shielding effects with voiding are taken in ERANOS, this is neglected in IGCAR code system calculations because of its small contribution to total reactivity change.

Table 4.1: Basic Design Parameters

Reactor Power	(MWe)	500
Fuel Type		MOX
Number of Fuel Enrichment Zones		2
Core Enrichments	(%)	20.7/27.7
Number of Fuel Sub-assemblies		85/96
Number of Sub-assemblies in Blanket		120
Maximum Linear heat Rating	(W/cm)	450
Fuel Pin Diameter	(cm)	0.66
Clad Thickness - Fuel	(cm)	0.045
Assembly Pitch	(cm)	13.5
Fuel Pins per Sub-assembly		217
Volume Fractions of Fuel/ Steel/ Sodium – Core Region	(%)	35.1/23.9/41.3
Number of Rows of Radial Blanket		2
Blanket Pin Diameter	(cm)	1.433
Clad Thickness – Blanket	(cm)	0.06
Pins per Blanket Sub-assembly		61
Volume Fractions of Fuel/ Steel/ Sodium in Blanket	(%)	52.3/19.5/28.2
Number of CSR		9
Number of DSR		3
Total Axial Blanket Height	(cm)	30+30=60

It has to be noted that the break-up of total leakage into axial and radial components and total scattering into elastic and inelastic components are only available with ERANOS and not with IGCAR codes. Therefore, the component of total leakage and scattering are only given in the results. Also the contribution from fission spectrum and (n, xn) reactions are also not available with PERTX. These contributions are also given in the results though these components are negligible in most of the cases of perturbation considered. Plutonium

equivalence of various fuel isotopes present in the cote are also estimated using both the schemes.

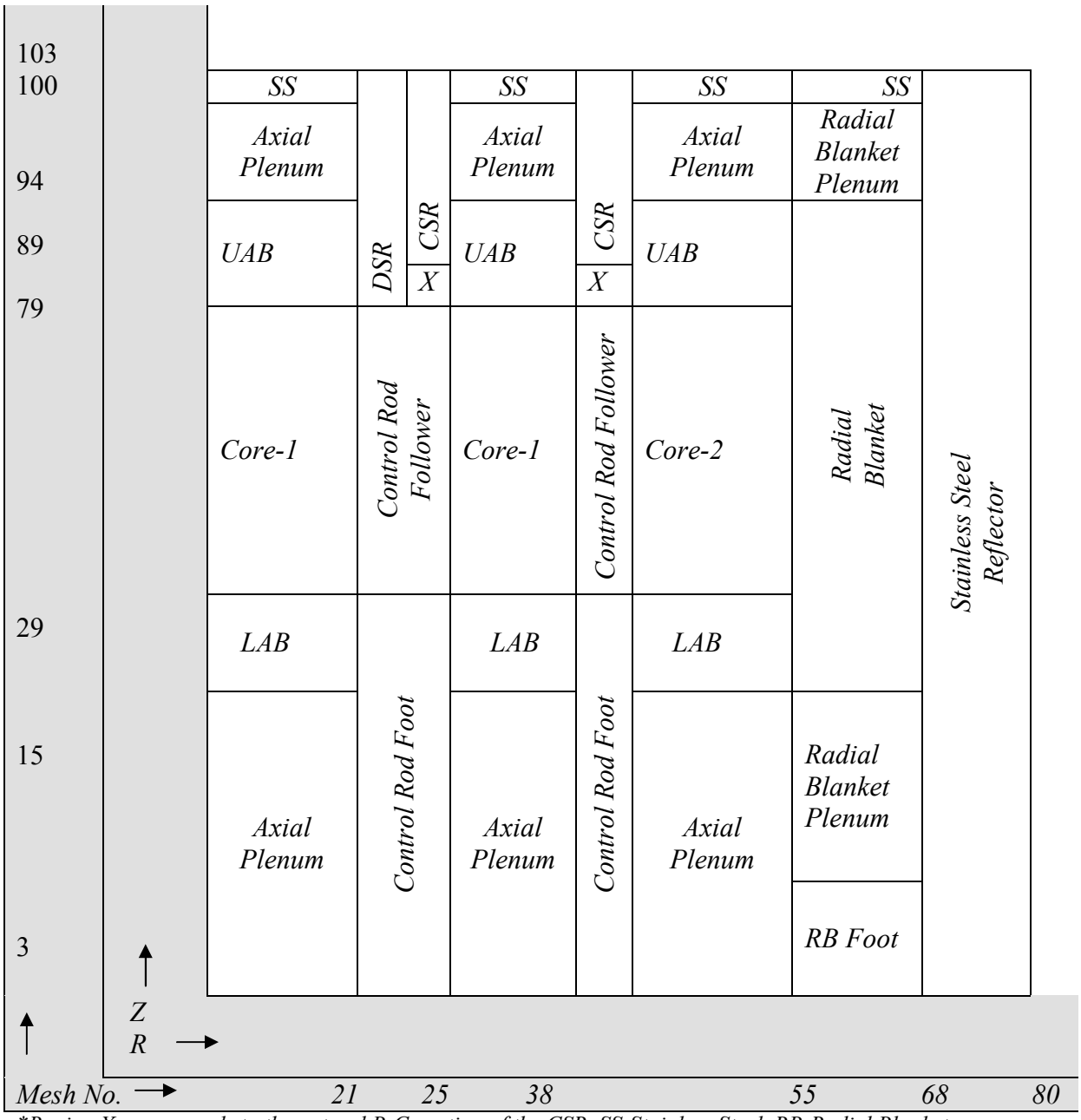

**Region X corresponds to the natural B_4C portion of the CSR, SS-Stainless Steel, RB-Radial Blanket LAB-Lower Axial Blanket, UAB-Upper Axial Blanket*

Fig.4.1.The RZ Model of the PFBR Oxide Core

4.4.1 Sodium Void Worth

Positive sodium void reactivity worth is an important safety concern of medium and large sized sodium-cooled fast reactors. Sodium void reactivity insertion is mainly due to four effects [Waltar and Reynolds, 1981]. First component is from the spectrum hardening effect caused by the reduced neutron moderation in the sodium voided core. This is a positive contribution to the total reactivity. Next component is from the reduction of neutron capture in sodium after voiding. It causes a reduction in neutron loss and a give a positive contribution to the reactivity of the core. Third component is from the enhanced neutron leakage in a sodium voided core and introduces a negative reactivity. Influence of self shielding during voiding is the fourth component and makes very small contribution to the total and hence can be neglected. Such decomposition of net sodium void reactivity in to different components are reported from literature [Kaichavo Sun et al., 2011].

All the individual components of the sodium void worth and hence the total void worth is space dependent as the neutron importance (adjoint) is a space dependent function. The positive contributions from spectral hardening and capture will be more at the core centre and reduces as moves to the core periphery. At the same time, the negative contribution from neutron leakage increases at peripheries compared to core centre. Also the magnitude of these components is decided by the fuel type. It means that, the sodium void reactivity can be reduced by a proper selection of core designs and fuel type [Hill and Khalil, 1980; Bruno Merk, 2011]. This is generally achieved by decreasing the positive components and/or increasing the negative leakage component [Wade and Fujitha, 1989].

For PFBR, which is a medium-sized, sodium cooled and MOX fuelled fast reactor, the core design is optimized by minimizing the plutonium requirement. The estimated

sodium void worth of this core is 2 $ at fresh core and increases to 3 $ at equilibrium with a delayed neutron fraction of 355 pcm. The reactivity worth due to the voiding of sodium from core-1 region of PFBR core as a function of void volume is found using IGCAR code system, and the results are shown in Table 4.2. For comparison, results from ERANOS are also shown. In general, first order calculation under-predicts the sodium void worth. It can be seen that for voiding volume less than 10%, error in the first order estimation is below 1% for both the scheme of calculations.

Table 4.2: Sodium Void Worth as a Function of Voiding Volume in Core-1 of PFBR

Void fraction (%)	IGCAR Code Systems			ERANOS 2.1		
	Perturbation Scheme (pcm)		Error in First order value (%)	Perturbation Scheme (pcm)		Error in First order value (%)
	First order	Exact		First order	Exact	
10	119.8	120.2	-0.3	122.8	123.8	-0.8
20	239.5	241.4	-0.8	244.1	248.2	-1.6
30	359.3	363.5	-1.1	363.6	373.0	-2.5
40	479.0	486.5	-1.5	481.2	498.1	-3.4
50	598.8	610.3	-1.9	594.0	623.7	-4.3
60	718.5	735.0	-2.2	710.6	749.5	-5.2
70	838.3	860.4	-2.6	822.0	875.6	-6.1
80	958.0	986.4	-2.9	931.1	1002.0	-7.1
90	1077.8	1113.1	-3.2	1037.9	1128.7	-8.0
100	1197.5	1240.3	-3.4	1142.6	1256.5	-9.1

As the voiding increases, the error in the first order estimation also increases. For full voiding of sodium from core-1 region, the first order method using IGCAR code system

under-predicts the worth by only 3.4%. But the first order estimation with ERANOS under predicts the full sodium void worth of core-1 by 9% as compared to the exact result.

Table 4.3: Comparison of Sodium Void Worth Predictions with IGCAR Codes and ERANOS2.1+JEFF3.1

No.	Voiding from	Sodium Void Worth Estimated with IGCAR Codes (ERANOS 2.1)		Error in 1st Order (%)
		Mode of Approximation		
		1st order	Exact	
1	Core-1	1197.5 (1142.6)	1240.3 (1256.5)	-3.5 (-9.1)
2	Core-2	-57.8 (-276.9)	-92.4 (-148.1)	-37.4 (+87.0)
3	Core1 and core-2	1139.8 (865.7)	1163.6 (1118.2)	-2.1 (-22.6)
4	Core, LAB, UAB	993.5 (636.5)	971.2 (908.2)	2.3(-30.0)
5	**Whole Core	869.4 (468.6)	824.0 (746.3)	5.5 (-37.2)

**The values obtained with ERANOS are given in brackets, **Whole Core-total core and blankets*

The error in the sodium void worth estimation of other core regions by first order method compared to the results of exact method is shown in Table 4.3. It can be seen that the difference between first order and exact predictions is less with IGCAR code system as compared with those obtained with ERANOS. As an example, the error in the 1st order prediction of void worth from core-1 and core-2 is 2.1% with PERTX, while it is 23% with ERANOS. For sodium voiding from a peripheral region, core-2, the error in the first order estimation is more in both the scheme of calculations. It may be noted that the sum of core-1 and core-2 sodium void worths do not add up to give the total core sodium void worth in exact perturbation unlike the first order case.

The difference between the first order estimations of sodium void worth using IGCAR and ERANOS schemes of calculation are shown in Table 4.4. Similar values obtained with exact method of both the schemes are also given. The percentage difference in the first order estimated value of sodium void worth from core-1 is 4.6%. As it changes to exact method, the difference between the two schemes reduces to 1.3%. For voiding from core-2, first order estimated value of IGCAR scheme shows very large difference with ERANOS predicted value, and it reduces as the method of estimation changes to exact. In general, the values estimated with first order method, between the two schemes show large errors, the difference decreases as the method changes to exact. The residual difference can be attributed mainly due to the difference between the leakage treatment in the two schemes, also to the difference between the nuclear data used.

Table 4.4: Percentage Difference in the Sodium Void Worth Predictions Between the Two Scheme of Calculations

Voiding from	1st order Perturbation (pcm)		Deviation %	Exact Perturbation (pcm)		Deviation %
	IGCAR	ERANOS		IGCAR	ERANOS	
Core-1	1197.5	1142.6	-4.6	1240.3	1256.5	1.3
Core-2	-57.8	-276.9	379.1	-92.4	-148.1	60.3
Core1, Core-2	1139.8	865.7	-24.0	1163.6	1118.2	-3.9
Core, LAB,UAB	993.5	636.5	-9.9	971.2	908.2	-6.5
*Whole Core	869.4	468.6	-46.1	824.1	746.3	-9.4

**Whole Core represents total core and blanket (both axial and radial) regions*

The difference between the two schemes of calculations can be more explained if the reactivity break-ups are available. Such a distribution is shown in Table 4.5 for the voiding from core-1 region. The total reactivity change due to voiding is split into the contributions from leakage, capture, fission and fission spectrum, scattering and (n,xn). The contribution of fission and fission spectrum and the contribution from (n,xn) reactions obtained from ERANOS are also provided, which are not available with PERTX, For IGCAR scheme of calculations, the contribution from fission and fission spectrum is zero as self shielding due to sodium voiding is not considered. Fission & fission spectrum and (n, xn) contributions do not have significant influence on the total worth.

It has to be noted that the results quoted above are from 2D diffusion studies. It is justified as this study is mainly intended for the comparison between the two calculation schemes and nuclear data. Transport calculation or transport corrected three dimensional diffusion estimation has to be performed for a better and realistic sodium void estimation.

Table 4.5: Reactivity Components of Full Sodium Voiding from Core-1

Method	Scheme	Contribution from (pcm)					Total
		Leakage	Capture	Fission + Spectrum	Scattering	(n, xn)	
1st Order	PERTX	-518.1	109.6	0	1606.0	-	1197.5
	ERANOS	-723.6	258.4	-17.1	1624.9	-0.02	1142.6
Exact	PERTX	-607.3	107.8	0	1739.8	-	1240.3
	ERANOS	-712.4	216.5	-12.4	1764.8	-0.02	1256.5

4.4.2 Doppler Constant

More negative Doppler constant is a desirable safety parameter of a fast reactor for limiting transients with power rise. For an oxide fuelled fast reactor, the Doppler coefficient dk/dT is assumed to have (1/T) dependence [Waltar and Reynolds, 1981]. The constant of proportionality is the Doppler constant. The Doppler constant is estimated in the temperature range 473 K-1173 K. Its value predicted with 1st order perturbation theory using IGCAR and ERANOS systems is given in Table 4.6. The difference in prediction is ~19%. Similar results using exact perturbation theory are given in Table 4.7. But with the same calculation scheme (either IGCAR or ERANOS), the difference between first order and exact predicted values decreases to ~6%. The individual components are also shows similarities in this case. The total Doppler constant is under predicted by IGCAR code systems relative to ERANOS by about 15%. This is true with both the perturbation schemes. Also in general, exact perturbation theory gives lesser magnitudes of Doppler constant.

Table 4.6: 1st Order Perturbation Predictions of Doppler Constant from IGCAR Codes and ERANOS

Scheme	Contributions from (pcm)					Total	Difference (%)
	Leakage	Capture	Fission+ Spectrum	Scattering	(n,xn)		
PERTX	16.9	-846.5	76.1	-18.3	-	-771.9	+18.8
ERANOS	24.3	-1049.1	112.0	-4.1	0.01	-916.9	

Table 4.7: Exact Predictions of Doppler constant from IGCAR Codes and ERANOS

Scheme	Contributions from (pcm)					Total	Difference (%)
	Leakage	Capture	Fission+ Spectrum	Scattering	(n,xn)		
PERTX	17.1	-801.9	71.1	-17.4	-	-731.0	+17.8
ERANOS	24.7	-984.8	102.6	-4.1	0.01	-861.5	

4.4.3 Fuel Void Worth

The fuel void worth values estimated with first order approximation using IGCAR code system and ERANOS are shown in Table 4.8. Three cases of fuel voiding have been considered. First is the removal of U^{238} from core-1 region. The first order estimation of reactivity change caused by this isotope removal is ~+8800 pcm from both the scheme of calculations. This addition of reactivity is mainly due to the reduced neutron capture in U^{238}. It is noted that ~40 pcm has contributed from the (n,xn) component in the U^{238} voiding from core-1, which is small. In the second case of fuel voiding, the fissile isotope Pu^{241} alone is removed from the core-2 region and causes core reactivity reduction. In the third and final case of fuel voiding, the fissile isotopes Pu^{239} and Pu^{241} are removed from core-1 and core-2. For this, both the scheme of calculations gives similar results.

As a summary, the first order estimation of total fuel voiding worth with IGCAR code system and ERANOS gives similar results, though the contributions from individual components are slightly different for leakage and scattering. The fuel void worth estimated with exact perturbation are given in Table 4.9. Here also, both the schemes give similar

results. Also, from the tables 4.8 and 4.9, it is clear that the first order perturbation underestimates the fuel void worth as expected, especially for bigger perturbations.

Table 4.8: First Order Perturbation Predictions Fuel Void Worth using IGCAR Codes and ERANOS

Voiding of	Method	Contributions from (pcm)					Total
		Leakage	Capture	Fission +Spectrum	Scattering	(n,xn)	
U^{238} from Core1	PERTX	-718.4	10570.0	-3308.7	2308.9	-	+8851.4
	ERANOS	-1023.5	10572.4	-3200.2	2574.6	-40.6	+8882.8
Pu^{241} from Core2	PERTX	-22.7	144.1	-2216.9	18.8	-	-2076.7
	ERANOS	-22.3	169.8	-2223.9	11.6	-0.7	-2076.0
Pu^{239} and Pu^{241} from core 1&2	PERTX	-428.7	5883.7	-55456.0	459.5	-	-49542.0
	ERANOS	-486.2	5983.7	-55440.8	372.6	-5.4	-49576.1

4.4.4 Steel Void Worth

The values of steel void worth values are estimated with IGCAR code systems and compared with the results obtained from ERANOS. Both 1st order and exact cases are analyzed. Two cases are analyzed here. First, the Iron (Fe) component of steel is voided from core-1 and core-2. In the second case, the entire steel material is voided from core-1 and core-2. As shown in Table 4.10, first order calculations with ERANOS gives lower values compared to IGCAR code systems. But the exact perturbation results are rather close. Fission and fission spectrum components cannot be neglected in the case of steel voiding. Studying the individual components in Table 4.11, the differences in leakage and capture components

are in opposite directions between IGCAR and ERANOS schemes. The difference between first order and exact calculation results obtained with ERANOS is more compared to similar values with IGCAR code systems.

Table 4.9: Exact Order Predictions of Fuel Void Worth using IGCAR Codes and ERANOS

Voiding of	Method	Contributions from (pcm)					Total
		Leakage	Capture	Fission+ Spectrum	Scattering	(n,xn)	
U^{238} from Core1	PERTX	-942.5	12234.0	-3244.7	2651.6	-	10698.0
	ERANOS	-1049.1	12129.5	-3237.4	3032.9	-45.1	10832.9
Pu^{241} from Core2	PERTX	-22.0	141.3	-2193.1	17.2	-	-2056.7
	ERANOS	-21.5	165.0	-2210.1	10.6	-0.6	-2056.7
Pu^{239} and Pu^{241} from core 1&2	PERTX	74.6	9417.40	-298740.0	+267.8.3	-	-288980.0
	ERANOS	59.9	10211.1	-308614.9	+203.5	-2.5	-298142.6

4.4.5 Plutonium Equivalence

A fast breeder reactor closed fuel cycle involves the recycling of the discharge fuel, after reprocessing and re-fabrication. The utilization of the un-burnt fuel and the freshly bred fissile material is possible here. The plutonium vector in a fast reactor changes with the burn-up. This can be either by the accumulation or depletion of fissile and non-fissile isotopes of plutonium with burn-up. Therefore, the worth of the fuel after burn-up will be different from that in the beginning, as the effectiveness of various isotopes of plutonium will be different for continuing the chain reaction. The change in the fuel worth can be compensated by the addition/removal of fissile plutonium to/from the fuel. The effectiveness of any fuel isotope

can be represented by its plutonium equivalence and is an important parameter if multiple recycling of fuel is considered in a fast reactor [Pandikumar et al., 2009]. It is the relative worth of a fuel isotope with respect to the main fissile isotope of plutonium, Pu^{239} [Riyas and Mohanakrishnan, 2006b]. The plutonium equivalence of different isotopes present in the core-1 region of PFBR equilibrium core is shown in Table 4.12 as computed by IGCAR perturbation code PERTX and ERANOS. Equivalence of Pu^{239} is taken as 1.0 in both the calculation schemes. By definition, equivalence of U^{238} is zero in ERANOS2. In PERTX, the equivalence is computed as the relative worth of a fuel isotope relative to that of Pu-239. Hence its value is non-zero for U-238, though it is very small. From table, it is clear that both the schemes give similar results for the main fuel isotopes except U-238. At the same time, for some isotopes like U^{234}, two schemes give different results. PERTX with ABBN-93 nuclear data give positive equivalence for U^{234}, but its value is slightly negative with ERANOS 2.1+JEFF 3.1 system. In the both cases, Am^{242} has the maximum plutonium equivalence, which is more than 2.0.

Table 4.10: 1st Order Predictions of Fe and Total Steel void Worth

Voiding of	Method	Worth (pcm)					Total (pcm)
		Leakage	Capture	Fission+ F.Sp.	Scattering	(n,xn)	
Fe from Core-1 and Core-2	PERTX	-1800.2	+1395.5	0	+2722.4	-	+2317.6
	ERANOS	-2430.6	+1822.2	-93.0	+2606.8	-1.2	+1954.2
Steel from Core-1 and Core-2	PERTX	-3162.9	+3569.3	0	+4144.0	-	+4550.4
	ERANOS	-5213.8	+4371.6	-212.0	+4180.2	-2.1	+3123.9

Table 4.11: Exact Perturbation Predictions of Fe and Total Steel void Worth

Voiding of	Method	Contribution from (pcm)					Total (pcm)
		Leakage	Capture	Fission+ spectrum	Scattering	(n,xn)	
Fe from Core-1 and Core-2	PERTX	-2087.9	1358.5	0	3074.1	-	2344.7
	ERANOS	-2209.0	1743.7	-73.8	2923.9	-1.6	2383.2
Steel from Core-1 and Core-2	PERTX	-4032.6	3451.8	0	5019.3	-	4438.4
	ERANOS	-4227.2	3850.8	-126.0	5038.3	-3.0	4532.3

Table 4.12: ^{239}Pu Equivalence of Fuel Isotopes

Isotope	Plutonium Equivalence	
	PERTX + ABBN 93	ERANOS 2.1+ JEFF 3.1
U234	-0.005	0.06
U235	0.80	0.76
U236	-0.07	-0.01
U238	-0.06	0.00
Np237	-0.19	-0.21
Pu238	0.56	0.69
Pu239	1.00	1.00
Pu240	0.09	0.17
Pu241	1.51	1.47
Pu242	0.04	0.11
Am241	-0.23	-0.27
Am242m	2.97	2.18

4.5 Conclusions

The exact and first order estimates of sodium, fuel and steel voiding worths in different regions of 500 MWe PFBR equilibrium core are estimated with the newly developed perturbation code system. It involves two dimensional diffusion code ALCIALMI, exact perturbation code PERTX and ABBN-93 nuclear data. The results are compared with those obtained from a similar analysis done using ERANOS system, which comprises diffusion and various perturbation theory modules available in ERANOS2.1 and JEFF 3.1 nuclear data.

For 100% sodium voiding from the central core-1, both the schemes gives similar results. But for voiding of sodium from other regions and from core peripheries, the results are not matching. The first order estimated sodium void worth from outer regions like core-2 using IGCAR methods shows large deviations compared to ERANOS predictions, but the deviation decreases with exact calculations. In general, ERANOS gives lower positive sodium void worth. Total steel and fuel void worths estimated with ERANOS and IGCAR perturbation code systems are nearly same. The first order approximation in both the schemes drastically under predicts the fuel void worth, as expected. The first order and exact predictions of Doppler constants estimated using IGCAR code systems in the temperature range of interest are found to be less negative as compared to the ERANOS results. The plutonium equivalence of most of the main fuel isotopes was similar with both the calculation schemes. The total neglect of fission and fission spectrum components are not advisable for total worth in IGCAR code system, as it gives notable contributions for certain voiding cases. The differences in some of the results (especially the reactivity components) obtained with the two schemes of calculations may be partially due to the difference between

the nuclear data used. The above diffusion theory based perturbation analysis done using ERANOS shows the adequacy of IGCAR code scheme for the safety analysis of PFBR core for transients up to sodium voiding. However, transport theory based perturbation worths are expected to be more correct and needed for cases with Na voiding.

The development of PERTX code helped to compute both first order and exact perturbation theory worth data. Also, it enabled to calculate safety parameters more accurately and also make a reliable assessment of core behaviour during transients.

Chapter 5

ULOF TRANSIENT BEHAVIOUR OF METAL FUELLED FBR CORES AS A FUNCTION OF CORE SIZE AND PERTURBATION METHODS

5.1 Introduction

It is known that, faster growth of nuclear power in India is possible through the use of metallic fuels in FBR cores. Out of possible metallic fuel compositions, ternary alloy of U-Pu-Zr with 6 wt% of Zr is chosen by considering breeding and irradiation experience. Also, because of the higher breeding and economic benefits, installation of bigger reactors are advisable provided their inherent safety behaviour during transients are demonstrated. Among these transients, the investigation on unprotected loss of flow accident (ULOFA) is important due to the consequences during its occurrence. The safety performance of metal fuelled FBR cores during ULOFA is studied as a function of core size and the results are discussed in this chapter.

Sodium void worth is an important safety concern for FBR cores and its value is positive for medium and large cores. Also its value become high positive with core size and has an important adverse influence on reactor safety as it provides positive reactivity contribution during ULOFA. The main negative feedback during such an accident is from core radial expansion. A sensitive study is performed to understand the influence of these two main feedback reactivity effects on the severity of the transient and the results are also summarised in this chapter.

For all analysis performed here, the core is assumed to be retained in the pre-disassembly phase during the transient. This study is important for an optimized economic and safe nuclear reactor strategy using FBRs using metal fuels. In the next section, properties

of the metal fuel used, reference cores chosen and the calculation scheme are briefly explained. The results are discussed in sections 5.3-5.5. Summary and conclusions of the study are given in section 5.6.

5.2 Reference Cores and the Calculation Scheme

To understand the influence of core size and the 1st order perturbation approximation on the ULOFA behaviour, metal-fuelled and sodium cooled FBR cores of three different sizes are taken. It consists of a small experimental fast reactor of power of 120 MWe (320 MMt), a medium sized reactor of power 500 MWe (1250 MWt) and large sized commercial reactor of power 2630 MWt (1000 MWe) respectively [Riyas and Mohanakrishnan, 2014]. The metallic ternary alloy of U-Pu-6%Zr is chosen as the fuel for all the cores considered. Detailed core design properties are given in chapter-3.

The ATOMIX-CONSYST-EFCONSY-ALCIALMI-ALEX-PERTX code system is used for the static core physics and perturbation analysis of the three FBR cores. The code ALCIALMI solves neutron diffusion equation in RZ-geometry. Pre-disassembly part of the ULOF analysis is carried out using the code PREDIS. The code uses point kinetics approximation for the calculation of reactor power and the net reactivity is calculated as the sum of input reactivity and feedback reactivity. The main feedbacks considered here are from the axial expansion of fuel and clad, Doppler effect, core radial expansion, and coolant density changes. The calculation scheme is explained in chapter-2.

5.3 Perturbation and Transient Analysis Using 1st Order Results

The results of ULOFA analysis performed on three FBR cores using 1st order worths are given in this section. Based on the mode of calculation, the study is divided in to two; the static and dynamic. The static calculations include diffusion and perturbation analysis, while

the dynamic calculation includes the response behaviour of core in a transient during ULOFA.

5.3.1 Material Void and Doppler Worths

First order perturbation theory based parameters used for pre-disassembly calculations are given in Table 5.1. The whole reactor values are given in the table. From the table, it can be seen that the sodium void increases and fuel void worth decreases with core size. The values of steel void worth and Doppler constant increase its value with core size. The variation of sodium void reactivity with core size is well known. The reduction in fuel worth with increase in core size is due to the reduced effect of fuel perturbation in cores with large amount of fuel. Even though the 1000 MWe reactor design considers higher fuel pin diameter and consequently higher fuel volume fractions compared to the other two reactors, the trends in perturbation worths are consistent with the increase in reactor size and corresponding fall in Pu enrichment.

The variation of sodium void worth with respect to core size will be more understood from Table 5.2, where the total reactivity change during sodium voiding is depicted as a sum of different components of leakage, absorption, fission and scattering. From the table, it can be seen that the decrease in neutron leakage is the main reason for the higher sodium void worth in bigger cores. It has to be noted that, for calculating the sodium void worth, sodium from core and blanket regions are voided, maintaining the sodium in the fuel pin bond. The region wise distribution of sodium void of the FBR cores is shown in Table 5.3. As the core size increases, core regions provide more positive contribution to the total sodium void reactivity change. It is important to understand that sodium voiding of core regions alone causes more positive reactivity worth compared to whole core (core and blankets) voiding.

The region wise contribution to the total sodium void worth of the three FBR cores are schematically given in Fig.5.1. It can be seen that the negative reactivity contributions from blankets are less. In addition, the positive contribution from the core region decreases and the negative contributions from blanket regions increases as the core size reduces and causes a reduced sodium void worth in smaller cores.

Table 5.1: First Order Perturbation Values of Material Void and Doppler Worths as a Function of Reactor Size (pcm)

Number	Reactivity Change due to	Reactor Size (Power-MWe)		
		Small (120)	Medium (500)	Large (1000)
1	Sodium Voiding*	+164	+1830	+2340
2	Fuel Voiding*	-43732	-38461	-34153
3	Steel Voiding*	+972	+4128	+5543
4	Doppler+	-336	-469	-524

**100% voiding* *+ Temperature range is 200 ^{o}C - 857 ^{o}C*

Table 5.2: Component wise Distribution of 1st Order Estimated Sodium Void Worth

Reactor Size (MWe)	Components of Reactivity Change				Total (pcm)
	Leakage	Absorption	Fission	Scattering	
120	-2596	+97	0	+2663	+164
500	-2076	+117	0	+3789	+1830
1000	-1311	+96	0	+3555	+2340

The sodium void worth have a spatial dependence in the reactor core as both the direct and adjoint fluxes have space dependence. The radial variation of direct and adjoint fluxes are shown in Fig.5.2. Even though both the fluxes follow same radial dependence,

they show different energy dependence. The spectrum of direct and adjoint fluxes at the core centre is shown in Fig.5.3.

Table 5.3: Sodium Void Worth with Region wise Distribution

Reactor Size (MWe)	Region wise Contribution (pcm)					Total (pcm)
	Core-1	Core-2	Core-3	Axial Blanket	Radial Blanket	
120	+389	-	-	-114	-111	+164
500	+1761	+231	-	-95	-67	+1830
1000	+1176	+1122	+109	-36	-31	+2340

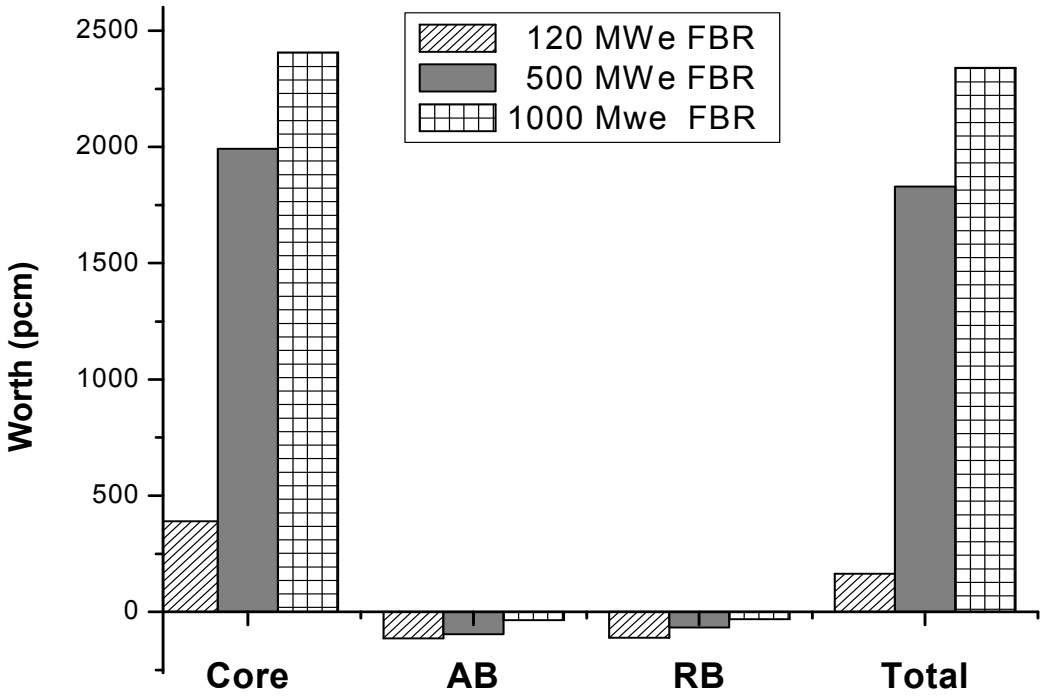

Fig.5.1. Comparison of Region wise Distribution of Sodium Void worth of Three FBR Cores

The difference in energy dependence between flux and adjoint flux can be explained using the concept of neutron importance. Higher neutron cross-sections at lower energies and

high reproduction factor at higher energies causes increase in the relative neutron importance and causes increase of adjoint flux at these energy ranges.

The radial variation of net sodium void worth and its components along the core centre plane of 1000 MWe FBR core is shown in Fig.5.4. The net positive reactivity of sodium voiding from core and blankets is 2340 pcm. Among the components, effects of self shielding on net voiding have not been considered as it is very small. The variation of sodium void worth per unit volume of sodium at the core centre plane has been taken. It can be seen that the leakage component is negative and the capture component is small positive. The main positive component is from the reduced scattering in the voided core. Because of the radial variation of these components, the net void worth becomes slightly –ve at the core peripheries.

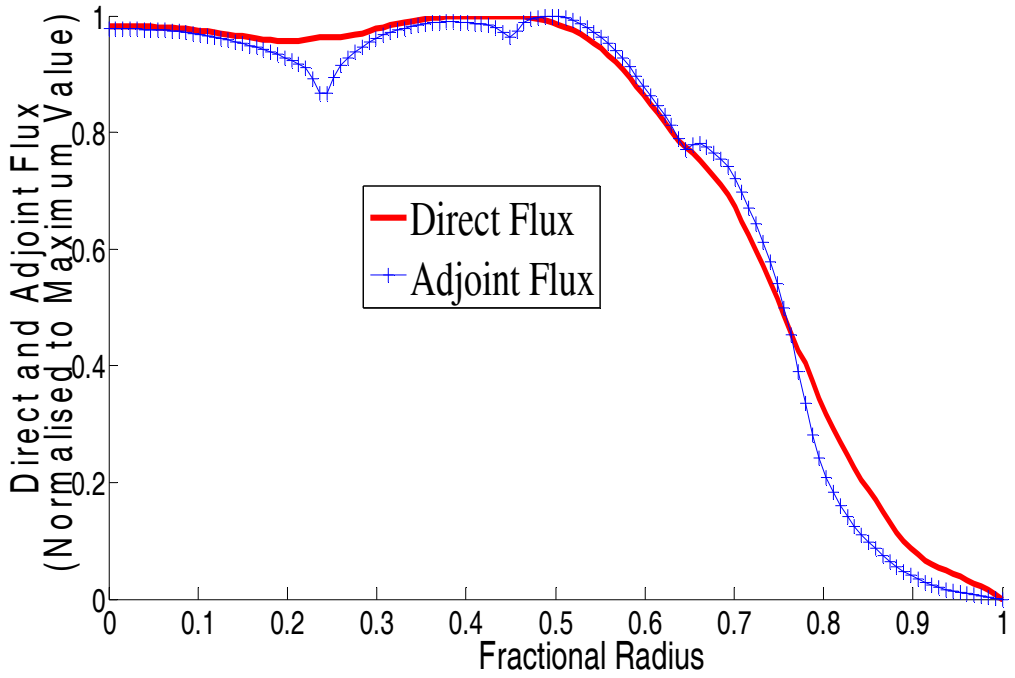

Fig.5.2. Radial Variation of Direct and Adjoint Fluxes for 1000 MWe FBR Core

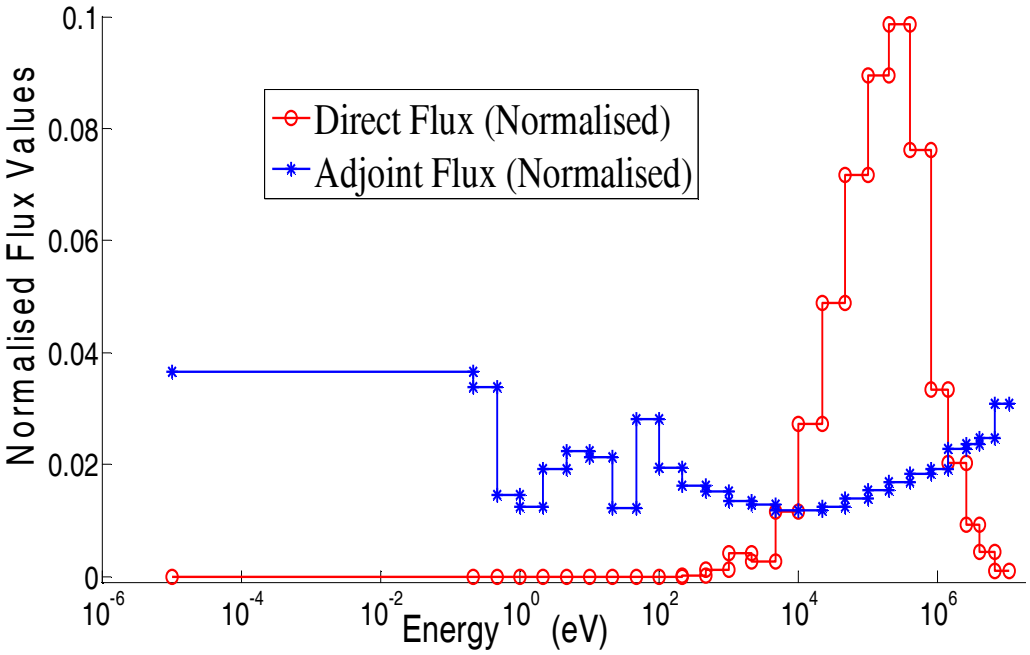

Fig.5.3. Energy Dependence of Direct and Adjoint fluxes at the Core Centre

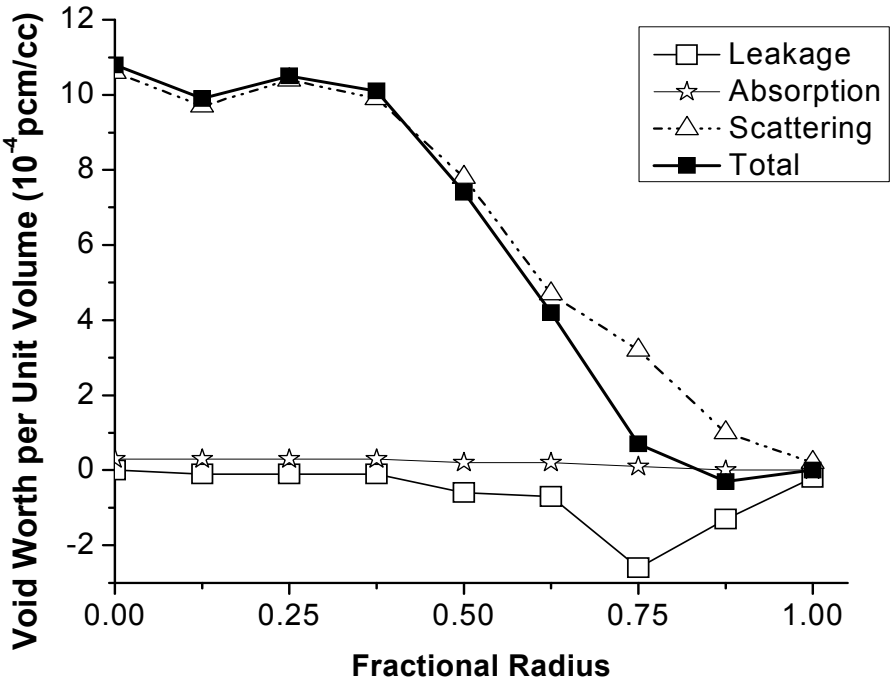

Fig.5.4. The Radial Variation of Sodium Void Worth and its Components (10^{-4}pcm/cc) for the 1000 MWe FBR Core (along the Core centre Plane)

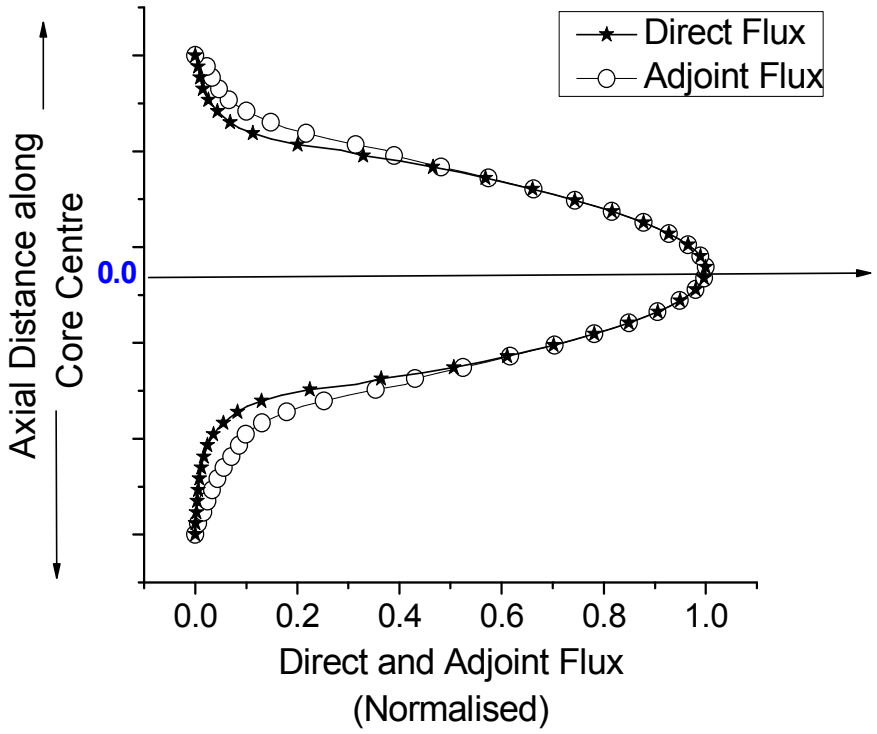

Fig.5.5. Axial Variation of Direct and Adjoint Fluxes for a 1000 MWe FBR Core

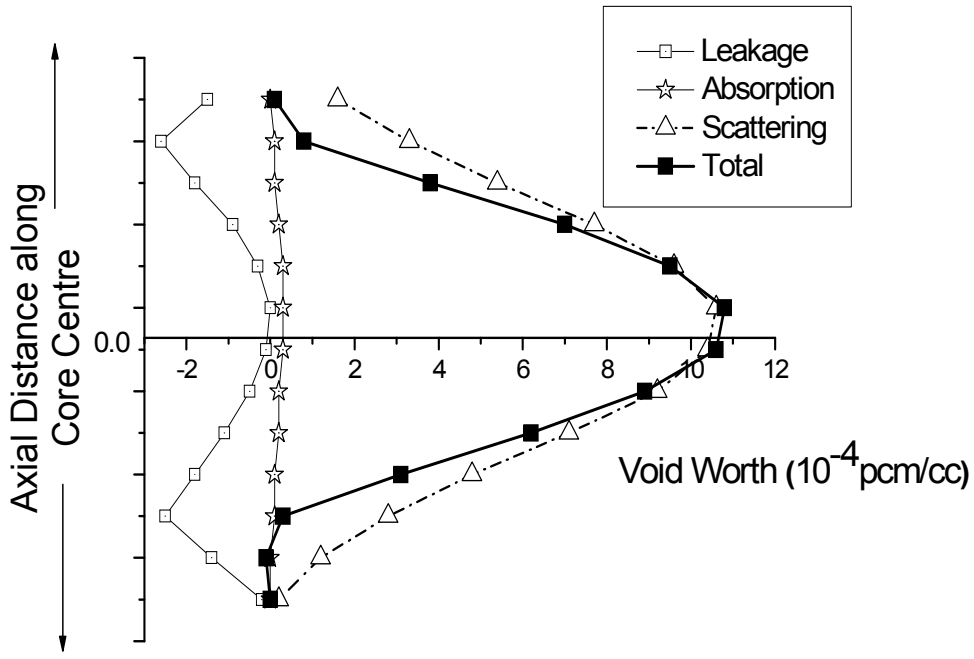

Fig.5.6. Axial Variation of Sodium Void Worth and its Components along the core Centre

The axial variation of direct and adjoint fluxes are shown in Fig.5.5. It is clear that, both the fluxes follow the same shape. Axial variation of the sodium void worth and its components are shown in Fig.5.6. Here also the voiding of unit volume of sodium is considered along the axial direction at the core centre (at the central fuel sub-assembly). The components and the net reactivity shows the similar trend as in radial variation.

The radial and axial variation of component wise and net reactivity of sodium voiding with respect to core size are also estimated. The radial variation of sodium void worth for the three FBR cores is shown in Fig.5.7. Voiding of sodium from unit volume is considered and it is estimated along the radial plane in the core centre. Even though the whole core voiding worth is more positive in the 1000 MWe case among the three cores, per unit volume values show a reverse trend as shown in figure. The negative contributions from the blankets are more in the 120 MWe core. Its value is 58% of the positive contribution from the core regions. For the 500 MWe and 1000 MWe cores, these values are 8% and 3% respectively. Also it has to be noted that the core volumes are more for bigger cores and causes more positive net void reactivity. The greater void worth per unit volume at the core centre of the 120 MWe core can be explained through the flux peaking in the core centre also.

The axial variation of sodium void worth per unit volume at the core centre is shown in Fig.5.8. It is clear that smaller cores have more –ve worth at top and bottom of the core, even though the core centre values show a reverse trend. During an ULOF accident, the sodium voiding initiates at the top of the central fuel SA. In addition, void reactivity values are more negative for smaller core. This is one of the reasons for the better benign behaviour of small core.

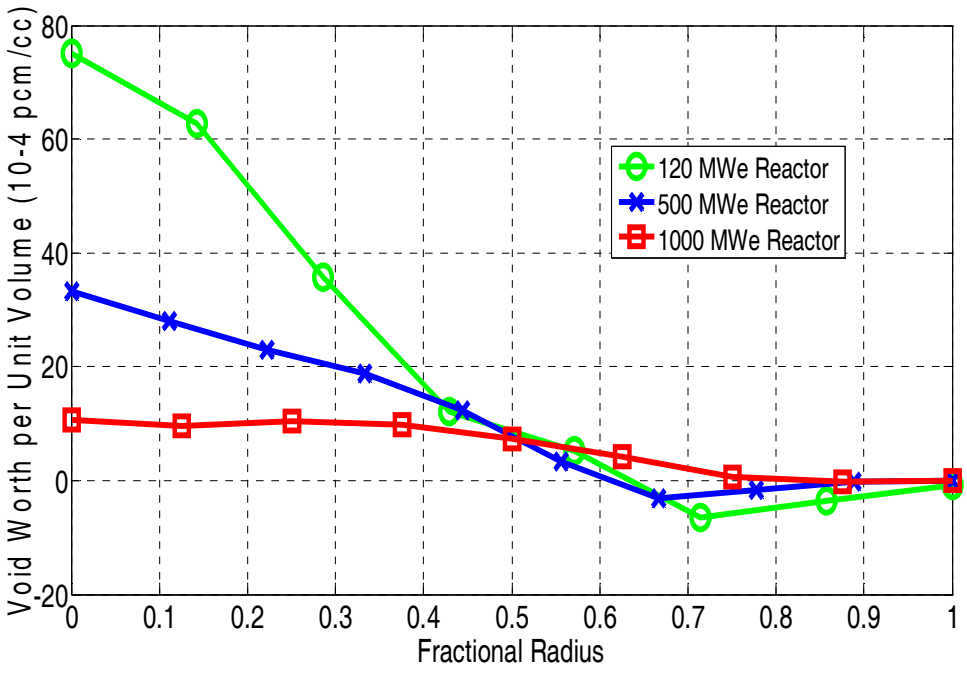

Fig.5.7. Radial Variation of Sodium Void Worth/cc of Three FBR Cores (along the core centre plane)

The increase of Doppler constant with core size is due to the spectrum softening, reduced fissile enrichment and the relative increase of U-238 amount in large cores. This fact can be well understood from Table 5.4, where the component wise distribution of Doppler constant is given. As the core size increases, resonant absorption increases due to higher U-238 content and causes more –ve Doppler feedback.

The components of steel void worth are shown in Table 5.5. The effect of core size on neutron leakage and amount of steel on scattering can be seen. Reduction in leakage is the main reason for the increase in steel void worth in large cores. Similar table for the 1st order estimated fuel void worth is shown in Table 5.6. The effect of neutron leakage, absorption, fission and scattering on the fuel size and amount is seen from table.

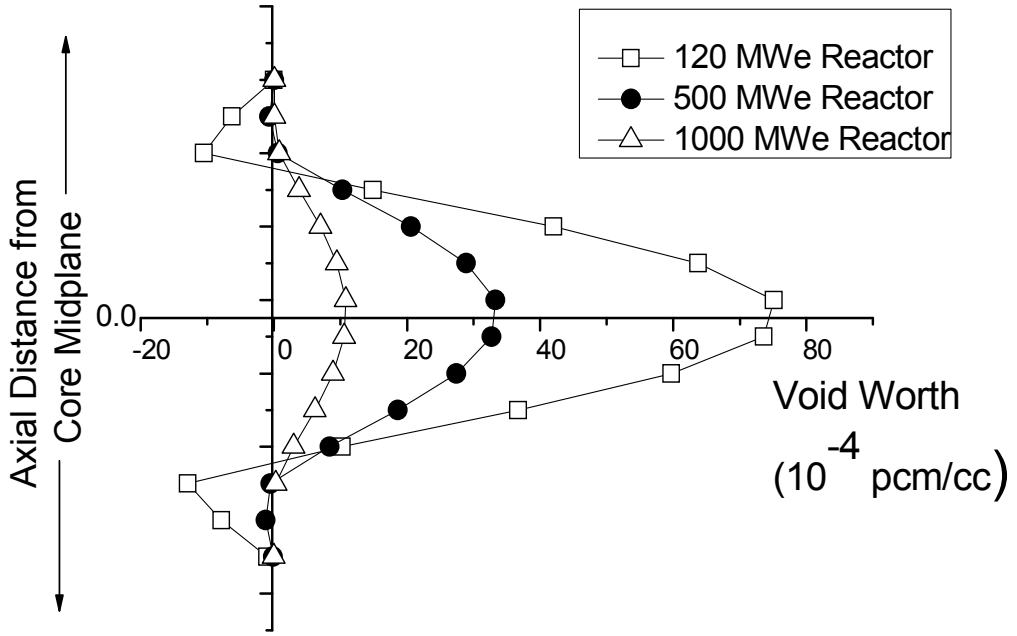

Fig.5.8. Axial Variation of Sodium Void Worth/cc of Three FBR Cores at the Core Centre

Table 5.4: Component wise Distribution of 1st Order Estimated Doppler Constant

Reactor Size (MWe)	Components of Reactivity Change (pcm)				Total (pcm)
	Leakage	Absorption	Fission	Scattering	
120	+27	-394	+38	-7	-336
500	+24	-510	+28	-11	-470
1000	+21	-551	+20	-14	-524

Table 5.5: Component wise Distribution of 1st Order Estimated Steel Void Worth

Reactor Size (MWe)	Components of Reactivity Change				Total (pcm)
	Leakage	Absorption	Fission	Scattering	
120	-5956	+2368	0	+4560	+972
500	-4780	+2829	0	+6079	+4128
1000	-3424	+2606	0	+6361	+5543

Table 5.6: Component wise Distribution of 1st Order Estimated Fuel Void Worth

Reactor Size (MWe)	Components of Reactivity Change (pcm)				Total (pcm)
	Leakage	Absorption	Fission	Scattering	
120	-9428	+51515	-93389	+7570	-43732
500	-7619	+54898	-95655	+9915	-38461
1000	-6330	+56791	-97086	+12472	-34153

5.3.2 Isothermal Temperature and Static Power Coefficients

Isothermal temperature coefficient of reactivity and power coefficient of reactivity will decide the reactivity changes due to the changes in temperature and power respectively during a ULOFA accident. The net temperature and power coefficients and its components estimated by the PREDIS code using 1st order estimated removal and Doppler worths for the three FBR cores are shown in Table 5.7.

Table 5.7: Static Temperature Coefficient (pcm/^{o}C) and Power Coefficient (pcm/MWt) of Three Reactors (averaged over zero to full power)

Reactivity Coefficient Components	Reactor Size (Power –MWe)					
	Small (120)		Medium (500)		Large (1000)	
	Temp. Coeff.	Power Coeff.	Temp. Coeff.	Power Coeff.	Temp. Coeff.	Power Coeff.
Doppler	-0.881	-0.165	-0.632	-0.092	-0.706	-0.056
Fuel axial expansion	-0.586	-0.244	-0.466	-0.074	-0.394	-0.033
Clad axial expansion	+0.019	+0.009	+0.083	+0.008	+0.111	+0.005
Coolant expansion	+0.047	+0.021	+0.522	+0.038	+0.667	+0.023
Core Radial Expansion	-1.197	-0.237	-1.056	-0.093	-0.971	-0.026
Total	-2.598	-0.616	-1.549	-0.213	-1.293	-0.087

Note: Temperature and Power Coefficients are having units of pcm/^{o}C and pcm/MWt respectively.

From the table it is clear that, both the temperature and power coefficients are more negative for smaller cores. It is due to the increase in net negative contributions from Doppler, fuel axial expansion and radial expansions with reduction in core size.

5.3.3 Transient Behaviour of the Three Reactor Cores during ULOFA

The transient behaviour of the FBR cores during an ULOF event with a flow halving time of 8 sec are discussed in this section. Voiding of steel, sodium, fuel and the Doppler constant in the operating range is used. The reactivity change produced by 100% voiding and its spatial distribution is considered in the first order method, and it is scaled linearly for the actual expansion or void undergone by different materials of the core during the transient. The Doppler feedback due to an actual temperature fluctuation during a transient is estimated by integrating dk/dT using the estimated Doppler constant which is computed for a wider operating temperature range. The Doppler constant is estimated in the range 200 ^{o}C to 827 ^{o}C, which is close to sodium boiling temperature and it is sufficient for transient in the pre-disassembly phase.

As flow reduces, the core reactivity and hence the reactor power varies due to the reactivity feedbacks caused by the changes in temperature and the associated changes in the geometry and composition of the core. The reactor power varies with flow reduction, the variation of normalized power to flow as a function of time after the initiation of the event is shown in Fig.5.9. The normalized power to flow ratio varies with time in the similar manner for 120 MWe and 500 MWe reactors, but 1000 MWe core shows a different trend. The value of peak power/flow ratio is significantly higher for 1000 MWe core.

This difference in reactor power with flow reduction can be explained by the feedback reactivity components and the net reactivity at the time of its peaking. The peak

occurs near around 60s for both the 120 MWe and 500 MWe reactors, while it is 90s for 1000 MWe reactor. The components of feedback reactivity and the net reactivity for the three

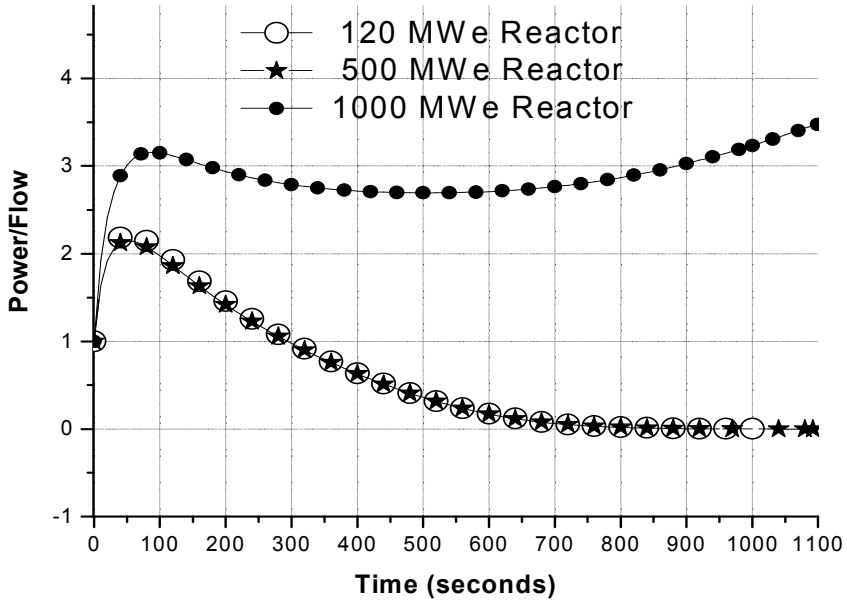

Fig.5.9. The Variation of Normalized Power to Flow Ratio of the Three Cores

cores at the respective peaks are given in Table 5.8. From the table it is clear that, the magnitude of the net reactivity feedback is smaller for 1000 MWe core as compared to the other reactors and hence causes a higher power and power to flow ratio. From Table 5.8, it can be seen that the more positive contribution from sodium expansion is the main reason for the reduced net negative feedback at peak power to flow ratio for large reactor.

As the cores is subjected to a ULOF accident with the same flow coast down time, the various reactivity feedbacks and the net reactivity vary with respect to time. The main reactivity feedbacks considered during ULOFA are from sodium expansion, core radial expansion, Doppler Effects, steel expansion and fuel axial expansion. These feedbacks changes with time and the variation with respect to time is shown in Fig 5.10 to Fig 5.14 respectively. Out of these, Fig.5.10 gives the combined reactivity feedback from sodium due

to its expansion and voiding during ULOFA. Also, the feedback reactivity components are compared in the figures with respect to the core size also. The variation of individual components and the net reactivity as a function of time after ULOFA is shown in Fig.5.15 for the 1000 MWe FBR core.

Table 5.8: The Net Feedback Reactivity and its Components at the Peak of Normalized Power to Flow Ratio for the Three Reactor Cores

Reactivity Feedback Components from	Reactor Size (Power MWe)		
	Small (120)	Medium (500)	Large (1000)
Sodium Expansion	+0.024	+0.156	+0.319
Steel Expansion	+0.006	+0.021	+0.043
Fuel Axial Expansion	-0.017	-0.035	-0.089
Doppler	-0.009	-0.036	-0.111
Core Radial Expansion	-0.278	-0.384	-0.355
Net Reactivity Feedback	-0.274	-0.278	-0.20

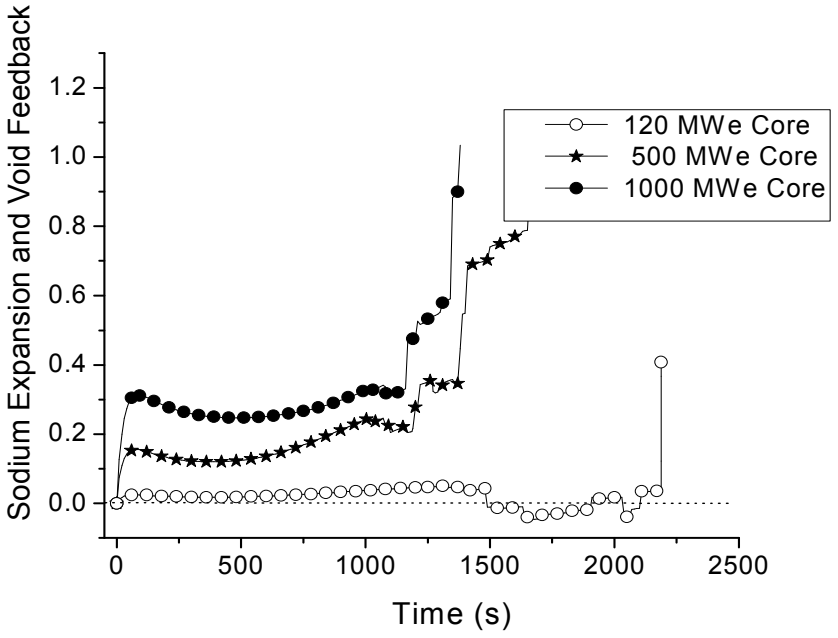

Fig.5.10. Reactivity Feedback from Sodium Expansion and Void for the during ULOFA

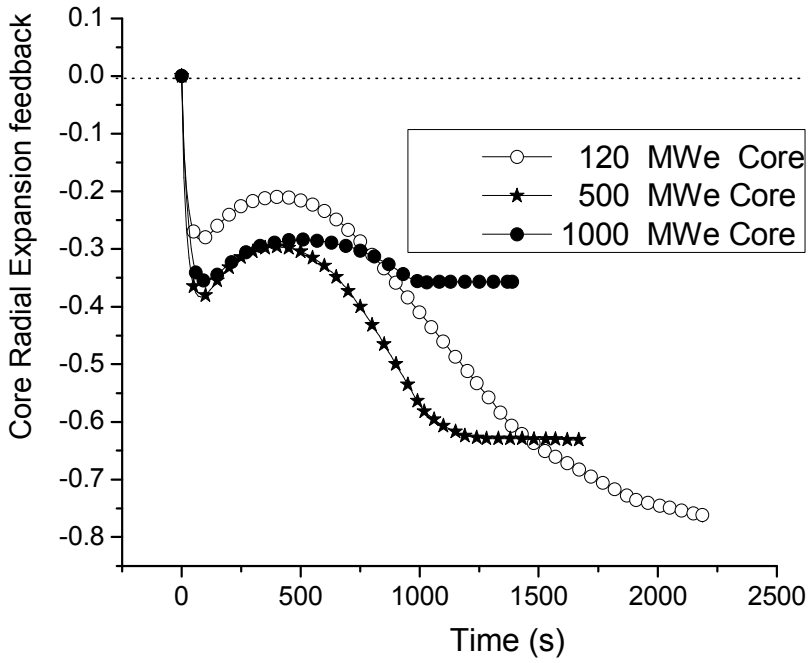

Fig.5.11. Reactivity Feedback from Core Radial Expansion for the 3 FBR Cores

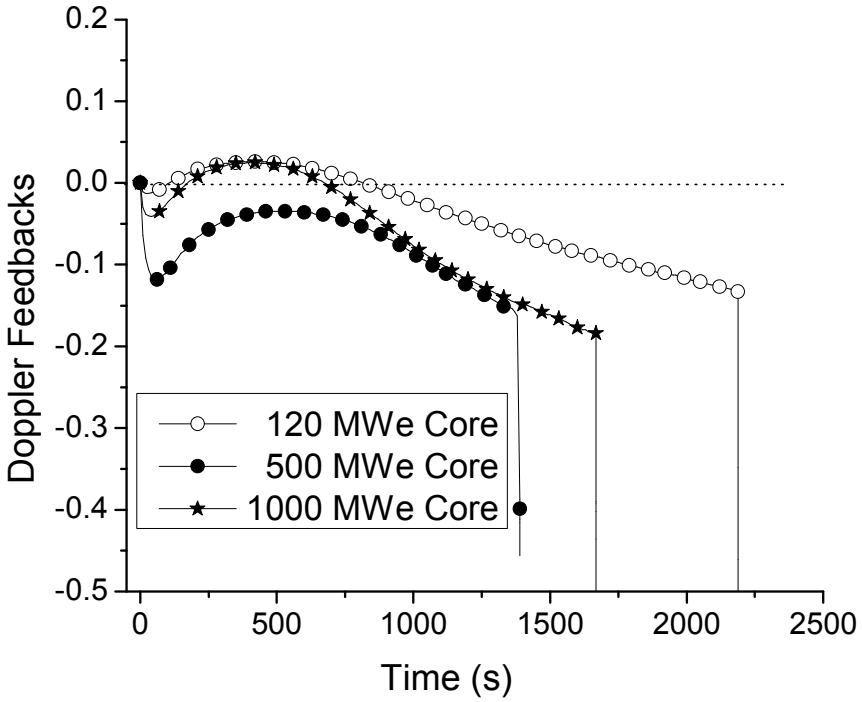

Fig.5.12. Doppler Reactivity Feedback from 3 FBR Cores during ULOFA

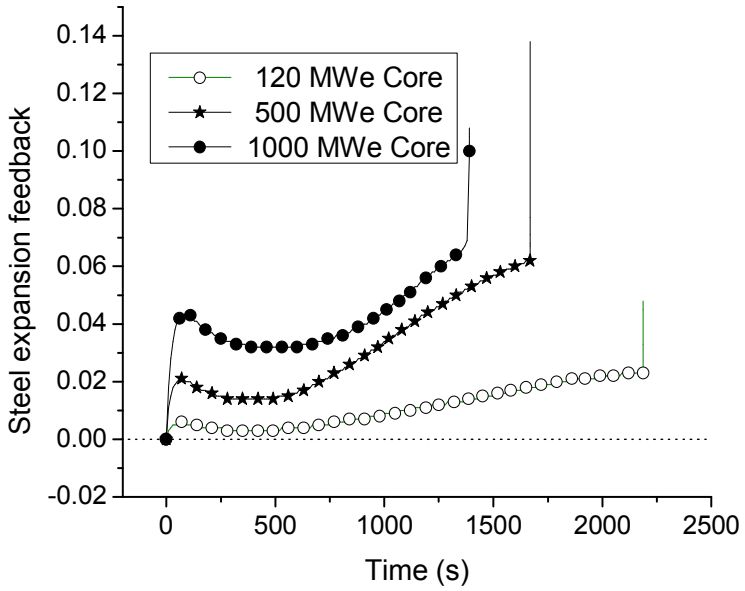

Fig.5.13. Steel Expansion Feedback during ULOFA from 3 FBR Cores

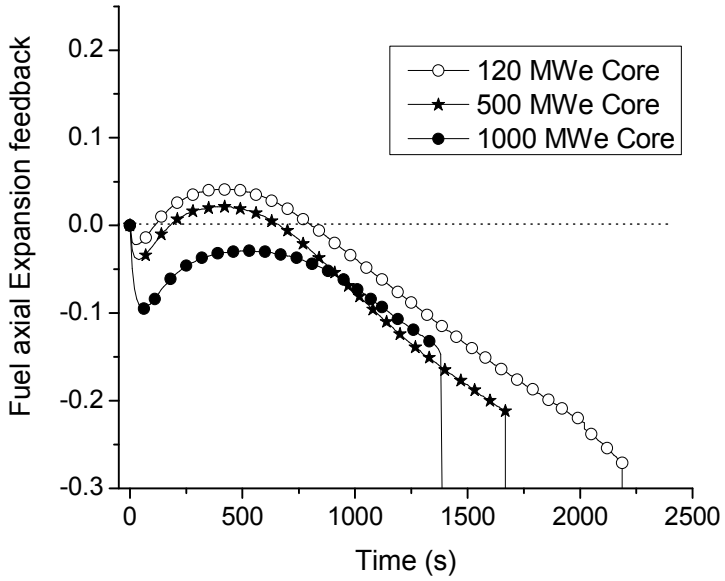

Fig.5.14. Fuel Axial Expansion Feedback from 3 FBR Cores during ULOFA

From the above figures it is clear that the main positive feedback during an ULOFA of metal fuelled FBR's is due to the expansion and voiding of sodium and the main negative feedback is from core radial expansion. However at the beginning of ULOFA, the positive feedback is only from sodium expansion as there is no initiation of sodium voiding. Also, the

negative core radial expansion overwhelms the positive contribution from sodium expansion and causes the net reactivity feedback negative. As this difference is more for smaller cores, 120 MWe FBR core shows more sub-criticality during ULOFA. Steel expansion feedback is small positive throughout the event. Fuel and Doppler feedbacks are small negative, but small and medium reactors show a positive contribution initially.

The time dependence of component and net reactivity of the 1000 MWe FBR during the ULOFA shown in Fig.5.15 can be explained. Transient behaviour of the core during ULOFA is reflected in the changes in sodium flow, temperatures of sodium, steel and fuel, different reactivity feedbacks and the net reactivity, reactor power and power to flow ratio (P/F). It has to be noted that all this parameters are inter-related to each other. The normalised power, normalised flow and their ratio are shown in Fig.5.16 and the variation of coolant, clad and fuel temperatures during the incident are shown in Fig.5.17. The behaviour of these parameters during ULOFA and the associated flow coast down for the 1000 MWe core can be explained as given below.

Pump seizure during ULOFA causes continuous flow reduction and rise in temperature of sodium, steel and fuel. This causes positive insertion of reactivity from sodium and steel and negative reactivity insertion from fuel axial expansion, core radial expansion and Doppler effect. Out of these, the major negative contribution is from core radial expansion and the major positive contribution is from sodium expansion and voiding. As the total negative contributions are more compared to the total positive components, net reactivity is negative and becomes more negative with flow coast down. The insertion of negative reactivity causes power reduction, but the power to flow ratio (P/F) shows an increase as the power reduction is less compared to flow reduction. As the negative reactivity

insertion increases, power reduces to still smaller values so that the P/F ratio saturates and then decreases leading to reduction of sodium, steel and fuel and temperatures.

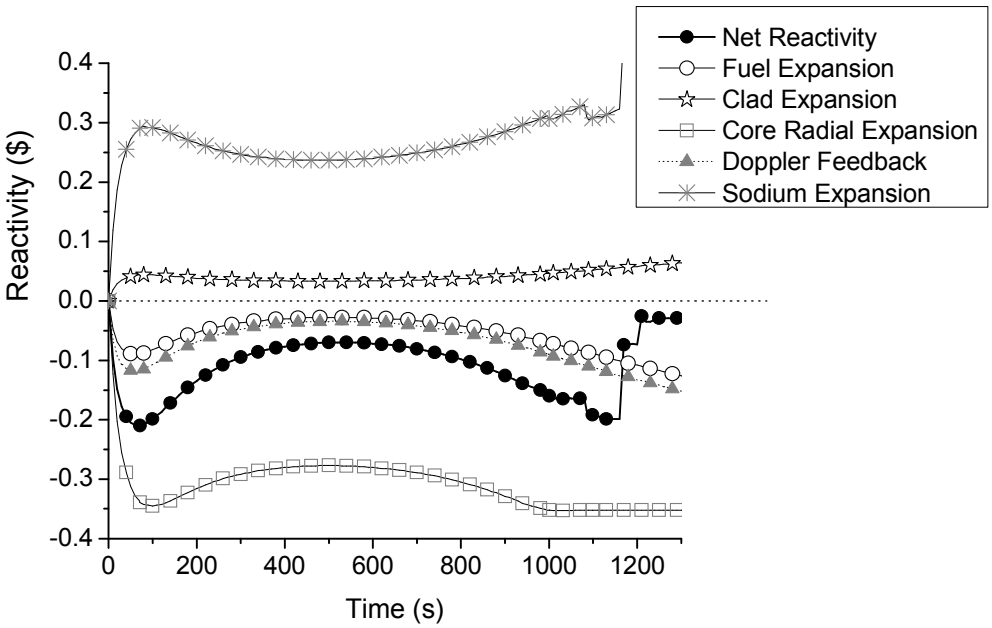

Fig.5.15. Variation of Net Reactivity and its Components of 1000 MWe Core during ULOFA

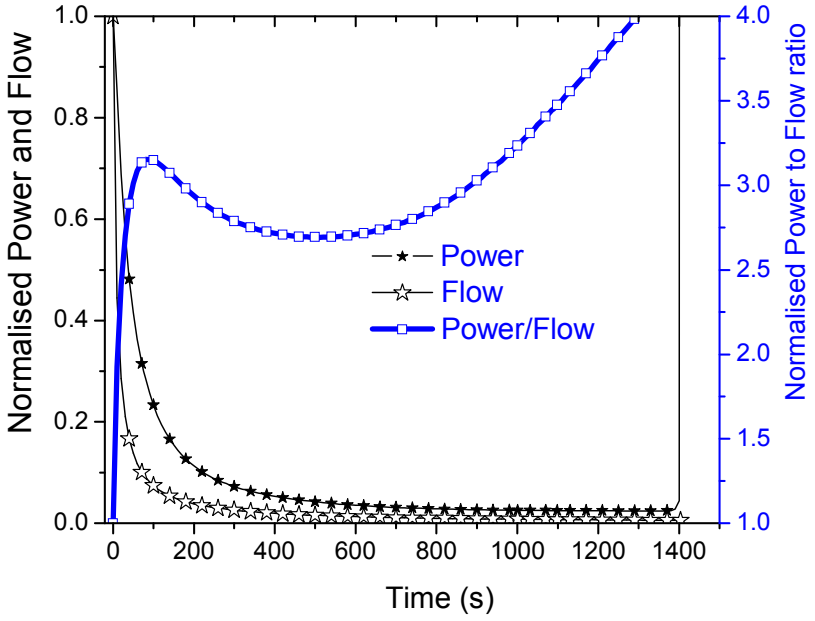

Fig.5.16. Variation of Normalized Power, Flow and Power to Flow Ratio for 1000 MWe FBR during ULOFA

With reduction of temperatures, feedbacks show decrease in its values (both +ve and –ve contributions), but the net reactivity continuous to be negative. But the net –ve reactivity shows a reduction in its value as the reduction in –ve components are more than the reduction in +ve components and causes a slow-down of power reduction.

As further flow coast down happens, P/F increases and causes a temperature hike. This causes increase in both +ve and negative reactivity components and the net becomes more –ve. But as the time elapses, the main –ve grid-plate expansion saturates, the main +ve sodium component continues to increase and the net reactivity to positive values. It causes further sodium voiding, boiling and a saturation of sodium temperature, but positive insertion of reactivity increases with time. These causes increase in clad and fuel temperatures hence leads to an initiation of CDA.

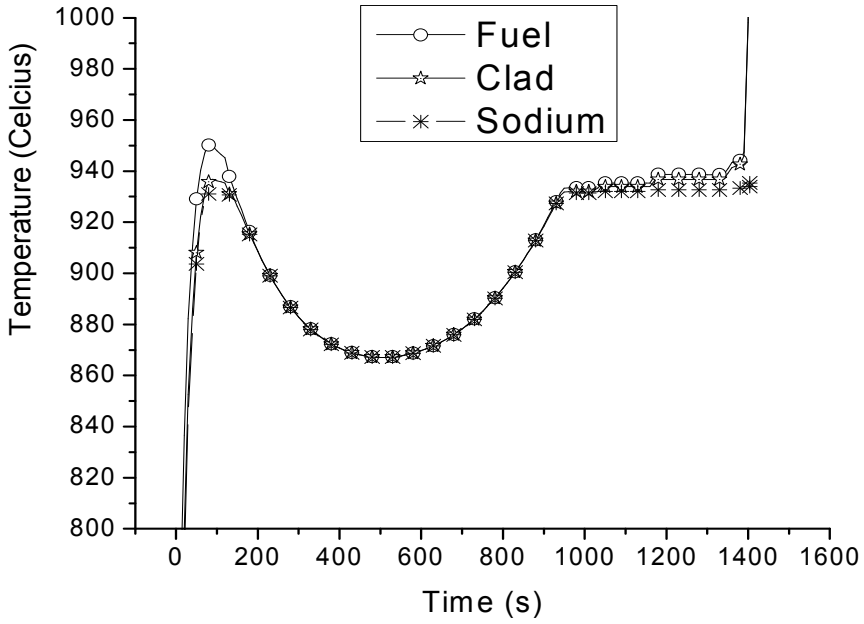

Fig.5.17. Temperature of Fuel, Clad and Sodium as a Function of Time during ULOFA of 1000 MWe FBR Core

It has to be noted that, even both the feedbacks from sodium and core radial expansion is due to the changes in sodium temperature, different material movements are contributing to these. Feedbacks from sodium are caused by its density changes during transient, but the feedbacks from core radial expansion are mainly provided by the fuel density changes and boundary movement worths.

As already mentioned the net reactivity is the sum of the feedback reactivity for all the cores and therefore will vary with core size. Its variation with respect to time for the three FBR cores is shown in Fig.5.18 [Riyas and Mohanakrishnan, 2014]. The figure shows that smaller reactors will be in pre-disassembly phase for longer time due to the lower positive reactivity addition from sodium density fall. In this respect, the pre-disassembly phase of ULOFA accident is safer for the 120 MWe FBR core as compared to the other reactors. In all the reactors, the prompt critical transient which indicates the end of pre-disassembly phase is caused by the large scale sodium voiding in core. As perturbation results are not accurate in such scenarios, the plots of reactivity are only indicative for large positive reactivity insertion.

As given in Fig.5.18, the FBR cores go to subcritical state during the initial times of transient and cause a reduction in fission power. Total power is the sum of fission power and decay power. For a flow coast down time of 8 sec assigned to the present analysis, power reduction of the cores during ULOFA is shown in Fig.5.19. It is seen from the figure that the total power decreases and asymptotically reaches to a value before entering in the dis-assembly phase. The asymptotic power value, time at which the power attains the asymptotic value and the time interval at which it retains in the asymptotic value are functions of core size. These asymptotic power values are 8 MWt, 33 MWt and 67 MWt for the small, medium

and large reactors respectively. It means that by providing decay heat removal systems having capacities equal to the asymptotic power levels, the power excursion and disassembly phase can be eliminated.

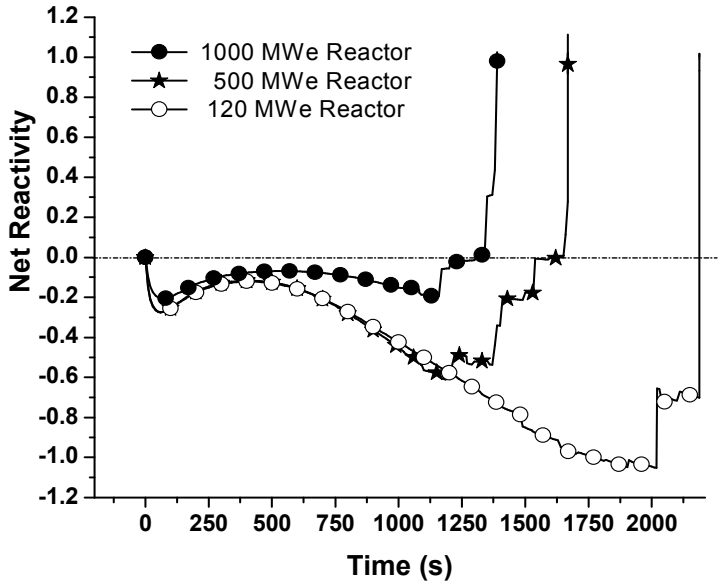

Fig.5.18.The Variation of Net Reactivity with Time of Three Reactors

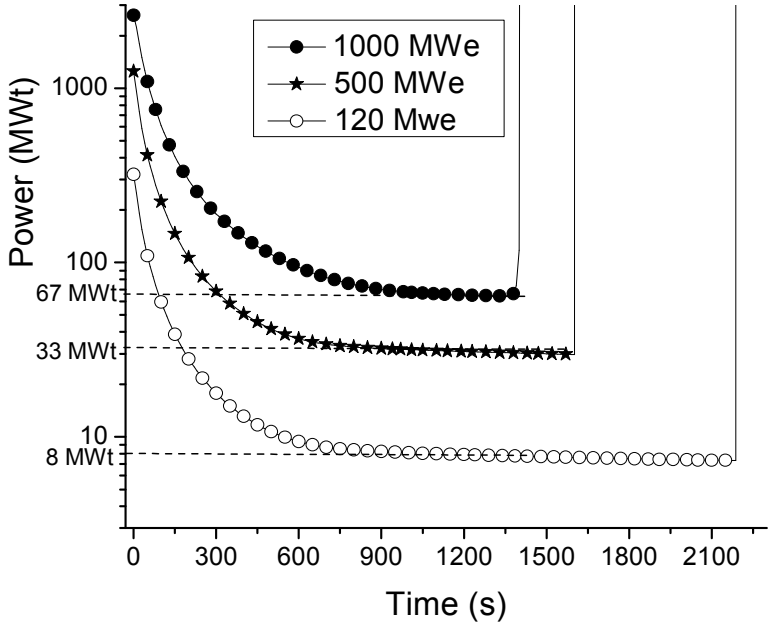

Fig.5.19.The Variation of Reactor Power with Time of Three Reactors during ULOFA

5.4 Exact Perturbation Worths and its Influence on Transient Analysis

In the previous section, the values of material removal worths and Doppler worths estimated with 1st order approximated methods are used for the ULOFA transient behaviour of an FBR core. A range of accuracy of the values computed with first order perturbation can be estimated by using the corresponding exact reactivity values of material void and Doppler worths. Also the effect of these exact perturbation values on the reactor transient behaviour is studied and the results are presented in this section.

The important reactivity worths involved in the prediction of ULOF transient are Na void reactivity worth, Doppler reactivity worth and radial expansion reactivity worth. By many comparisons with experiments (John, 1998; Devan et al, 1999; Mohanakrishnan,2008) involving ABBN data and neutron diffusion theory codes used, the uncertainty of Na void worth, steel worths and Doppler worth have been estimated as 20%. The above comparisons were based on two k_{eff} computations which are expected to match with exact perturbation theory application. No experimental measurements were available for comparing predicted radial expansion reactivity worths. In the transient studies for metal FBR reported earlier (Harish et al., 2009, Sathiyasheela et al., 2011), only first order perturbation reactivity worths were used. Thus it is of interest to quantify the additional uncertainty of the worths arising from first order perturbation instead of exact perturbation.

5.4.1 Removal Worths and Doppler Constant

The values estimated for the removal worths and Doppler constant by the exact method are shown in Table 5.9. For comparison, the values of first order values are given in brackets. It can be seen that the 100% material void worth and Doppler constant predicted

by the exact perturbation method show the same trend of variation with core size as of 1st order results.

But for a particular reactor, the values predicted by the exact method shows difference with respect to the corresponding first order estimated values. The important safety parameter of sodium void worth is over predicted (higher positive) by the first order method for the smallest core, but the medium and large cores shows a reverse trend. The component-wise distribution of sodium void worth in the small (120 MWe) and large (1000 MWe) reactors is shown in Table 5.10 and Table 5.11 respectively.

Table 5.9: Exact and First order Perturbation Values of Material Void and Doppler Worths for Three Reactor Cores (pcm)

Case	Reactivity Change due to	Reactor Size (Power-MWe)		
		Small (120)	Medium (500)	Large (1000)
1	Sodium Voiding*	-8 (+164)	+1863 (+1830)	+2475 (+2340)
2	Steel Voiding*	-110 (+972)	+3442 (+4128)	+5360 (+5543)
3	Fuel Voiding**	-2298(-2186)	-2029(-1923)	-1807(-1708)
4	Doppler Constant+	-324(-336)	-446 (-469)	-498 (-524)

** 100% voiding* *** 5% Voiding* *+ temperature range 200 °C- 827 °C*

Table 5.10: Reactivity Components of Sodium Void Worth of Small FBR Core (pcm)

Perturbation Method	Components of Reactivity Change (pcm)				Total
	Leakage	Absorption	Fission	Scattering	
1st Order	-2596	+97	0	+2663	+164
Exact	-3034	+92	0	+2934	-8

From Table 5.9, it is found that the steel void worth is also over predicted with 1st order method because of the underestimation of leakage component of reactivity. As the

core size increases, contribution from leakage decreases and the error in the first order values reduces. The magnitude of Doppler constants are slightly over predicted by the 1st order method, and can be explained by the use of reduced perturbed flux for the estimation of exact reactivity change.

Table 5.11: Reactivity Components of Sodium Void Worth of 1000 MWe FBR Core (pcm)

Perturbation Method	Components of Reactivity Change (pcm)				Total
	Leakage	Absorption	Fission	Scattering	
1st Order	-1311	+96	0	+3555	+2340
Exact	-1503	+91	0	+3887	+2475

The relative error in the first order worths with respect to exact worths of sodium and steel void as a function of voiding fraction is studied on the 1000 MWe core and the results are given in Fig.5.20 and Fig.5.21 respectively. It can be seen from figure that, the error in the first order estimated sodium void worth is less than 6% even for 100% voiding. Also the maximum error in steel voiding is less than 4%. Similar results can be obtained with other reactors too.

The comparison of fuel void worth estimated with first order and exact perturbation methods are shown in Fig.5.22 as a function of voiding fraction. The relative error in the first order estimation is also shown. It is clear from figure that for small fuel void fractions, the error is small. But as the void fraction increases beyond 10%, the error in the first order values increases significantly. Evidently as fuel void fraction increases, the flux distortion increases resulting in failure of first order approximation.

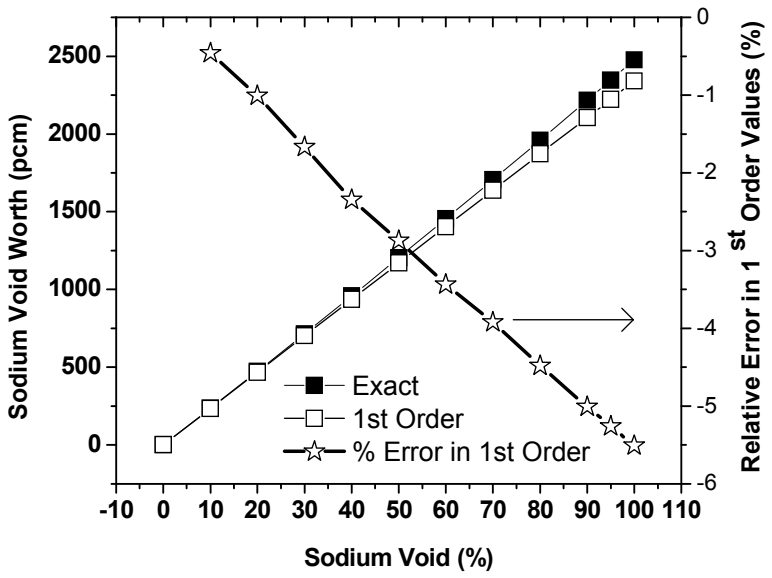

Fig.5.20. 1st Order and Exact Sodium Void Worth and the Relative Error in the 1st Order Prediction for 1000 MWe Core

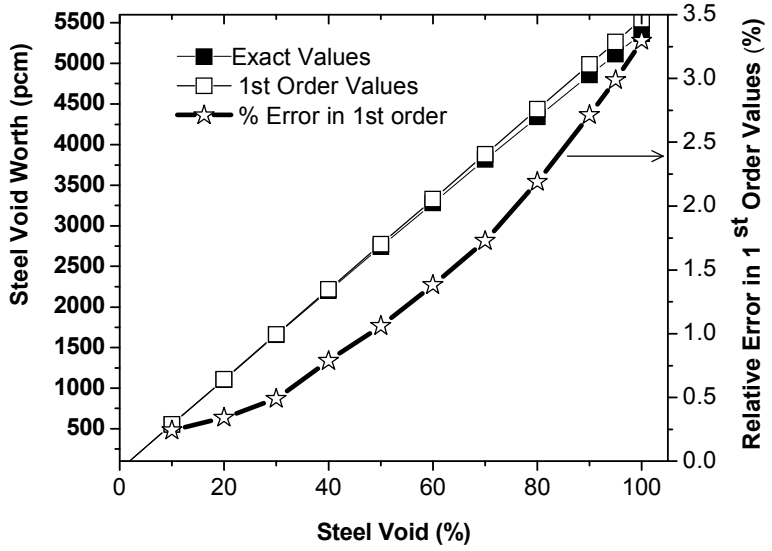

Fig.5.21. First Order and Exact Perturbation Steel Void Worths and the Relative Error in the First Order Prediction for 1000 MWe Core

Because of the higher negative fuel void worths predicted with exact perturbation, it is important to investigate the actual fuel displacement a core undergoes during a ULOFA transient. It is found out from our earlier pre-disassembly analysis that the overall fuel expansion and the amount of fuel displaced from the chosen mesh is less than 5%, provided

that the core is in the pre-disassembly phase (Sathiyasheela, 2014). Since the analysis discussed in this study is strictly constrained to pre-disassembly phase, the maximum void fraction of 5% fuel voiding may be applied for the exact perturbation studies. The values corresponding to 5% fuel voiding with first order and exact perturbation values are also given in Table 5.9. It can be seen that, the exact perturbation slightly over-predicts the fuel void worth with 5% voiding.

From the above discussion, it is clear that 100% voiding worths of steel and sodium and 5% fuel voiding gives comparable results. Therefore, the use of 100% steel and sodium removal obtained from 1st order and exact perturbation methods and its linear scaling for an actual material expansion for a transient analysis is justified. But for the small 120 MWe reactor, steel and sodium voiding by 100% shows difference in the predicted values as seen in Table 5.9 (sign change) and the use of these in the transient analysis has to be verified. The distribution of total sodium void worth in the RZ-geometry and along the 112 zones of the 120 MWe core using exact perturbation are shown in Fig.5.23. First order values are given in brackets for comparison and the shaded area represents the core and the other portion represents blankets. It can be seen that for axial blankets, the exact values are small and slightly more negative as compared to first order perturbation values, but at the core area, both are giving a similar worth distribution. In the case of a transient, sodium voiding initiates at the core top and then spread to the core centre. Since the worths are small at the core top (axial blankets) and similar in the core centre, the use of these worths (either 1st order or exact) on the transient analysis give similar results for the small reactor too.

The distribution of 100% steel void worth for the 120 MWe reactor is shown in Fig.5.24. Both the exact and first order values (in brackets) are given. As the core centre

values are similar and due to the small steel expansion during the transient, the use of first order perturbation voiding worths may not affect ULOFA analysis results of 120 MWe reactor also.

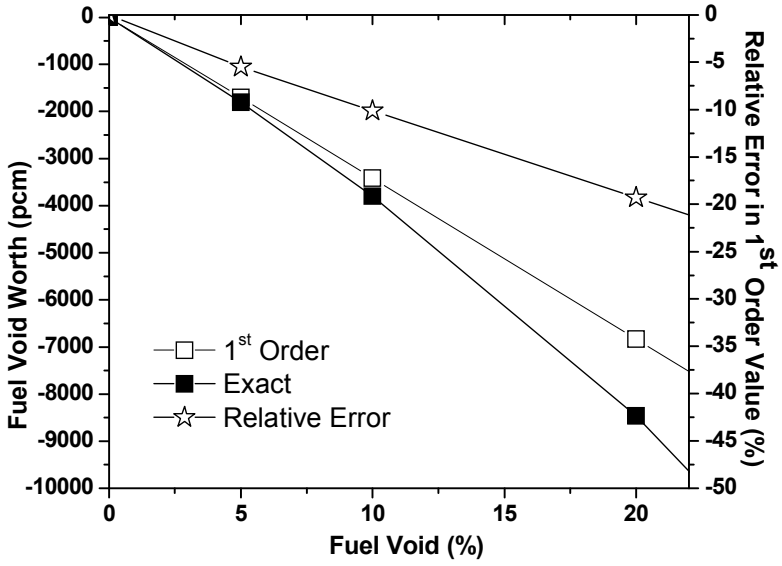

Fig.5.22. First Order and Exact Perturbation Fuel Void Worths and the Relative Error in the First Order Prediction for 1000 MWe Core

-2(-2)	-12(-9)	-21(-17)	-21(-16)	-14(-10)	-11(-8)	-2(-1)	-1(0)
-3(-2)	-13(-11)	-24(-20)	-27(-22)	-20(-16)	-23(-18)	-5(-4)	-1(-1)
1(2)	4(6)	-3(1)	-14(-10)	-11(-8)	-26(-21)	-8(-6)	-2(-2)
6(6)	24(25)	23(25)	2(5)	-1(1)	-27(-23)	-10(-9)	-3(-2)
10(10)	42(42)	46(47)	17(18)	8(10)	-28(-24)	-12(-11)	-4(-3)
12(12)	52(52)	61(60)	26(26)	14(15)	-29(-25)	-13(-12)	-4(-3)
12(12)	53(53)	62(62)	27(27)	15(15)	-29(-25)	-14(-12)	-4(-3)
10(10)	45(45)	51(51)	20(21)	11(11)	-28(-24)	-13(-11)	-4(-3)
7(7)	29(29)	30(31)	7(9)	2(4)	-28(-23)	-11(-9)	-3(-3)
2(2)	9(10)	4(6)	-8(-5)	-8(-5)	-26(-22)	-8(-7)	-3(-2)
-2(-2)	-10(-9)	-20(-16)	-21(-17)	-17(-13)	-24(-19)	-5(-4)	-2(-1)
-2(-2)	-9(-7)	-13(-10)	-12(-9)	-12(-9)	-11(-9)	-2(-1)	-1(0)
0(0)	0(0)	0(0)	0(0)	-1(-1)	-1(-1)	0(0)	0(0)

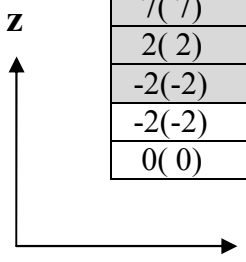

Fig.5.23. The Distribution of Sodium Void Worths (pcm) Using First Order and Exact Perturbation for 120 MWe Reactor

-2(-1)	-9(-5)	-15(-8)	-12(-6)	-7(-3)	-7(-3)	-2(-1)	-1(0)
-8(-6)	-41(-28)	-77(-52)	-79(-51)	-54(-34)	-42(-24)	-10(-6)	-5(-2)
-6(-4)	-33(-21)	-66(-41)	-81(-51)	-63(-39)	-67(-43)	-20(-14)	-8(-5)
5(7)	18(27)	3(21)	-31(-8)	-30(-11)	-70(-47)	-31(-23)	-13(-9)
17(18)	73(78)	79(90)	22(37)	3(17)	-71(-49)	-41(-32)	-18(-12)
27(28)	120(122)	145(150)	66(76)	31(41)	-71(-51)	-49(-39)	-22(-15)
33(33)	148(149)	184(186)	93(99)	48(55)	-70(-52)	-54(-43)	-24(-17)
34(34)	152(152)	190(190)	97(102)	50(57)	-70(-52)	-55(-43)	-24(-17)
29(29)	130(130)	160(162)	78(84)	38(46)	-70(-51)	-51(-40)	-23(-16)
20(20)	87(89)	101(107)	39(50)	13(25)	-71(-50)	-44(-34)	-19(-13)
7(9)	31(37)	25(38)	-10(8)	-18(-2)	-71(-48)	-35(-26)	-15(-10)
-5(-3)	-25(-15)	-49(-29)	-56(-32)	-49(-29)	-71(-46)	-24(-17)	-10(-6)
-7(-5)	-36(-25)	-58(-37)	-53(-31)	-51(-32)	-48(-29)	-13(-8)	-6(-3)
-1(-1)	-7(-4)	-11(-6)	-11(-5)	-13(-7)	-10(-5)	-3(-1)	-1(-1)

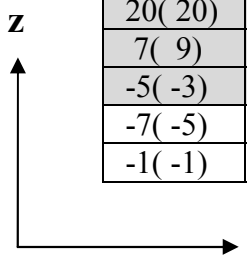

Fig.5.24.The Distribution of Steel Void Worths (pcm) Using First Order and Exact Perturbation for 120 MWe Reactor

5.4.2 Power and Temperature Coefficients

The values estimated with exact perturbation results are used for the estimation of power and temperature coefficients. Doppler constant, 100% steel and sodium removal worths and 5% fuel void worths estimated with exact perturbation are used for the analysis. Also, for better understanding and clarity, only two reactors (small and large) are considered for further comparison as it was found that the medium size reactor behaviour is similar to that of the small size reactor. The results given in Table 5.12 show that, the exact perturbation worths leads to more negative total coefficients. Also the different coefficient components estimated by exact perturbation are close to those estimated by 1st order perturbation results (differences less than 10%).

Table 5.12: Temperature Coefficient (pcm/^{o}C) and Power Coefficient (pcm/MWt) Estimated by Exact and First order Perturbation Results

Reactivity Coefficient Components	Reactor Size (Power –MWe)			
	Small (120)		Large (1000)	
	Temperature Coefficient	Power Coefficient	Temperature Coefficient	Power Coefficient
Doppler	-0.848 (-0.881)*	-0.160 (-0.165)	-0.670 (-0.706)	-0.053 (-0.056)
Fuel axial expansion	-0.629 (-0.586)	-0.262 (-0.244)	-0.427 (-0.394)	-0.036 (-0.033)
Clad axial expansion	+0.019 (+0.019)	+0.008 (+0.009)	+0.107 (+0.111)	+0.005(+0.005)
Coolant expansion	+0.045 (+0.047)	+ 0.020 (+0.021)	+0.705 (+0.667)	+0.024(+0.023)
Spacer pad expansion	-1.288 (-1.197)	-0.255 (-0.237)	-1.045 (-0.971)	-0.029 (-0.026)
Total	-2.701 (-2.598)	-0.649 (-0.616)	-1.330 (-1.293)	-0.089 (-0.087)

**First Order values are given in the brackets*

5.4.3 Effects of Exact Perturbation Results on the Transient Behaviour

The effect of exact perturbation values on the reactor transient behaviour is studied on 120 MWe and 1000 MWe reactors. At each time step of the pre-disassembly analysis, net reactivity feedbacks is calculated based on the change in material temperature with respect to the steady state conditions. The expansion feedbacks are calculated based on the difference in temperatures, thermal expansion coefficient and removal worth. The analysis results are shown in the Fig.5.25 and Fig.5.26. Values of first order perturbation worths use are also given for comparison. As shown in Fig.5.25, the power to flow ratio is not showing any significant change with respect to the use of first order values. Similarly the net reactivity variation with transient given in Fig.5.26 also show close results between the use of exact and perturbation worths. The analysis shows that, first order perturbation values gives accurate results, since the material voiding and expansion are small in the actual ULOF transient in the pre-disassembly phase.

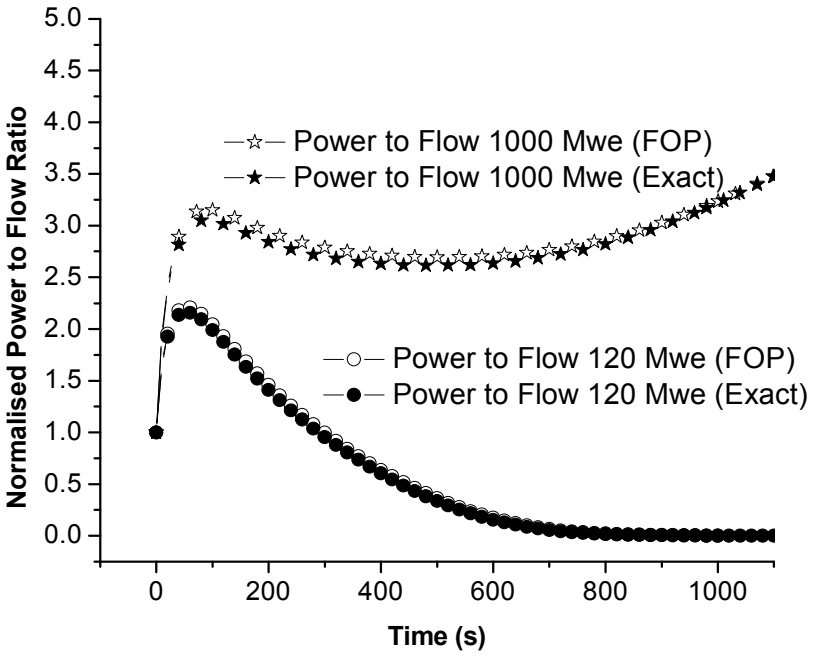

Fig.5.25. Variation of Normalized Power to Flow Ratios for 120 MWe and 1000 MWe Reactor Cores Using First Order and Exact Perturbation Results

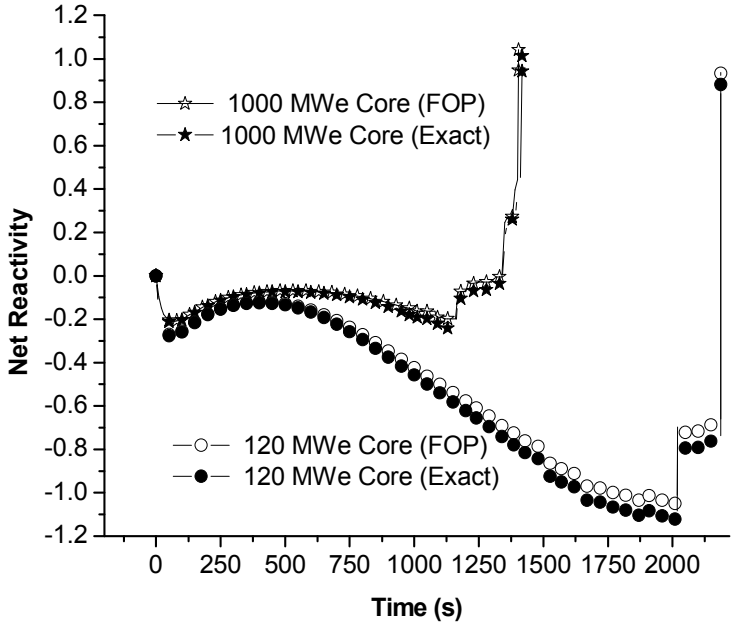

Fig.5.26. Variation of Net Reactivity of 1000 MWe Core with First Order and Exact Perturbation Results

5.5 Sensitivity Analysis

Sensitive analysis is essential for any safety analysis to assess the spread in predicted parameters due to the uncertainties in the data. As seen from Section 5.3 that the main contributions to the net reactivity during ULOFA is from the components of coolant expansion and core radial expansion. This fact was clear from Fig.5.15 where the net reactivity and its components during ULOFA are plotted as a function of time for the 1000 MWe FBR core. It is clear that the main positive contribution is from coolant expansion and main negative contribution is from core radial expansion. This trend is same for the other two cores too. The sensitivity analysis is to be carried out with respect to uncertainties of these feedbacks. An assigned uncertainty of 20% is taken for these main feedbacks in the unfavorable direction.

A sensitivity analysis is performed on the 500 MWe metal fuelled FBR core with respect to the main sensitive parameters of coolant expansion and core radial expansion [Harish et al., 2009 and Sathiyasheela et al., 2011]. The results are depicted in Fig.5.27. Reference case represents the time dependence of reactor power during the ULOF transient, which is obtained with the predicted feedbacks. In case-1, sodium expansion feedback is retained to its original predicted value, but the negative radial expansion is reduced by 20%. Case-2 denotes the response of reactor power with an uncertainty of 20% in the unfavorable direction for the main feedback components. In other words, in this case, reactor power is estimated with an increase of positive sodium expansion feedback by 20% and a reduction of core radial expansion feedback by 20%. It is found that, in both the cases of sensitivity analysis considered, the reactor power drops to the asymptotic value as in the reference case and hence can be handled by decay heat removal system. Otherwise, the benign behaviour

predicted is unaltered with the uncertainties in the main feedbacks and the present analysis shows the inherent safety of 500 MWe metal fuelled FBR. As 500 MWe FBR core is safe with the uncertainties in the feedback components, it is expected that 120 MWe core also will be necessarily safe with a similar allocation of uncertainties. The inherent safety of the small reactor with the uncertainty in the main sensitive feedbacks is mainly due to its lower sodium void worth.

Similar sensitivity analysis is performed on 1000 MWe FBR core and the results are shown in Fig.5.28 [Sathiyasheela, Riyas et al., 2013]. Reference case denotes to the reactor power variation during ULOF transient and obtained using predicted feedbacks with no uncertainties. As given early, reactor power safely drops to the capacity of SGDHR. It is shown that (case-1) with 20% reduction in core radial expansion feedback, the reactor power drops to the assigned capacity of SGDHR. But in case-2, besides 20% reduction in core radial expansion, sodium expansion feedback is assumed to be increased by 20% and it is found that, reactor power abruptly rises to higher values at 60 s itself. It means that, the sensitivity analysis of 1000 MWe FBR core with respect to the main feedback parameters (with uncertainties of 20% in the unfavorable direction) shows that, the reactor safety during ULOFA can be ensured only if the sodium void worth could be reduced by a minimum of 20%.

The results of the sensitivity analysis performed on ULOFA behaviour of 1000 MWe FBR core will be more clear from Table 5.13. With the predicted core sodium void worth (with no uncertainty) of 5.6 $, the reactor safety during ULOFA is ensured. Now with the same sodium void worth of 5.6 $ and 20% reduced core radial expansion feedback, the ULOFA safety is also proved (Case-1). In case-2, 1000 MWe core is found to be unsafe with

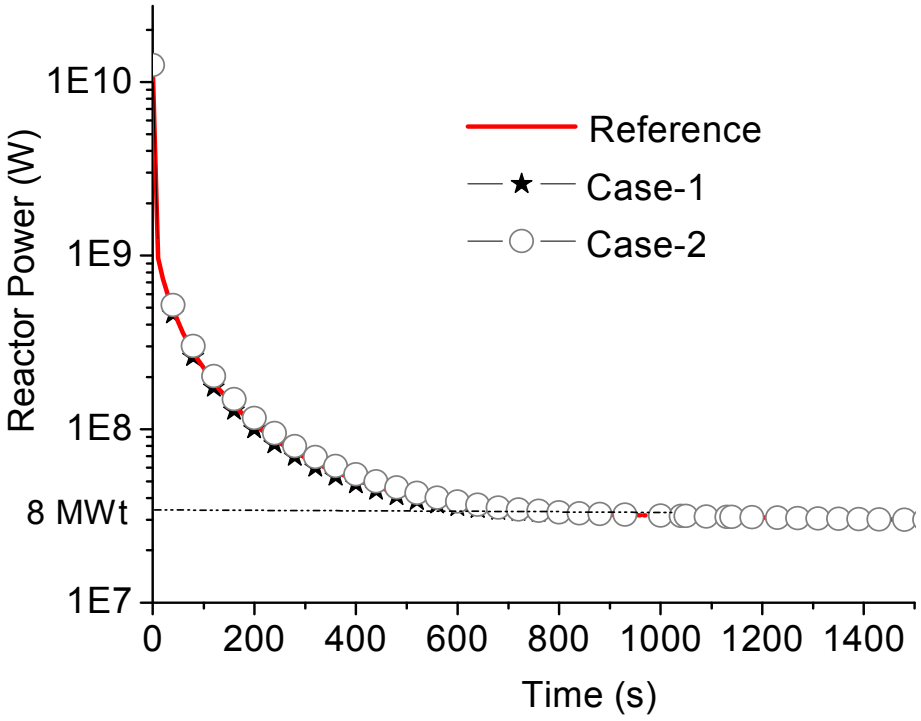

Fig.5.27. Performance of ULOF behaviour of 500 MWe FBR Core during ULOFA with Uncertainty in the Main Feedback Parameters

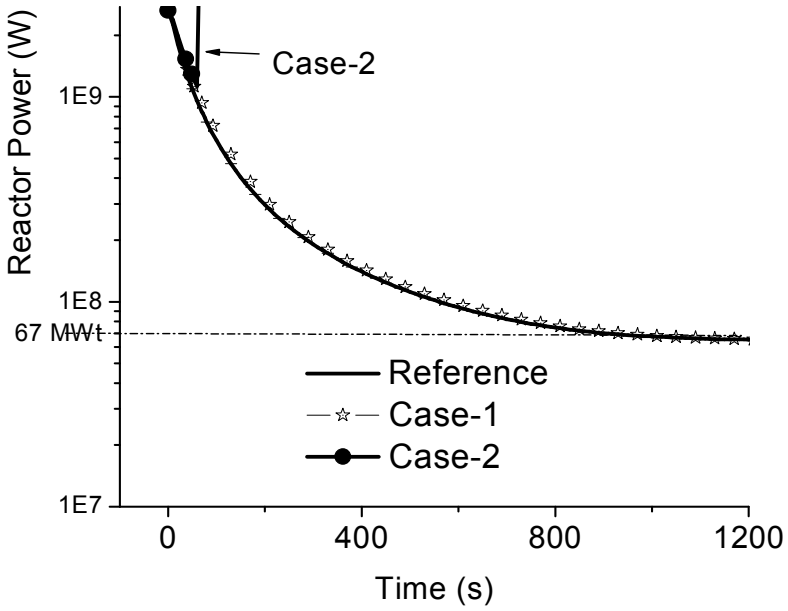

Fig.5.28. Performance of ULOF behaviour of 1000 MWe FBR Core during ULOFA with Uncertainty in the Main Feedback Parameters

Table 5.13: ULOF behaviour of 1000 MWe FBR Core during ULOFA with Uncertainty in the Main Feedback Parameters

Cases Studied	Sodium Void Worth ($)	Uncertainty of Feedback Reactivity from		Remarks
		Sodium Voiding	Core Radial Expansion	
Reference	5.6	0	0	Safe
Case-1		0	-20	Safe
Case-2		+20	-20	Unsafe
Case-3	4.5	+20	-20	Safe

20% uncertainty of both the main feedback reactivities of sodium expansion and core radial expansion in the unfavorable directions. The sodium void worth of the present core is 5.6 $. By combining the case-1 and case-2, it is clear that the 1000 MWe FBR core can be safe with the assigned uncertainties (in unfavorable direction) provided the present sodium void worth could be reduced by 20% (4.5 $). This is given as a separate case (case-3) in Table 5.13.

As uncertainties are inevitable to any reactor calculation, discussion on sensitivity analysis shows the necessity of design and development of advanced FBR cores with lesser sodium void worth and hence inherent safety during transients.

5.6. Summary and Conclusions

An analysis is performed to find the ULOF transient behaviour of metal fuelled FBRs as a function of core size and the approximations used in the estimation of reactivity worths and feedbacks. A small (120 MWe), medium (500 MWe) and large (1000 MWe) reactor cores are used for the analysis with metallic ternary fuel U-Pu-6%Zr. The study reveals the core size dependence of transient behaviour. It is found that the time interval of pre-

disassembly phase during an ULOFA transient decreases with core size. The analyses use the voiding worths of sodium, steel, fuel and the Doppler worths estimated by the first order approximated perturbation methods.

If the exact perturbation method is used, conservative (safer) reactivity coefficients and worths are observed relative to those of first order except for the Doppler constant, whose value becomes less negative with exact perturbation method. The differences of individual reactivity coefficient components estimated by exact perturbation compared to first order perturbation is less than 10%.

The effect of worths and reactivity coefficients derived from first order and exact perturbation methods on the transient behaviour of metal fuelled FBR core during an ULOF accident is studied on 120 MWe and 1000 MWe cores. The study shows that the use of exact perturbation worths do not result in significant change on the transient behaviour of these reactors relative to the use of first order perturbation worths. The effect of exact perturbation worths on the transient behaviour is small as the actual expansion and voiding of core materials during the transient is small when the core is in the pre-disassembly phase. However, exact perturbation theory based reactivity worths are recommended for use in future studies as the effort involved in deriving them is only slightly higher.

The study shows that, with U-Pu-6%Zr fuel and with pessimistic uncertainties in the main feedback parameters from first order perturbation theory, 500 MWe FBR core is benign under ULOFA transient. The 1000 MWe core can be benign with 20% reduction in sodium void worth.

Chapter 6

CONCLUSIONS AND SCOPE OF FUTURE STUDIES

6.1 CONCLUSIONS

Energy is essential for the economic growth and improvement of quality of life in a country. Nuclear energy has a greater role to play for this. In India, metal FBRs are planned to be launched during its second-stage of nuclear energy programme with the aim of achieving energy security. This choice was due to their attractive characteristics of higher fissile fuel breeding potential which enables faster growth in nuclear energy. They are also well suited for incinerating long lived minor actinides, by which the radio-toxicity of nuclear waste can be reduced. In addition, multiple recycling of reprocessed fuels is possible in FBR cycle. With respect to non-proliferation, metal fuelled reactors with closed fuel cycle and using pyro-processing of spent fuel are an ideal choice. Though, the benefits of metal FBRs are well understood, no commercial power reactors have been built so far based on metal fuels, and the limited data available today for the design is based on the published data of American experimental reactors, EBR-I, II and FFTF. The core safety aspects of metal FBRs are also experimentally demonstrated in these experimental reactors.

Even though metal FBRs have very attractive core characteristics, it has higher positive sodium void coefficient compared to oxide and other ceramic fuelled reactors. It is therefore essential to ensure core safety even after accounting all the uncertainties involved in the estimations. Accurate knowledge of reactivity coefficients, reactivity worth data of fuel, coolant and structural materials are essential for performing such study. These parameters, in general, vary for reactor size, power and the types of fuel used.

The present study is based on three main objectives. The first objective of the study is to understand the breeding and safety characteristics of metal fuelled FBR cores of different size and type of fuel. The second objective of the study is to find the effectiveness of the first order approximated material removal worths on transient analysis. Third objective of the study is to analyse the unprotected loss of flow accident (ULOFA) behaviour of metal fuelled FBR cores as a function of core size and perturbation method.

To accomplish these aims, three metal FBRs having a small (120 MWe), medium (500 MWe) and a large (1000 MWe) sized reactors using ternary metallic fuel U-Pu-Zr are used. The criteria adopted for the core optimization is higher BR and improved safety parameters for safe and sustainable energy production. In these cores, the impact of various safety coefficients and reactivity worth data on transient behaviour during severe accidental conditions are obtained. The sensitivity of first order and exact perturbation approximations for computing reactivity worth data is analysed and their impact on core transient behaviour is also assessed. This study helped the development of a computer code for estimating reactivity worth data based on exact perturbation theory. The main results of the study are briefly summarised below:

A systematic variation of core physics parameters of metallic ternary U-Pu-Zr fuelled FBRs as a function of zirconium content in the fuel and core size is studied. It shows that both BR and sodium void worth increases with core size and reduction in zirconium. It is found that, the BR achievable with these cores (small, medium and large) using U-Pu-6%Zr fuel is 1.1, 1.36 and 1.49 respectively. The estimated values of sodium void worth for these cores is 0.4 $, 4.5 $ and 5.6 $ respectively. Two methods are presented for the reduction of

sodium void worth in large FBR cores. In a study conducted on a 1000 MWe FBR core shows that, its value can be reduced to 43% of its original value by replacing the upper axial blanket by a sodium plenum.

A computer code PERTX is developed for computing reactivity worth data based on exact perturbation theory. The deviation in reactivity worth data between first order and exact perturbation theory is studied. The study shows that up to 50% voiding of steel and sodium from whole core or inner core regions, first order and exact perturbation methods show comparable results. For voiding from outer core regions, first order estimates show larger deviations from exact values. Fuel voiding worths are largely under predicted by first order methods for void fractions more than 10%. Both the first order and exact perturbation worths as well as Pu-239 reactivity equivalence values with IGCAR code systems are validated against the European code ERANOS version 2.1. The adequacy of scheme of safety analysis at IGCAR with 1^{st} order perturbation worth data is also verified.

Using the results of first order perturbation theory, the ULOFA analysis is performed for three FBR cores of 120 MWe, 500 MWe and 1000 MWe. The study shows that the 1000 MWe reactor enters the disassembly phase within a shorter interval after the initiation of the event. This is due to the significantly more positive contribution from sodium expansion feedback in this core. Also, it is found that the ULOFA transient behaviour of these FBR cores are unaltered by the use of material removal and Doppler reactivity worths estimated using exact perturbation theory. During the accident, the above conclusion is valid only up to the end of pre-disassembly phase, within which, the core is subjected only to relatively small perturbations.

In summary, the study shows that with U-Pu-6%Zr fuel and with pessimistic uncertainties in the main feedback parameters from first order perturbation theory, 120 MWe and 500 MWe FBR cores are benign under ULOFA transient. The 1000 MWe core can be benign with 20% reduction in sodium void worth.

The study presented in the thesis is important for the choice of core size and safe implementation of FBR cores in India.

6.2 SCOPE OF FURTHER STUDIES

The above studies show that, sodium void worth is an important parameter with respect to core safety. Hence, these studies can be extended to get core design modifications for near zero sodium void worths and their influence on transient behaviour. Core designs with heterogeneous concept could be attempted toward reducing sodium void coefficient. Multichannel representation in a coupled code with neutron diffusion theory and sub-assembly wise thermal hydraulics computation can be also studied. Also, detailed 3D burn-up and perturbation studies of metallic fuels can be carried out.

REFERENCES

1. Azekura, K., Hayase, T., 1989. Three-Dimensional First-Order Perturbation Calculation Method for Reactivity Changes Due to Core Deformations of Fast Breeder Reactors, Journal of Nuclear Science and Technology, 26[3], pp.374-378.
2. Bruno Merk et al., 2011. On the Use of a Moderation Layer to Improve the Safety Behaviour in Sodium Cooled Fast Reactors, Annals of Nuclear Energy, 38[5], pp.921–929.
3. Cahalan, J.E. et al., 1990. Performance of Metal and Oxide Fuels during Accidents in a Large Liquid Metal Cooled Reactor, International Fast Reactor Safety Meeting, Snowbird, USA, Vol. IV, 73.
4. Carmack, W.J. et al., 2009. Metallic Fuels for Advanced Reactors, Journal of Nuclear Materials, 392, pp.139-150.
5. Chang, Y.I., 2007. Technical Rationale for Metal Fuel in Fast Reactors, Nuclear Engineering and Technology, 39 (3), pp.161-170.
6. Chellapandi,P. 2103. Severe Accident Scenarios: Indian Perspective, FR13, 4-7 Mar 2013, Paris.
7. Chetal, S.C., et al., 2006. The Design of the Prototype Fast Breeder Reactor, Nuclear Engineering and. Design, 236, pp.852–860.
8. Chetal, S.C., 2009. A Perspective on Development of Future FBRs in India, Int. Conf. Fast Reactors and Related Fuel Cycles (FR09)-Challenges and Opportunities, Dec. 7-11, Tokyo, Japan.
9. Chetal, S.C. et al., 2011. Current Status of Fast Reactors and Future Plans in India, Energy Procedia, 7, pp.64-73.

10. Chetal, S.C., Chellapandi, 2013. Indian Fast Reactor Technology: Current Status and Future Programme, Sadhana, 38/5, Indian Academy of Sciences, pp.795–815.
11. Chernock, W., Horton, K.E., 1994. Status of Liquid Metal Fast Reactor Development in the United States of America, IAEA TECDOC-791, pp.68-87.
12. Daniel Fieno, 1972. A Shielding Application of Perturbation Theory to Determine Changes in Neutron and Gamma Doses due to Changes in Shield Layers, Technical Paper Proposed for Presentation at National Topical Meeting on New Development in Reactor Physics and Shielding, American Nuclear Society, New York.
13. Debanwita Paul et al., 2014. Physics Design of an Advanced Oxide 600 MWe FBR, RDG/RND/CPS/154, IGCAR Report.
14. Devan, K. et al., 1999. Benchmark Analysis with ABBN-93 and CV2M Cross-Section Sets to Recommend a Cross-Section Set for PFBR Core Calculations, REG/RPD/NDS/78, IGCAR Report.
15. Devan, K. et al., 2003. ATOMIX -A Code for Calculating Atom Densities of Nuclides in a Mixture, RPD/CPS/24, IGCAR Report.
16. Devan, K., 2003. An Interface between CONSYST/ABBN-93 and IGCAR Diffusion Theory Codes. RPD/NDS/90, IGCAR Report.
17. Devan, K. et al., 2011. Physics Design of Experimental Metal Fuelled Fast Reactor Cores for Full Scale Demonstration. Nuclear Engineering and Design, 241, pp.3058-3067.
18. Devan, K. et al., 2011a. Approach to Equilibrium Fuelling Scheme of 500 MWe PFBR Based on 3-D Core Burn-up Modeling, Nuclear Engineering and Design, 241, pp.1596-1605.

19. Devan, K. et al., 2012. A Comparative Study of FARCOB and ERANOS-2.1 Neutronics Codes in Predicting the Phenix Control Rod Withdrawal End-of-life Experimental Results, Nuclear Engineering and Design, 245, pp.89-98.
20. Dubberley, A.E. et al., 2000. Super Prism Oxide and Metal fuel Core Designs. Proceedings of ICONE8, 8th International Conference on Nuclear Engineering, Baltimore, USA.
21. Dubberley, A.E. et al., 2003. S-PRISM High Burn-up Metal-Fuel Core Design. Proceedings of ICAPP, Paper 3142, Cordoba, Spain.
22. Endo, H. et al., 1990. Safety Features of Fast Reactor with Metallic Fuelled Core, Proceedings of the 1990 International Fast Reactor Safety Meeting: Snowbird, Utah, US.
23. Fujita, E.K., Wade, D.C., 1990. The Neutronic and Fuel Cycle Performance of Interchangeable 3500 MWth Metal and Oxide Fuelled LMRs, International Conference on the Physics of Reactors, Marseille, France.
24. Gandini, A., 1967. A Generalized Perturbation Method of Bilinear Functionals of the Real and Adjoint Neutron Fluxes, Journal of Nuclear Energy, 21, pp.755-765.
25. Gandini, A., 1978. Implicit and Explicit Higher Order Perturbation Methods for Nuclear Reactor Analysis, Nuclear Science and Engineering, 67, pp.347-355.
26. Gandini, A., 1981. On the Standard Perturbation Theory, Nuclear Science and Engineering, 79, pp.426-430.
27. Gandini, A., 1986. Equivalent Generalized Perturbation Theory (EGPT), Annals of Nuclear Energy, 13, Number 3, pp.109-114.
28. Grover, R. B., Chandra, D., 2006. Scenario for Growth of Electricity in India, Energy Policy, 34, pp.2834-2847.

29. Harish, R. et al., 1999. KALDIS: A Computer Code System for Core Disruptive Accident Analysis of Fast Reactors, IGC-208, IGCAR Report.

30. Harish, R. et al., 2009. A Comparative Study of Unprotected Loss of Flow Accident in 500 MWe FBR Metal Core with PFBR Oxide Core, Annals of Nuclear Energy, 36, pp. 1003-1012.

31. Hofman, G.L., 1980. Irradiation Behaviour of Experimental Mark-II EBR-II Driver Fuel, Nuclear Technology, 47, pp.7-22.

32. Hofman, G.L., et al., 1997. Metallic Fast Reactor Fuels, Progress in Nuclear Energy, 31, pp.83-110.

33. Hummel, H.H., Okrent, D., 1970. Reactivity Coefficients in Large Fast Power Reactors, ANS Publication, Hinsdale.

34. Hill, R. N., Khalil, H., 1980. Evaluation of LMR Design Options for Reduction of Sodium Void Worth. In: Proc. of Int. Conf. on Physics of Reactors, Marseille, France, volume 1, pp.11–19.

35. IAEA-RC-803.3, 2001. Working Material, RCM-3 of IAEA CRP on Updated Codes and Methods to Reduce the Calculational Uncertainty of LMFBR Reactivity Effects. IAEA, Vienna.

36. IAEA, 2010. BN-600 Hybrid Core Benchmark Analyses, IAEA-TECDOC-1623.

37. IAEA, 1994. Evaluation of Benchmark Calculation on a Fast Power Reactor Core with Near Zero Sodium Void Effect, Final Report of Benchmark Program Supported by the IAEA and European Commission, TECDOC-731. IAEA, Vienna.

38. IAEA, 2000. Transient and Accident Analysis of BN-800 type LMFR with Near Zero Void Effect, TECDOC-1139.

39. IAEA, 2011. Energy, Electricity and Nuclear Power Estimates for the Period up to 2050. IAEA-RDS-1/31, Vienna.

40. IGC Newsletter, 2014. 100, ISSN 0972-5741. IGCAR.

41. John T.M., 1984. NEWPERT–Perturbation Code for Two Dimensional Diffusion Equations. REDG/01150/RP-253, REDG/01150/RP-253, IGCAR Report.

42. John, T.M., 1998. Comparison of Calculated and Experimental Neutronics Parameters for the Critical Assembly BFS-44, RPD/CPS/08, IGCAR Report.

43. Kakodkar, A, 2008. Evolving Indian Nuclear Programme, Rationale and Perspective. Available at http://dae.nic.in/writereaddata/.pdf_33.

44. Kappler, F. et al., 1984. Analysis of Small-zone Sodium Void Experiments Performed in Heterogeneous Fast Reactor Core, ANS Topical Meeting on Reactor Physics and Shielding, Chicago, USA.

45. Kittel, J.H. et al., 1993. History of Fast Reactor Fuel Development, Journal of Nuclear Materials, 204, pp.1-13.

46. Kobayashi, K., Hirakawa, N., 1987. New Treatment of Sodium Void Effect in Fast Reactor Transient Study, 24[4], pp.257-265

47. Koning, A.J. et al., 2006. The JEFF-3.1 Nuclear Data Library. JEFF Report 21, Nuclear Energy Agency, Paris.

48. Khalil, H.S., Hill, R.N., 1991. Evaluation of Liquid-Metal Reactor Design Options for Reduction of Sodium Void Worth, Nuclear Science and Engineering 109, pp.221-266.

49. Lamarsh, J.R., 1965. Introduction to Nuclear Reactor Theory, Addison Wesley, USA.

50. Lewis, E. E., Miller, W. F., 1993. Computational Methods of Neutron Transport, American Nuclear Society, Inc, USA.

51. Manturov, G.N., 1997. ABBN-93 Group Data Library Part I: Nuclear Data for the Calculation of Neutron and Photon Radiation Functions INDC (CCP-409), IAEA, Vienna.

52. McMurry, H.L., 1956. Perturbation Theory and Applications, AEC Research and Development Report, UK.

53. Mohanakrishnan, P., 2005. Revised Estimates of ^{239}Pu Reactivity Equivalence and PuO_2 Content for Fabrication of MOX Fuel Pin, PFBR/01113/DN/1054/R-A, IGCAR Report.

54. Mohanakrishnan P., 2008. Development and Validation of Fast Reactor Core Burn-up Code-FARCOB, Annals of Nuclear Energy, 35, pp.158-166.

55. Mohanakrishnan, P. et al., 1999. PSAR Chapter 5.1 on Reactor Physics. IGCAR Report.

56. Mohanakrishnan and Om Pal Singh, 2000. Eigen-value Separation and Spatial Neutronic Coupling, PFBR/01113/DN/1041, IGCAR Report.

57. Ott, K.O., 1988. Inherent Shutdown Capabilities of Metal-fueled Liquid Metal Cooled Reactors during Unscrammed Loss of Flow and Loss of Heat Sink Incidents, Nuclear Science and Engineering, 99 (1), pp.13–27.

58. Pandikumar, G. et al., 2009. Multiple Recycling of Fuel in Prototype Fast Breeder Reactor, Pramana-Journal of Physics, Indian Academy of Sciences, Vol.72, No.5, pp.819-832.

59. Pahl, R.G. et al., 1990. Experimental Studies of U-Pu-Zr Fast Reactor Fuel Pins in EBR-II, Metallurgical Transactions A, 21, Issue 7, pp.1863-1870.

60. Pahl, R.G. et al., 1992. Irradiation Behaviour of Metallic Fast Reactor Fuels, Journal of Nuclear Materials, 188, pp.3-9.

61. Pitterle, A., Paik, N.C., 1972. Summary of Analysis of Plate Vs Pin Measurements Emphasizing Reactivity and Sodium Void Effects, Topical Meeting on New Development in Reactor Physics and Shielding, New York.
62. Planchon, H.P. et al., 1987. Implications of the EBR-II Inherent Safety Demonstration Test, Nuclear Engineering and Design, 101 (1), pp.75–90.
63. Rimpault, G. et al., 2002. The ERANOS Code and Data System for Fast Reactor Neutronic Analyses. Proceedings of PHYSOR 2002 Conference, Seoul, Korea.
64. Riyas, A., Mohanakrishnan, P., 2008. Studies on Physics Parameters of Metal (U–Pu–Zr) Fuelled FBR Cores, Annals of Nuclear Energy, 35, pp.87–92.
65. Riyas, A., Devan, K., Mohanakrishnan, P., 2013. Perturbation Analysis of Prototype Fast Breeder Reactor Equilibrium Core using IGCAR and ERANOS Code Systems, Nuclear Engineering and Design, 255, pp.112-122.
66. Riyas, A., Mohanakrishnan, P., 2005a. A Comparative Study of Physics Parameters of Oxide and Metal Fuels in PFBR. RDG/RPD/CPS/37, IGCAR Report.
67. Riyas, A., Mohanakrishnan, P., 2005b. Study of Physics Parameters for 1000 MWe Metal Fuelled FBR, RDG/RPD/CPS/39, IGCAR Report.
68. Riyas, A., Mohanakrishnan, P., 2005c. Studies on Physics of FBR's with U-Pu-Zr (10%) and U-Pu Fuels, RDG/RPD/CPS/48, IGCAR Report.
69. Riyas, A., 2011. Comparison between First Order and Exact Perturbation Theory Results of PFBR Core Analysis, REG/RPhG/RND/CPS/98, IGCAR Report.
70. Riyas. A., Mohanakrishnan. P., 2011. Exact perturbation Theory Code for 2D diffusion Equation- PERTX, REG/RPhG/RND/CPS/107, IGCAR Report.

71. Riyas, A., Mohanakrishnan, P., 2006a. Physics Parameters of Metal Fuelled 500 MWe FBR as a Function of Zirconium Content in the Fuel, RDG/RPD/CPS/51, IGCAR Report.
72. Riyas, A., Mohanakrishnan, P., 2006b. ^{239}Pu Equivalence of Fuel Isotopes Using XSET-98, RDG/RPD/CPS/64, IGCAR Report.
73. Riyas, A., Mohanakrishnan, P., 2007a. Physics Characteristics of a Metal Fuelled FBR with Modified Fuel Pin Design, RDG/RPD/CPS/71, IGCAR Report.
74. Riyas, A., Mohanakrishnan, P., 2007b. Study of Metal Fuelled FBR having Zirconium Liner in the Fuel Pin, RDG/RPD/CPS/73, IGCAR Report.
75. Riyas, A., Mohanakrishnan, P., 2009a. A Report on Physics Studies of Metallic Fuels for 500 MWe Fast Breeder Reactor, RPD/CPS/80/Rev-1, IGCAR Report.
76. Riyas, A., Mohanakrishnan, P., 2009b. 1000 MWe metallic Fuelled FBB with 2 Rows of Radial Blanket, REG/RPD/CPS/83, IGCAR Report.
77. Riyas, A., Devan, K., 2013. Studies of Reactor Doubling Time Dependence on Fuel Pin Diameter in a 1000 MWe MFBR, RDG/CDG/RND/CPS/129, IGCAR Report.
78. Riyas, A., Mohanakrishnan, P., 2014. ULOF Transient Behaviour of Metal Fuelled FBR Cores as a Function of Core and Perturbation Method, Nuclear Engineering and Design, 278, pp.141-149.
79. Ronen, Y., 1986. CRC Handbook of Nuclear Reactors Calculations. Volume III, CRC Press, Florida-USA, pp.63-188.
80. Royl, P. et al., 1990. Influence of Metal and Oxide Fuel Behaviour on the ULOF Accident in 3500 MWth Heterogeneous LMR Cores and Comparison with Other Large Cores, International Fast Reactor Safety Meeting, Snowbird, USA.

81. Ruggieri, J.M. et al., 2006. ERANOS 2.1: International Code System for GEN IV Fast Reactor Analysis, Proceedings of ICAPP'06, Reno, NV, USA.

82. Saito, R., Katsuragi,S., 1969. Higher Order Perturbation in Reactor Calculation, Journal of Nuclear Science and Technology, 6(6), pp.303-307.

83. Samuel Glasstone and Alexander Sesonske, 1994. Nuclear Reactor Engineering, Chapman & Hall.

84. Sathiyasheela, et al., 2011. Comparative study of Unprotected Loss of Flow Accident Analysis of 1000 MWe and 500 MWe Fast Breeder Reactor Metal (FBR-M) Cores and their Inherent Safety, Annals of Nuclear Energy, 38, pp.1065–1073.

85. Sathiyasheela, et al., 2013. Inherent Safety Aspects of Metal Fuelled FBR Nuclear Engineering and Design, 265, pp.1149-1158.

86. Sathiyasheela, et al., 2014. IGCAR Report (published soon).

87. Singh, O.P. et al., 1994. Analysis of Passive Shutdown Capability of Loss of Flow Accident in a Medium Sized LMFBR, Annals of Nuclear Energy, 21 (3), pp.165–170.

88. Shikhov, S.B., 1960. The Effect of Dimensional Changes on the Critical Mass of a Fast Reactor Calculated by Perturbation Theory. Journal of Nuclear Energy, Part A. Reactor Science, 11, Issues 2-4, pp.214-219.

89. Srinivasan, G, et al., 2006. The Fast Breeder Test Reactor—Design and operating experiences, Nuclear Engineering and Design, 236, Issues 7–8, pp.796-811.

90. Till, C.E et al., 1997. The Integral Fast Reactor, Progress in Nuclear Energy, Vol. 31, No. 1/2, pp.3-11.

91. Tommasi, J., 2007. ERANOS User's Manual-Applications of Perturbation Theory with Finite Difference Diffusion and SN Transport Flux Solvers, CEA, France.

92. Tommasi, J. et al., 2010. Validation of the Sodium Void Reactivity Effect Prediction using JEFF-3.1 Nuclear Data, Annals of Nuclear Energy, 37, Issue 11, November 2010, pp.1534-1553.

93. Vasudeva Rao, et al., 2013. A Perspective on the Indian Programme on Fast Reactors and Associated Fuel Cycles, International Conference on Fast Reactors and Related Fuel Cycles: Safe Technologies and Sustainable Scenarios, FR13, Paris, France.

94. Wade, D.C., Chang, Y.I., 1988. The Integral Fast Reactor Concept: Physics of Operation and Safety. Nuclear Science and Engineering, 100, pp.507-524.

95. Wade, D.C., Fujita, E.K., 1989. Trends Versus Reactor Size of Passive Reactivity Shutdown and Control Performance, Nuclear Science and Engineering, 103, pp.182–195.

96. Walter, A.E., Reynolds, A.B., 1981. Fast Breeder Reactors, Pargamon Press Inc., New York.

97. Walters, L.C., 1999. Thirty Years of Fuels and Materials Information from EBR-II, Journal of Nuclear Materials 270, pp.39-48.

98. Wright, A. E., et al., 1990. Fast Reactor Safety Testing in TREAT in the 1980s, Submitted to the 1990 International Fast Reactor Safety Meeting, Snowbird, USA.

99. Wyckoff, H.L., Greebler, P., 1974. Definitions of Breeding Ratio and Doubling Time, Nuclear Technology, 21, Number 3, pp.158-164.

100. Yokoo,T., Ohta, H., 2001. ULOF and UTOP Analyses of a Large Metal Fuel FBR Core Using a Detailed Calculation System, Journal of Nuclear Science and Technology, 38, No.6, pp.444-452.